2013

PROCEEDINGS OF
SUMMER UNDERGRADUATE RESEARCH PROGRAM

COLLEGE OF SCIENCE AND TECHNOLOGY
TEXAS SOUTHERN UNIVERSITY
HOUSTON, TX

TSU COLLEGE OF SCIENCE AND TECHNOLOGY
Summer Undergraduate Research Program (SURP) 2013

TABLE OF CONTENTS

TABLE OF CONTENTS
(Continued)

*SURP Fellowship Recipient
#Faculty Mentor

MESSAGE FROM THE DEAN

I would like to take this opportunity to congratulate all students who have participated in the College of Science and Technology (COST) Summer Undergraduate Research Program (SURP) 2013! I want to thank all faculty members who have spent their valuable summer time to dedicate to the mentoring of students in their research. This compendium of research accomplishments by the student participants is a clear evidence of the value and productivity of the COST SURP 2013.

The most critical need in our community is to produce more scholars and scientists. TSU has a long history of producing many of the nation's African American scientists. However, today fewer students are choosing to study for careers in science, technology, engineering, and mathematics, the so-called STEM fields. Our Science Building and the new Leonard H. O. Spearman Technology building have many highly automated laboratories, which are used for the most contemporary research. These facilities are cutting-edge and we want students to experience working in these laboratories so that they will see what the work of a researcher is like.

At one time there was almost no place where an undergraduate could gain experience in research. A similar situation existed in industry. But industry began to provide more internships to give students work experience and to provide an opportunity for industry to see the best students. Today, a growing number of companies use internships to attract the best students to hire.

Higher education has the same issues as industry. We need to attract more students to our enterprise of teaching, scholarship, and service. By providing research opportunities for our undergraduate students, they gain a deeper understanding of the subjects they studied and may see a clearer career path in higher education. Like industry, graduate schools are becoming more attracted to students who have shown promise in an undergraduate research experience.

I feel very strongly that more students should take advantage of the summer undergraduate research program and the College will continue to provide research experiences for as many undergraduate students as possible. I congratulate all those who participated in these research experiences. Keep up the good work!

Sincerely,

Lei Yu, Ph.D., P.E.
Professor of Transportation and
Dean, College of Science and Technology

PREFACE

During the summer of 2013, the College of Science and Technology (COST) at Texas Southern University (TSU) launched its inaugural Summer Undergraduate Research Program (SURP) to support active undergraduate student participation in science, technology, engineering, and mathematics (STEM) research. The 9-week program (6/2/13-8/2/13) was designed to provide valuable and exciting STEM research experiences for many talented students through their participation in cutting-edge research employing state-of-the-art instruments and techniques. A total of 16 undergraduate students were trained by 13 faculty mentors from 6 departments (Biology, Chemistry, Engineering Technologies, Environmental and Interdisciplinary Sciences, Mathematics, Transportation Studies) within the COST. Each undergraduate student received a $2,000 of fellowship and each faculty mentor received $1,000 for the purchase of research supplies.

Hands-on research experience is one of the most effective ways to retain students in STEM field, prepare them for their careers, and funnel them into graduate programs. Through their SURP participation, students learned how to use various state-of-the-art instruments such as: gas chromatograph-mass spectrometer (GC-MS) and a multimode inverted microscope. They were also exposed to meaningful research techniques such as: polymerase chain reaction (PCR), western blot analysis, in vitro XTT cytotoxicity assay, algal biofuel production, gel electrophoresis, and emerging concepts such as bioinformatics and life cycle assessment. Additionally, students investigated adverse impacts of exposure to electromagnetic radiation, grapheme oxide, bisphenol A, and nanomaterials. They also investigated impacts of microgravity on human cells. They tested effectiveness of phenols in Fries rearrangement and radio-frequency identification devices in order to reduce the risk of vehicle accidents as well as demonstrated potentials of soil-free hydroponic system in building a green roof and environmentally friendly community garden.

All student participants had a very productive summer through their participation in the program and also generated high-quality research data. Through our end-of-summer program symposium, students also learned how to effectively disseminate their findings orally through either PowerPoint (2 students) or poster presentations. Following their SURP participation, students are inspired to pursue summer programs in research institutes in other regions such as Mississippi and New York that will help them build nation-wide networks with other researchers. The COST is very proud of all students who successfully completed this 9-week summer research program while generating high-quality data evidenced by these students' manuscripts. I have no doubt that all of these future TSU alumni will become leaders in STEM fields in the near future.

Hyun-Min Hwang, Ph.D.
COST SURP Coordinator

LIST OF PARTICIPANTS
(STUDENTS)

Ariam Abraham, Senior
Department of Biology
Mentor: Dr. Shodimu-Emmanuel Olufemi

Muhammad Alghali, Senior
Department of Biology
Mentor: Dr. Shishir Shishodia

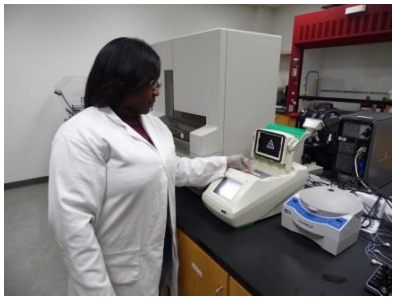

Kayla Burrell, Junior
Department of Biology
Mentor: Dr. Audrey Player

Mohamed Coulibaly, Junior
Department of Chemistry
Mentor: Dr. Jade Clement

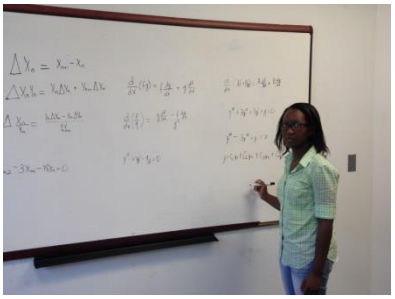

FranChell Davidson, Freshman
Department of Mathematics
Mentor: Dr. Willie Taylor

Damon Hall, Senior
Department of Transportation Studies
Mentor: Dr. Fengxiang Qiao

LIST OF PARTICIPANTS
(STUDENTS)

Kaness Khan, Junior
Department of Electronics Engineering Technology
Mentor: Dr. Graham Thomas

Ray Mbonu, Sophomore
Department of Chemistry
Mentor: Dr. Jade Clement

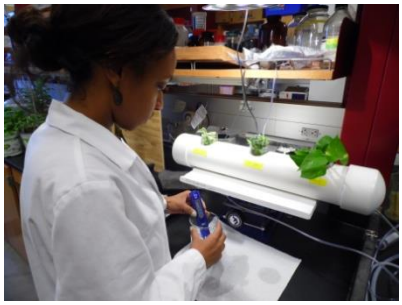

Kelly Newton, Sophomore
Department of Biology
Mentor: Dr. Hyun-Min Hwang

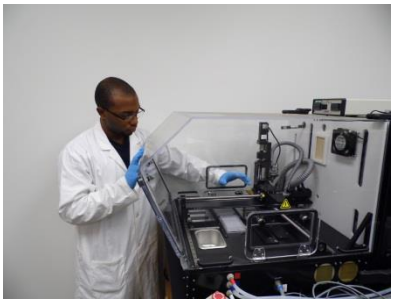

Richard North, Sophomore
Department of Biology
Mentor: Dr. Audrey Player

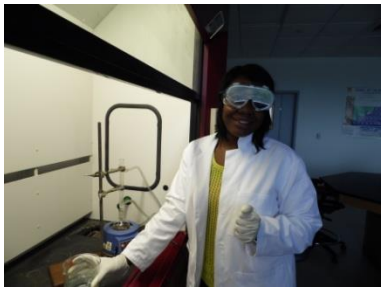

Uchechi Ogueri, Junior
Department of Chemistry
Mentor: Dr. John B. Sapp

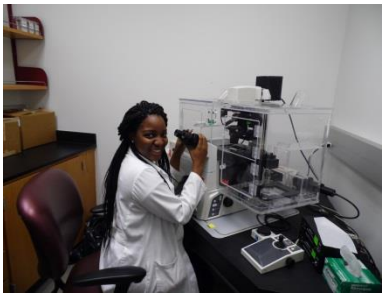

Nafisat Omotayo, Junior
Department of Biology
Mentor: Dr. Audrey Player

LIST OF PARTICIPANTS
(STUDENTS)

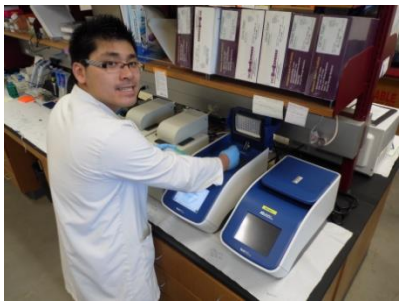

Tommy Quach, Sophomore
Department of Biology
Mentor: Dr. Hector Miranda

Raven B. Reed, Sophomore
Department of Chemistry
Mentor: Dr. Bobby L. Wilson

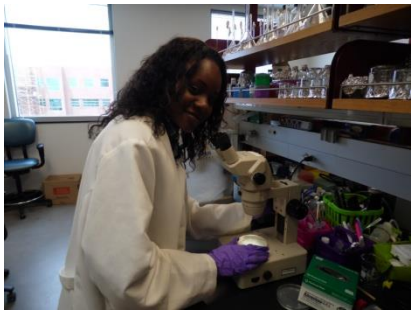

Sarah Sejoro, Sophomore
Department of Biology
Mentor: Dr. Fawzia Abdel-Rahman

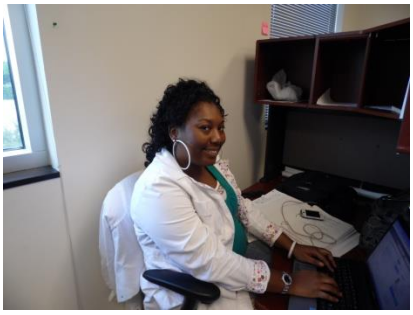

Tyneshia Thomas, Senior
Department of Biology
Mentor: Dr. Hyun-Min Hwang

LIST OF PARTICIPANTS
(MENTORS)

DR. JADE CLEMENT
Department of Chemistry

DR. HYUN-MIN HWANG
Department of Environmental and Interdisciplinary Sciences

DR. HECTOR MIRANDA
Department of Biology

DR. SHODIMU-EMMANUEL OLUFEMI
Department of Biology

DR. AUDREY PLAYER
Department of Biology

DR. FENGXIANG QIAO
Department of Transportation studies

DR. FAWZIA ABDEL-RAHMAN
Department of Biology

DR. JOHN SAPP
Department of Chemistry

DR. SHISHIR SHISHODIA
Department of Biology

DR. AYODOTUN SODIPE
Department of Biology

DR. WILLIE E. TAYLOR
Department of Mathematics

DR. GRAHAM THOMAS
Department of Electronics Engineering technology

DR. BOBBY WILSON
Department of Chemistry

ACKNOWLEDGEMENTS FROM PARTICIPANTS

Last summer I was afforded the opportunity to participate in the COST Summer Undergraduate Research Program (SURP) under the mentorship of Dr. Willie Taylor. At first I was apprehensive to do research after just completing my freshman year of college. I was nervous because I felt I didn't have adequate knowledge to successfully contribute to the program and that I was not going to be able to catch up fast enough. However, I was very wrong. I adapted to the program in no time with the assistance of my patient and understanding mentor. Our research entailed studying calculus from both the continuous and discrete points of view. This meant I have to first understand the concept of function and how it applies in both the continuous and discrete worlds. Then, I was able to study the solutions of linear differential equations and linear difference equations. By the end of my research I had learned how very different Discrete Calculus is in comparison to Continuous Calculus. However, when finding their solutions similar methods are utilized. The better understanding of these concepts helped me significantly this Spring Semester in my Differential Equations course. I was able to sit in the classroom with previously acquired knowledge, so I wasn't as lost as some of my fellow classmates. It was a great feeling to be able to actually interact and comprehend the lessons being presented. This made me feel as though if I keep doing these research experiences I will be able to graduate school with more confidence and drove me knowing that I will acquire great in-depth knowledge on any subjects one day if I keep trying and researching though I don't currently know much on them.

From *Franchell Davidson, Sophomore of Mathematics*

During my study with the Summer Undergraduate Research Program (SURP) in the College of Science and Technology (COST) at Texas Southern University under the leadership of Dr. Jade Clement, I learnt about the molecular and cellular responses to the space environment through research on two major space environmental hazards; radiation and microgravity. Microgravity and radiation are major hazardous factors in space due to their ability to cause damage to the body's cells and tissues. We conducted a study on microgravity and bisphenol A (BPA) and their combined effects on human cells. Over the 9-week program, I spent an average of 25 hours per week, in both the lab and library. Through extensive literary research I was able to get a view on current understanding of molecular and cellular responses to space environmental factors. In the lab, we were able to observe the toxicity of bisphenol A on human liver cells that experienced simulated-microgravity for 25 days versus the parental cell line that had never been exposed to the simulated microgravity. We performed time-course XTT cytotoxicity assay for cell viability analysis using various doses of BPA. As an aspiring Chemistry major and engineer, the COST SURP internship benefitted by helping me develop new research habits, refreshing and enhancing my lab practice with the use of more advanced lab equipment, as well as instilling a safety first mindset when in the lab, and providing research experience I was eager to acquire.

From *Ray Mbonu, Junior of Chemistry*

ACKNOWLEDGEMENTS FROM PARTICIPANTS

I would like to express my gratitude to the COST Summer Undergraduate Research Program (SURP) 2013 for their support. The program was outstanding because it allows many undergraduate students to participate in research at their own institution and showcase the research and the potential of several of the COST faculty members. In addition, it gave an undergraduate student, Ms. Ariam Abraham, the opportunity to conduct her scholastic summer 2013 research works in my laboratory, where we utilized different bioinformatics' tools and bio-technique approaches to generate microRNA-GFP DNA constructs that were expressed in mammalian cells. The research work she conducted in my lab was very exciting to her because she actually did the work "Hands on Research" and was able to present her research findings as a poster presentation at the Joint End-of-Program Symposium for TSU URP and COST SURP 2013.

I am also grateful for the monetary support that the program provided for my lab and Ms. Ariam to conduct the research. I sincerely thank all the participants and those who worked diligently and hard to make the COST SURP 2013 a very successful program for the students and COST.

From *Dr. Shodimu-Emmanuel Olufemi, Assistant Professor of Biology*

STUDENT ACTIVITIES

RESEARCH IN THE LABORATORIES

STUDENT ACTIVITIES

ORAL AND POSTER PRESENTATIONS

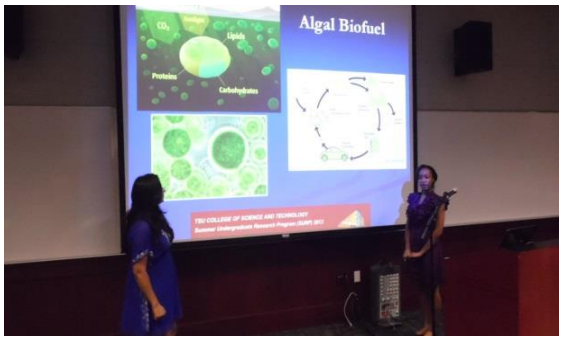

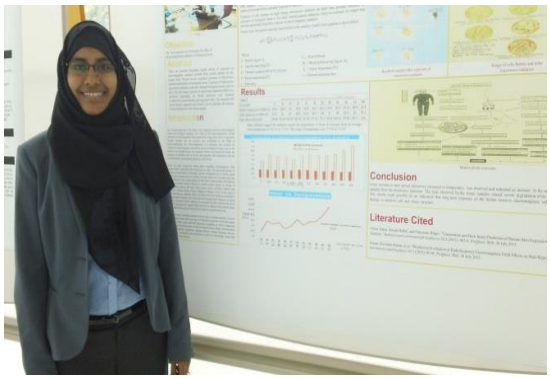

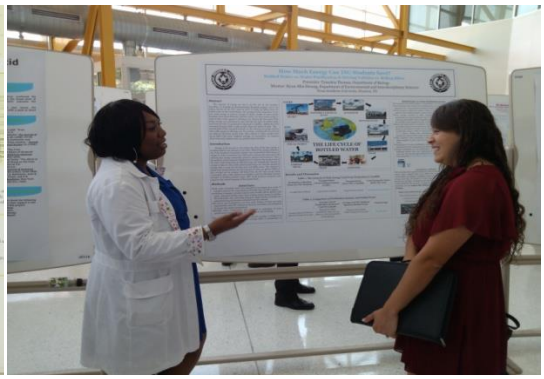

CLONING AND EXPRESSION OF PRE-miRNA FRAGMENTS IN TM3 CELLS

Ariam Abraham* and Shodimu-Emmanuel Olufemi#

Department of Biology
College of Science and Technology, Texas Southern University
3100 Cleburne Street, Houston, TX 77004

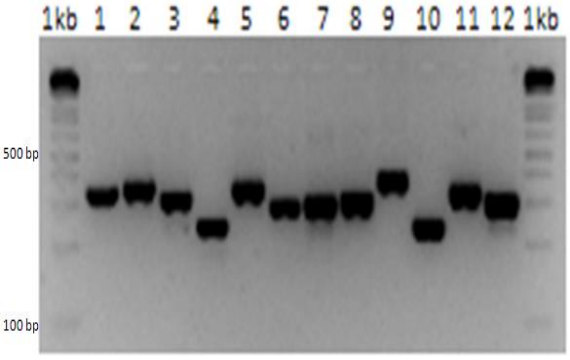

ABSTRACT

MicroRNAs (miRNAs) are a class of small non-coding RNA that are 15-25 nucleotides and are encoded by highly conserved genes. They are expressed in both unicellular and multicellular organisms and regulate different cellular processes, such as cell proliferation, cell differentiation and apoptosis. Here we embark on a specific, effective and practical method of cloning pre-miRNA fragments into expression vectors. First we identified the miRNA sequence at the miRBase and determined the pre-miRNA sequence at the UCSC Genome Browser and the NCBI database. Second, we designed both forward and reverse primers and confirmed alignment of the pre-miRNAs using two software, AmplifX 1.1 and Sequencher 5.0. The pre-miRNA primers were used for PCR amplification of either genomic DNA or cDNA. The PCR-amplified products were cloned into TOPO-2.1 or TOPO-4 vectors. The presence of the pre-miR fragment was confirmed by double restriction enzyme digestion using BamHI and HindIII or BamHI and NheI. The restriction enzyme digested fragments were further cloned into miRNA fluorescence expression vectors, pEGP miR expression vector and pmR-ZsGreen1 expression vector. We confirmed the presence of the pre-miRNA fragments in the miR expression vectors by double restriction enzyme digestion and we successfully cloned and expressed the pre-miRNAs in TM3 cells.

Key words: *MicroRNAs, Cloning, PCR amplification, Double restriction enzyme digestion*

*SURP Fellowship Recipient
#Faculty Mentor

INTRODUCTION

The ground breaking discovery of microRNA (miRNA) came to light by Dr. Victor Ambrose and his co-workers while studying normal larval development in *Caenorhabditis elegans* (C. elegans) and identified a single RNA molecule that they termed miRNA (Lee et. al., 1993). miRNAs are a class of small non-coding RNAs, which are involved in post transcriptional regulation, and they consist of approximately 15-25 nucleotides in length. miRNA genes are highly conserved and have been found in multicellular and unicellular organisms (Zhao et. al., 2007). miRNAs regulate gene expression by inducing RNA cleavage or translational inhibition, and regulate different cellular processes, such as cell proliferation, cell differentiation and apoptosis (Qin et. al., 2013). Both computational prediction and biological data from several investigations of genome-wide studies show that a single miRNA may target tens to hundreds of genes (Krek, et. al., 2005; Lim, et. al., 2005; Grimson, et. al., 2007). Our current

research focuses mainly on the fundamental steps which are essential in exploring the effects of miRNAs in cell-lines. Based on miRNAs sequences information at the miRBase, UCSC Genome Browser and the National Center for Bioinformatics (NCBI) database, we designed and aligned pre-miRNA primer sets using two software, AmplifX 1.1 and Sequencher 5.0. The primer sets are designed to amplify the pre-miRNA fragments with additional extension sequences on both sides. The pre-miRNA-products were obtained by amplifying genomic DNA or cDNA using Polymer Chain Reaction (PCR). The amplified pre-miRNA PCR-products were first cloned into TOPO-2.1 or TOPO-4 and removed by restriction enzyme digestion and were successfully cloned into pEGP miR expression vector or pmR-ZsGreen1 expression vector, which is expressed in TM3 cells. We envision that our pre-miR constructs will serve as resources for future studies in understanding miRNAs regulatory functions in mammalian cells.

METHODS

MicroRNAs (miRNAs) were identified at the miRBase and the miRNA sequences were used to deduce pre-miRNA sequences at UCSC Genome Browser and National Center for Biotechnology Information (NCBI) database. Both forward and reverse primers were designed based on pre-miRNA sequence using AmplifX 1.1 (New Dream Network, LLC, Los Angeles, CA) and the primer alignments were confirmed using Sequencher 5.0 software (Gene Codes Corporation, Ann Arbor, MI). The primer sequences were modified by tagging the 5′ ends of each primer with multiple restriction enzyme sites; and the primers were synthesized (Sigma Aldrich, St. Louis, MO).

Polymerase chain reaction (PCR) was performed on genomic DNA or cDNA templates using both forward and reverse primers. The PCR reaction mixture was carried out in a total volume of 15.0 µl (contains 2.5 µl of gDNA (250 ηg) or cDNA , 7.5 µl of master mix (Qiagen, Valencia, CA), 1.0 µl (10 nM) of forward primer, 1.0 µl (10 nM) of reverse primer and 2.5 µl of nuclease free water). PCR was performed using BioRad C1000 thermocycler (BioRad, Hercules, CA) and the PCR condition is as follows: 95°C for 15 min, 94°C for 45 sec, 60°C for 30 sec, 72°C for 60 sec, 45 cycles, 72°C for 10 minutes and 4°C. First, 5.0 µl of amplified PCR-products were analyzed on a 2% agarose gel stained with ethedium bromide. The PCR-products were ligated into TOPO-2.1 or TOPO-4 vectors (Life Technology, Grand Island, NY). The ligated products were transformed into F10 competent E. coli cells and streaked on Luria-Bertani (LB) kanamycin plates, containing X-gal (5-bromo-4-chloro-3-indolyl-β-D-galactoside) for white and blue colonies selection. The plates were incubated at 37 °C overnight for 18 hours. Two to four white colonies were picked and grown in LB medium at 37 °C overnight for 18 hours and DNAs were isolated and tested for presence of pre-miRNA fragments by PCR or restriction enzyme digestion.

The isolated DNA constructs were digested with restriction enzymes and analyzed on a 1% low melting agarose gel and pre-miRNA fragments were excised from the gel and purified using Geneclean (MP Biolab, Solon, OH). The purified pre-miRNA fragments were further ligated into pEGP-miRNA expression vector (Cell Biolabs, San Diego, CA) or pmR-ZsGreen1 expression vector (Clontech, Mountain View, CA), and then transformed into DH5α competent E. coli cells (Life Technology, Grand Island, NY). The cells were streaked on LB kanamycin or LB ampicillin plates and incubated at 37°C overnight for 18 hours. Two to four colonies were picked from the plates and grown in LB medium at 37°C overnight for 18 hours. DNAs were isolated from the LB medium and tested for presence of pre-miRNA fragments by PCR or restriction enzyme digestion. Insertion of pre-miRNA fragments were confirmed by double restriction enzyme digestion using restriction enzymes, BamHI and HindIII or BamHI and NheI (New England Biolabs, Ipswich, MA). The pre-miR-pEGP DNA constructs or the pre-miR-pmR-ZsGreen1 DNA constructs were transfected using Lipofectamine 2000 (Life Technology, Grand Island, NY) and expressed in TM3 cells (ATCC, Manassas, VA).

RESULTS AND DISCUSSION

In Figure 1a, the highlighted yellow and green sequences show the positions of the primers on the genomic DNA (gDNA) sequence obtained from UCSC Genome Browser. Figure 1b shows restriction enzyme tagged primer set for hsa-miR-574 pre-miR, which was identified in an ongoing project using

microsatellite sequences in the mammalian genome (unpublished). The gDNA sequence containing hsa-miR-574 is located in intron 1 of the FAM114A1 gene on human chromosome 4.

PCR results showed the exact pre-miR fragment sizes for all the amplified miR sequences that were analyzed on a 2% agarose gel stained with ethidium bromide (Figure 2). The amplified pre-miR fragments are cloned into miR-expression vectors. Figure 3 shows the structure of one of the miR expression vectors, pmR-ZsGreen1 expression vector.

(a)

Ggtggtgggaacaccataccttggcgcctcgtccgggacccacgaatcctgccctctgcgttagtgagaagcagtggtcagggaggacccggctctg

gggtgagggtctggggcggcgcggccgagggacctgcgtgggtgcgggcgtgtgagtgtgtgtgtgagtgtgtgtcgctccgggtccacgctcat

gcacacacccacacgcccacactcagggtctgccccctcggcctgcgtgaacctccgcggagcctgcctggatctcccaaagtatccagtcctggcac

caagcaagtctggaaaagtgcccccaatggctcggggccaagtcagaggtgggc

(b)

Flf-miR574-F ----- GCTAGCGCTACCCTCGAGCTCAAGCTTCgtggtgggaacaccataccttg

Flf-miR574-R ----- GACCGGTGGATCCCGGGCCCGCGGTACCGTcattgggggcacttttccagact

Figure 1. (a) Pre-hsa-miR-574 (flank by extra 125 base pair sequences at both the 5´ and 3´ ends) and **(b)** One of the tagged-miR primer sets and the bold letter is the restriction enzyme tagged sequence and the small letter is primer specific sequence. The expected PCR-product Size is 370 bp.

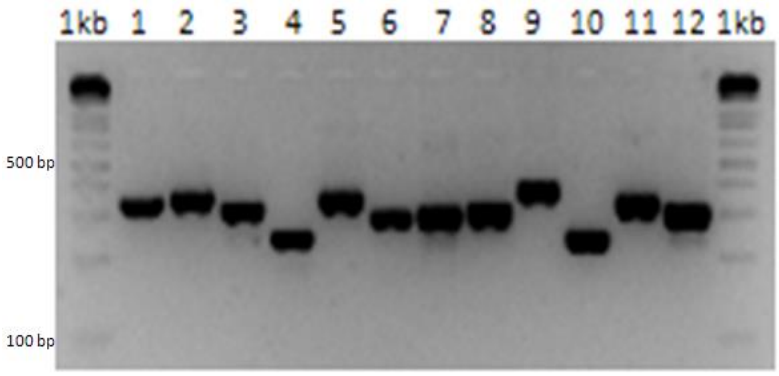

Figure 2. Analysis of PCR- amplified pre-miRNA fragments separated on a 2% agarose gel stained with ethidium bromide. The amplified pre-miRNA fragments are in lanes 1-12, and the two outside lanes contained the 1 kb ladder size marker.

Gel electrophoresis result of BamHI and HindIII double restriction enzyme digested pre-miR-pmR-ZsGreen1 DNA constructs separated on 2% agarose gel stained with ethidium bromide confirmed the presence of pre-miR fragments cloned into pmR-ZsGreen1 vector (Figure 4). The cloned pre-miR-pmR-ZsGreen1 DNA constructs are successfully transfected and expressed in TM3 cell-lines (data not shown).

It is 20 years ago when the first miRNA (Lee et. al., 1993) was identified and the numbers of miRNAs identified have increased and are found in many organisms. In most tissues, miRNAs producing genes constitute a small fraction of the non-coding RNA producing genes (Axtell, 2013). miRNAs regulate gene expression at the post-transcription level and computational approach has been used to determine mRNAs that are targeted by miRNAs. So far, most of the miRNA functions have not been deciphered due to lack of cloning of the miRNA sequence into expression vectors for functional studies.

In our studies, we show that pre-miRNA fragments can be cloned into expression vectors and expressed in mammalian cell lines that can be used for functional studies.

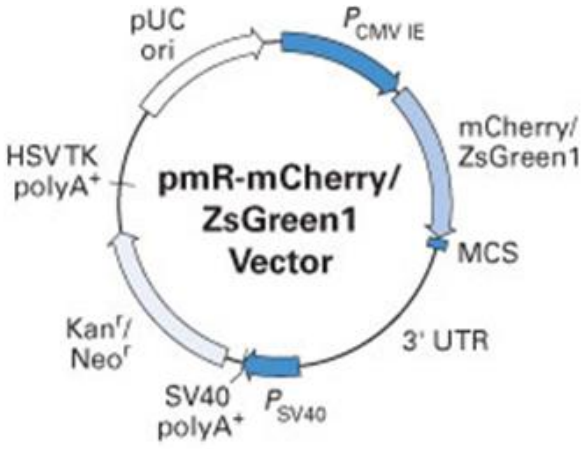

Figure 3. Schematic representation of one of the cloning vectors, pmR-ZsGreen1.

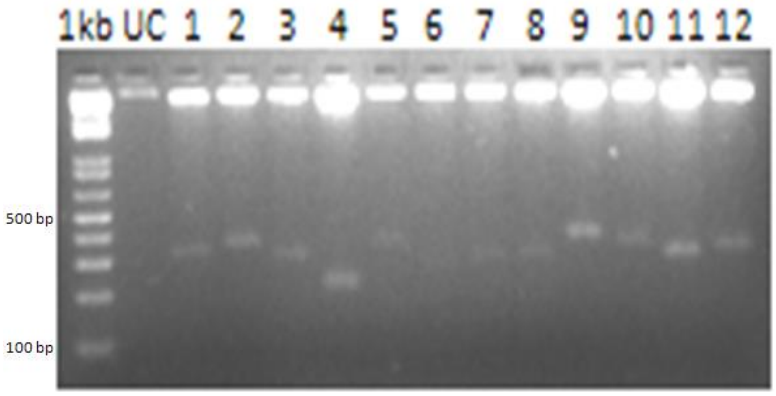

Figure 4. Gel electrophoresis result of double restriction enzyme digested pre-miR-pmR-ZsGreen1 DNA constructs using BamHI and HindIII restriction enzymes, confirming the presence of pre-miR fragments cloned into pmR-ZsGreen1 vector. Lanes 1-12 consist of digested pre-miR-pmR-ZsGreen1 DNA construct, including a 1kb (kilobase) ladder size maker (not shown is restriction enzyme digestion for pre-miR-pEGP-miRNA DNA constructs).

CONCLUSION

Pre-miR fragments are successfully cloned into miR fluorescence expression vectors and the pre-miR fragment DNA constructs are expressed in TM3 cells. The expression of the pre-miR fragments in the TM3 cells is confirmed through expression of green fluorescence protein (GFP).

ACKNOWLEDGEMENTS

This study was supported by Summer Undergraduate Research Program (SURP) of the College of Science and Technology at Texas Southern University. We also express our gratitude to the Department of Biology for supporting this study and providing equipment. We also would like to thank Hoda Eltayeb, Olusegun Ogunniyi, Jihan Asad, Angel Ryals, Tommie Johnson, Fatima Alhassan, Imani Bethel, Jennifer Mosley, and Everton Brown for their help.

REFERENCES

Axtell MJ. (2013) ShortStack: comprehensive annotation and quantification of small RNA genes. *RNA* 19:740-751.

Grimson A, Farh KK, Johnston WK, Garrett-Engele P, Lim LP, Bartel DP. (2007) MicroRNA targeting specificity in mammals: determinants beyond seed pairing. *Molecular Cell* 27:91-105.

Krek A, Grün D, Poy MN, Wolf R, Rosenberg L, Epstein EJ, MacMenamin P, da Piedade I, Gunsalus KC, Stoffel M, Rajewsky N. (2005) Combinatorial microRNA target predictions. *Nature Genetics* 37:495-500.

Lee RC, Feinbaum RL, Ambros V. (1993) The *C. elegans* heterochronic gene *lin-4* encodes small RNAs with antisense complementarity to *lin-14*. *Cell* 75:843-84.

Lim LP, Lau NC, Garrett-Engele P, Grimson A, Schelter JM, Castle J, Bartel DP, Linsley PS, Johnson JM. (2005) Microarray analysis shows that some microRNAs downregulate large numbers of target mRNAs. *Nature* 433:769-773.

Qin DN, Qian L, Hu DL, Yu ZB, Han SP, Zhu C, Wang X, Hu X. (2013) Effects of miR-19b overexpression on proliferation, differentiation, apoptosis and Wnt/β-catenin signaling pathway in P19 cell model of cardiac differentiation in vitro. *Cell Biochemistry and Biophysics* 66:709-722.

Zhao T, Li G, Mi S, Li S, Hannon GJ, Wang X, Qi Y. (2007) A complex system of small RNAs in the unicellular green alga *Chlamydomonas reinhardtii*. *Genes and Development* 21:1190-1203.

EFFECTS OF MICROGRAVITY ON APOPTOTIC CELL DEATH

Muhammad Alghali* and Shishir Shishodia#

Department of Biology
College of Science and Technology, Texas Southern University
3100 Cleburne Street, Houston, TX 77004

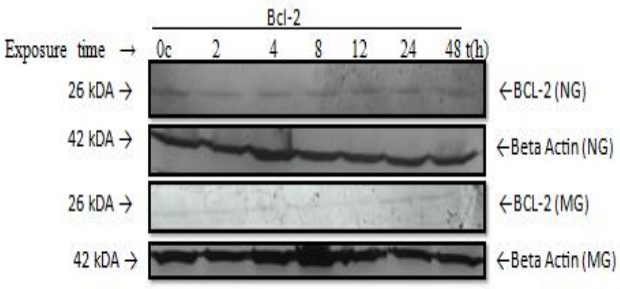

ABSTRACT

Astronauts are subjected to several environmental stress factors during space travel. One of which is microgravity. Studies have shown that microgravity exposure can lead to changes in muscle atrophy, blood, and plasma volume, bone loss and the deregulation of the immune system. In this study, we investigated the effect of microgravity on apoptotic cell death to determine whether microgravity is detrimental to the health of the immune system. Human T-lymphocyte (Jurkat) cells were subjected to microgravity conditions that were simulated using the Rotary Cell Structure System (RCCS) equipped with High Aspect Ratio Vessel (HARV) from Synthecon (Houston, TX). Cell viability due to microgravity was observed by counting cells using trypan blue exclusion method with a hemocytometer. Trypan blue is a stain that colors dead cells blue while the viable (live) cells remain unstained. Data from normal gravity (NG) and simulated microgravity (SMG) proved that there was indeed a change in cell viability. Proteins were extracted from cells grown in NG and SMG, and separated using SDS-PAGE gel. Our results showed that cells grown in simulated microgravity activated caspases that led to apoptotic cell death. The increased levels of the cleaved caspase proteins indicates that cells grown under SMG conditions were headed for self destruction whereas cells grown in normal gravity had very little cleaved caspase proteins present. These results show that reduced gravity may alter cellular activity by inducing cell death.

***Key words**: MicroRNAs, Cloning, PCR amplification, Double restriction enzyme digestion*

*SURP Fellowship Recipient
#Faculty Mentor

INTRODUCTION

Apoptosis (programmed cell death) is a form of naturally occurring cell death that plays fundamental roles for a) embryonic development to shape organs and tissues, b) homeostatic maintenance of cell population in tissues, and c) defense mechanism such as in immune reactions or when cells are damaged by disease or noxious agents to remove them in a neat orderly manner.

Apoptosis is characterized by cell shrinkage, chromatin condensation, disassembling of DNA, nuclear fragmentation, and packaging of the nuclear fragments into apoptotic cell bodies (Wyllie et al, 1980) – all these events lead to death of the cell. Every cell has to die, but it is crucial to the surviving organism that cell death is regulated because an inappropriate cell death is as detrimental to the organism as an inappropriate cell division. Therefore cell death must be regulated. Defective apoptotic processes have

been implicated in an excessive variety of diseases. Excessive apoptosis causes atrophy (tissue death), whereas an insufficient amount results in uncontrolled cell proliferation, such as cancer.

Alteration of the gravity vector is one of the external apoptosis inducers that also include UV radiation, ionization and heat shock. Gravity vector changes have been reported to damage the cytoskeleton of lymphocytes (Gmunder *et al*, 1990) during space flight and in simulated microgravity on ground-conducted experiments. Neurophysiological impairment signs were seen during space flights in astronauts (Krasnov, 1994). Whereas gravity is defined by NASA as force which governs motion throughout the universe, there is also the presence of some other gravity, called microgravity, also referred to as "zero gravity" which is located in space and can also be experienced during free-fall. Exposure to microgravity is known to cause several extensive effects and possibly have the ability to cause apoptosis. Apoptosis was observed in lymphocytes during spaceflight (Lewis et al, 1998; Cubano and Lewis, 2000). To determine whether microgravity induces apoptosis in immune cells, a ground-based system called the High Aspect Rotating Vessel (HARV) bioreactor was used to mimic microgravity environment here on earth. The apparatus includes 4 vessels each with a capacity of 10 ml – each containing Jurkat cells which were rotated at 8 RPM.

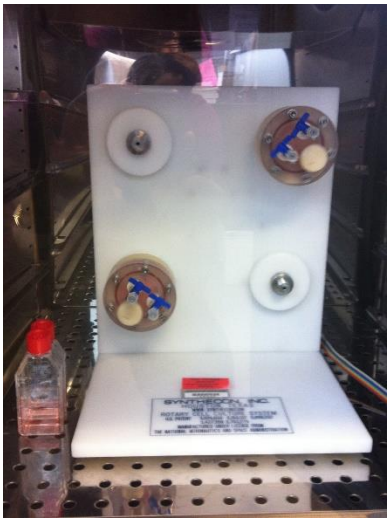

Figure 1. The High Aspect Rotating Vessel (HARV) simulating a microgravity environment. The vessel contains Jurkat cells in RPMI media.

METHODS

Jurkat cell lines (human T lymphocyte cell) obtained from American Type Culture Collection (ATCC) (Manassas, VA) was used in this experiment. The cell culture was performed using RPMI 1640 medium from Invitrogen. The RPMI medium was enhanced by a 10% FBS (Fetal Bovine Serum) plus 1% antibiotic containing 100 U/ml penicillin and 100 µg/ml streptomycin. The antibiotics help to maintain a sterile product free from contamination.

The cells were grown in the High Aspect Rotating Vessel (HARV) and in ground condition within a sterile environment of cell culture maintained at 5% CO_2 at 37 °C – the controls were cultured in a 25 ml culturing flasks in an incubator of 5% CO_2 at 37 °C. Jurkat cells were exposed to simulated microgravity for time points of 0, 2, 4, 8, 12, 24, and 48 hours using the HARV bioreactor developed by NASA. Cells obtained from each time points were prepared for whole cell extraction using lysis buffer solution. Both cells under simulated microgravity and the control in normal gravity were stained with trypan blue and counted using a hemocytometer.

Extraction buffer was used to perform whole cell extraction in a Western blot analysis. The Western blot or immunoblot is an analytical technique to detect specific proteins in a given sample tissue or

extract. It uses gel electrophoresis to separate native proteins by 3-D structure or denatured proteins by the length of the polypeptide. 50 µg of whole cell proteins were resolved on 7.5% or 12.5% SDS-PAGE (Biorad) depending on the molecular weight of the protein. After electrophoresis, the gel was electro-transferred to a nitrocellulose membrane (Biorad) and probed with desired antibodies. Gel electrophoresis is a method of separation and analysis of macromolecules (DNA, RNA, and proteins) and their fragments based on size and charge under an electrical field. Cytoplasmic and nuclear proteins were extracted from the cells. Other nitrocellulose membranes used were cleaved caspase 3, caspase 3, caspase 9, polyadipose ribose polymerase (PARP), BCL-2, and BAX as per manufacturer's protocol. The nitrocellulose membranes were then blocked with 5% non-fat blocking agent and probed with the desired antibodies. They were later washed with Tris Buffer Saline-Tween 20, and probed with antibodies against each antigen. Finally the BCIP-NBT reagent was used to detect the presence of the targeted proteins according to manufacturer's protocol.

RESULTS AND DISCUSSION

The pattern of cell death due to microgravity was observed by counting the cells using the trypan blue exclusion method with a hemocytometer. Trypan blue will penetrate the cell membranes of dead cells giving them a dark color and the cells which remain clear of the dye are live cells. Cell count was performed before and after exposure to microgravity and the same was done for the cells grown in parallel time point under normal gravity in the incubator.

Data from the experiment proved that there was indeed a change in cell count which indicates that the experiment worked. The experiment was also designed to determine the pathway that led to programmed cell death of these cells by probing for certain proteins associated with apoptosis. BCL-2 is a protein known to regulate apoptosis for proper development, tissue homeostasis, and protection against certain pathogens. This protein is localized in the outer mitochondrial membrane and the endoplasmic reticulum of nuclear membranes and it has the ability to promote the survival of cells by inhibiting the activation of apoptosome complex formed from the binding of the released cytochrome c from the mitochondria to the apoptotic protease activating factor-1 (Apaf-1), thereby stabilizing the mitochondria membrane

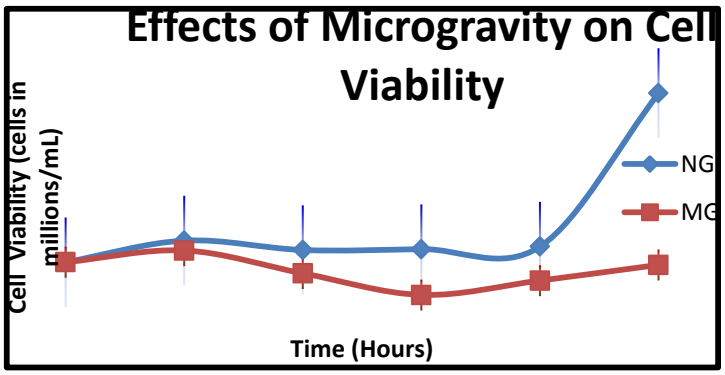

Figure 2. Trypan blue viability of Jurkat cells exposed to artificial microgravity simulated by High Aspect Rotating Vessel.

Two million Jurkat cells per milliliter were induced to microgravity and normal gravity for the indicated exposure time points. Fifty micrograms of whole cell protein extracts were prepared and resolved on a 12% SDS-PAGE gel electro transferred onto a nitrocellulose membrane and probed for BCL-2. According to the results obtained, the bands of BCL-2 (Anti-apoptotic) proteins appeared to be more pronounced in cells induced to normal gravity than those subjected to microgravity. This could be an indication that there was the presence of trophic factor in cells induced to normal gravity and the absence of trophic factor to those induced to microgravity and hence cell death. In normal gravity the presence of this signal could have led to a signaling cascade that will eventually lead to the release of the

protein Bad (pro-apoptotic) being phosphorylated. Bad protein is a Bcl-2 associated death promoter which is involved in initiating apoptosis. When phosphorylated, Bad loses its ability to bind and inhibit the activity of BCL-2, and hence have more cell survival in controlled cells than microgravity induced cells. From the bands produced at the 24 hours under normal gravity, the cells had doubled themselves indicating the presence of BCL-2 – in contrast under microgravity after 24 hours when doubling time should have occurred, the bands seemed to be less expressed when compared to its original control.

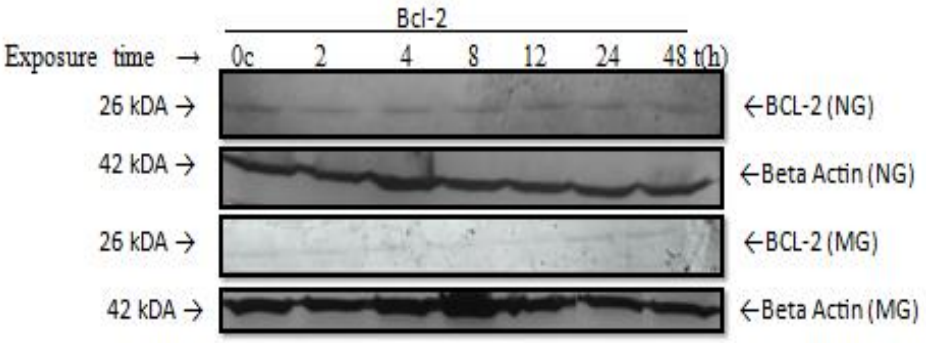

Figure 3. Western Blot analysis of Jurkat cells exposed to artificial microgravity simulated by High Aspect Rotating Vessel

Another Bcl-2 associated family member is the Bax protein, a pro-apoptotic protein that promotes apoptosis by competing with Bcl-2 proper. In healthy mammalian cells, the majority of Bax is found in the cytosol, but upon initiation of apoptotic signaling, Bax undergoes a conformation shift. When a cell is damaged, the Bax protein migrates to the mitochondria inhibits the anti-apoptotic activity of Bcl-2 and creates passages for the outflow of cytochrome c to bind to Apaf-1 forming the apoptosome complex.

From the Western blot analysis, the low expression bands of Bcl-2 in the Bcl-2 graph MG and the high expression bands of Bax in the Bax graph under microgravity MG is as a result of cell death. This shows that there are more cells dying than surviving under MG induced environment than under normal gravity NG induced environment.

Caspase or cysteine aspartic proteases are a family of cysteine proteases that play essential roles in apoptosis, necrosis and inflammation. Caspases are essential in cells for apoptosis (PCD) in development and most other stages in adult life. There are two types of apoptosis caspases namely, the initiator caspase which includes caspase 9 and the effector caspase which includes caspase 3. Caspase 9 is an important member of the cysteine aspartic acid protease (caspase) family. When a cell is stimulated to undergo apoptosis, the release of cytochrome c, due to the inhibition of Bcl-2 activity from the mitochondria associates itself with apoptotic protease activating factor (Apaf-1). This complex then binds to the inactive 47 kDa procaspase 9. The binding will lead to self cleavage of these large fragments to small active fragments of 37 kDa cleaved caspase 9 which is the active form of caspase 9 protein.

Data obtained showed that there were thicker bands of the inactive caspase 9 produced on a Western blot by normal gravity cells than microgravity cells. There were also lighter active cleaved caspase 9 protein bands produced by normal gravity cells than microgravity cells. Possible indication that the MG cells were on a path to be programmed for cell death are the positive feedback produced by MG cells, low caspase 9 and the high cleaved caspase 9. Since there is more cleaved caspase 9 produced in MG cells than NG cells, it means that these cells still had to go through certain caspase cascade. Caspase 3 is a 35 kDa protein known for being a critical executioner of apoptosis and interacts with caspase 9. Sequential activation of caspases plays a central role in the execution phase of cell apoptosis. The result from the caspase 3 graph shows a higher expression of the inactive executioner of apoptosis in normal gravity cells stating that these cells are not programmed to die at the rate as high as those programmed to die under microgravity induced cells and hence, more cells tend to survive in NG than in simulated MG environment.

CONCLUSION

It is shown that stress from microgravity indeed was the cause for cell death in the human T lymphocyte cell. The stress led to a change in normal cellular function and this may have depleted ATP energy in the mitochondria by the release of cytochrome c (which is normally used in the mitochondria as an electron carrier molecule) thereby altering the hydrogen ion concentration gradient which is responsible for creating potential energy needed to power ATP synthase to synthesize more ATP. The opening of the mitochondria membrane resulted in the release of cytochrome c which formed a complex with APAF-1 called the apoptosome complex which cleaved and activate caspase 9 which on its own cleaved caspase 3 and hence apoptosis. Microgravity resulted in a decrease in cell count as time increases leading to the inhibition of anti-apoptotic proteins, activation of Pro-apoptotic proteins, to caspase cascade and then apoptosis.

ACKNOWLEDGMENTS

This study was supported by Summer Undergraduate Research Program (SURP) of the College of Science and Technology at Texas Southern University. My sincere thanks to Dr. Marian Hillar who took an interest in me and introduced me to Dr. Lu who asked me to apply for the research program. Thanks to Ms. Nkem Azu who taught me all the laboratory techniques that I now know. Thanks are also due to Ms. Linda Noukeu who allowed me to use some of her materials and reagents.

REFERENCES

Boen B. (2008) NASA-Microgravity Research Program Fact Sheet, *NASA*.

Zona K. (2009) What is Microgravity? *NASA*.

Jeffery S. (2005) How does spending prolonged time in microgravity affect the bodies of astronauts? *Scientific American*.

Droppert PM. (1990) The effects of microgravity on the skeletal system – a review. *Journal of the British Interplanetary Society* 43:19-24.

Strollo F. (1999) Hormonal changes in humans during spaceflight. In Advances in Space Biology and Medicine Vol. 7. Ed Bonting SL, Elsevier Science. pp 99-129.

Uva BM, Masini MA, Sturla M, Bruzzone F, Giuliani M, Tagliafierro G, Strollo F. (2002) Microgravity-induced apoptosis in cultured glia cells. *European Journal of Histochemistry* 46: 209-214.

Cohen GM. (1997) Caspases: the executioners of apoptosis. *Biochemical Journal* 326:1-16.

CHARACTERIZATION OF TRANSCRIPTION FACTOR 1 GENE IN TRIPLE NEGATIVE BREAST CANCER

Kayla Burrell* and Audrey Player#

Department of Biology
College of Science and Technology, Texas Southern University
3100 Cleburne Street, Houston, TX 77004

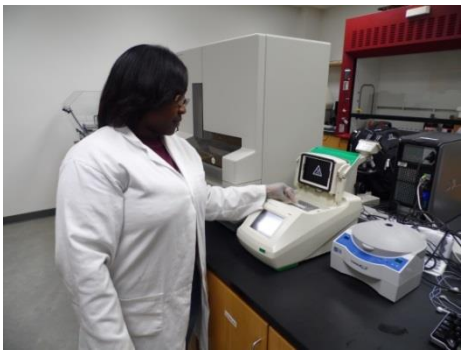

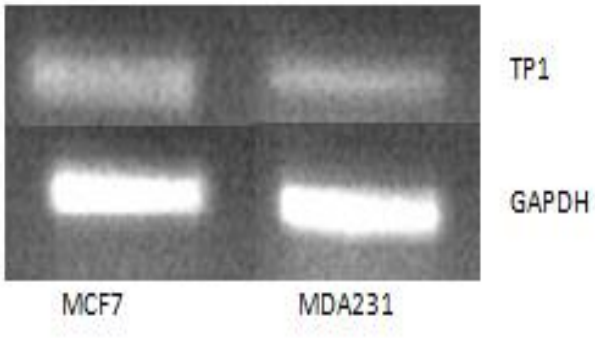

ABSTRACT

The goal of this study was to identify genes that reliably define triple negative (TN) aggressive breast cancers. Once identified, the genes would be examined further for their use as biomarkers. The experimental approach was to compare gene expression in breast cancer cell lines representing TN, to breast cancer cell lines characterized as 'non-TN'. Differentially expressed genes were identified and compared to publically available datasets as validation. Transcription factor 1 (TP1) gene was one of the genes identified as differentially expressed in TN. TP1 (RNA) expression was validated using cell line samples by qualitative polymerase chain reaction (PCR) and found to be down-regulated. For further validation, protein levels were examined using commercially available clinical patient samples. Clinical patient samples were diagnosed and defined by genetic signatures as TN or non-TN patient samples. Similar to results observed using RNA, protein levels were down-regulated. Some 33% of TN clinical samples demonstrated substantially lower TP1 gene expression compared to TP1 in non-TN clinical samples. Preliminary data suggest TP1 might be a promising gene to examine further as a biomarker for TN breast cancers.

Key words: *Breast cancer, Transcription factor 1 gene, PCR, Biomarker*

*SURP Fellowship Recipient
#Faculty Mentor

INTRODUCTION

There are many different types of breast cancer, often described as different subtypes. So far there are 5 subtypes, designated basal (also defined as TN), ERRBB2+-like, normal-like and luminal A and B. The types of breast cancers were defined based on their ability to 'cluster' following gene expression analysis, independent of diagnoses. Although there are several types of breast cancer, much of the focus and interest has been on trying to understand TN cancers. The TN breast cancer represent 10-20% of breast cancers (2) and are defined as negative for 3 genes, estrogen receptor (ER), progesterone receptors (PR) and ERBB2 (v-erb-b2 erythroblastic leukemia viral oncogene homolog 2) (1). It is important to characterize TN cancers because they are deadly (i.e., aggressive and prone to metastasis), are poorly defined on the genomic level, and lack effective therapies. There are therapies available for other types of breast cancer, but none for TN (2). Because TN cancers are aggressive, and lack effective therapies, TN

patients tend to die sooner compared to patients with other breast cancer types. If biomarkers can be identified, they might be useful as therapeutic targets and improve patient survival. Before therapies can be identified, however, scientists must first characterize TN cancers and identify genes reliably associated with the disease. The aim of this study was to first characterize TN cancers and identify reliable genetic signatures. If proven reliable, such signatures might ultimately be studied for their role as a biomarker and/or therapeutic targets.

The experimental approach was to compare gene expression of a TN cell line (MDA MB231) to a non-TN cell line (MCF7). Objective was to identify TN genes or genes that possibly define aggressive behavior associated with TN genotype. Genes identified by group comparison were then compared to publically available datasets deposited on GEO (http://www.ncbi.nlm.nih.gov/geoprofiles). Genes common to both this study and GEO datasets were further examined using other analyses, including signaling pathways and transcriptional regulation to start. Genes demonstrating a relationship via these analyses were chosen for further study. TP1 was one of several genes selected following this approach. Purpose of the study described below was to first validate differential expression of TP1 in TN samples. Analyses show that consistent with microarray, TP1 RNA was down-regulated in TN cell line RNA. And, consistent with RNA results, TP1 protein levels appear down-regulated in clinically diagnosed patient samples. Preliminary analyses of patient samples show ~33% of TN samples analyzed show down-regulation, far greater than would be expected under random conditions.

METHODS

Affymetrix U133 plus 2 gene expression hybridizations were performed previously following suggestions of the manufacturer (Affymetrix.com) using MDA MB231 (TN) cell line and MCF7 (non-TN) cell line, each in triplicate. Affymetrix microarray contained 54, 675 genes and Expressed Sequence Tags (EST) corresponding to all known and purported genes. Datasets generated from hybridizations were deposited on National Cancer Institute's mAdb website (https://madb.nci.nih.gov/). For data analysis, MDA MB231 (TN; group 1) was compared to MCF7 (non-TN; group 2). Grouped samples were normalized using Robust Multiarray analysis (RMA), and group comparisons performed using T-test. Gene expression differences between the 2 groups were identified using the T-test, and filtered based on genes showing at least 2-fold difference, with statistical p-values <0.01. A list of 49 (of 54,675) genes were identified as different between the 2 groups. The 49-gene-list was then compared to publically available patient datasets deposited on Gene Expression Omnibus (GEO); this allowed for comparisons between cell line and patient datasets and to some degree comparison to datasets generated by other investigators. Data associated with clinical samples was retrieved from Gene Expression Omnibus (GEO; http://www.ncbi.nlm.nih.gov/geoprofiles) using search-terms "Affymetrix and triple negative breast cancer". The GEO-GDS4069 dataset was one of the GEO datasets used for comparison to cell line datasets. GDS4069 included normal, non-basal/luminal, and basal breast cancer samples. Basal-breast cancer samples were all TN aggressive type samples. Hierarchical clustering (HC) analysis was performed using programs available on mAdb.

RNA gene expression levels were examined by converting mRNA to cDNA and analysis of the relative quantities between the different cell lines. For generating cDNA, one microgram of total RNA (from cell lines) was mixed with iScript Reverse Transcriptase (RT) and master mix (BioRad.com) and processed as suggested by the manufacturer. Master Mix included dNTPs, RT buffer and oligo dT primer.

For comparative analysis of the gene expression levels, qualitative polymerase chain reaction (PCR) was performed. GAPDH (control) and TP1 gene primers used for PCR were generated using Primer3 (http://Bioinfo.ut.ee/primer3-0.4.0/primer3). Primer specificity was validated by analysis of the amplicon at UCSC (http://genome.ucsc.edu/cgi-bin/hgPcr?command=start). Primers were synthesized by IDTDNA. PCR was performed by adding 1ul cDNA, 10ul 10X AmpliTaq Gold (AppliedBiosystems), 2ul left/right primers and 7ul water. PCR amplifications were carried out using the following parameters: 95 °C hot start (5 min), 57 °C annealing (30 s), less than 29 cycles, followed by (30 s) at 72 °C for extension. By limiting the number of PCR cycles, one is able to detect log-phase amplification of the PCR products.

PCR products were analyzed on a 1% agarose gel (in Tris Acetate EDTA buffer with ethidium bromide). Gels were visualized and photographed using a trans-UV illuminator.

Immunohistochemistry (IHC) analysis of tissue microarray (TMA) was used to examine the protein levels in tissues formerly diagnosed as triple negative or other subtypes of breast cancers. TMAs contained tissue cores representing 96 clinical patient samples. Antibodies were purchased from Abcam. IHC was performed using the protocol suggested by the manufacturer, inclusive of the antigen retrieval of TMA tissues. To ensure tissue quality, CD31 staining was used as a control. CD31 protein is associated with blood vessels, so positive CD31 staining should localize to vascularity. For interpretation of TP1 results, only core-samples demonstrating positive CD31 staining were used. Protein levels (i.e., intensity of staining) were scored from 0-5 with 5 being the most intense staining or protein level.

RESULTS AND DISCUSSION

With the goal of the current study being to identify and begin validation of genes that might serve as biomarkers to distinguish TN breast tumors, preliminary analysis suggests TP1 might be one such gene. Hierarchical cluster analysis of microarray data show TP1 differentially expressed in MDA MB231 (representing TN) compared to MCF (representing non-TN sample). TP1 appeared down-regulated in MDA MB231 (Figure 1). Similar results were observed when cDNA from the corresponding cell lines were examined following PCR; MDA MB231 transcript levels were lower (Figure 2). Results might appear more dramatic had densitometer analysis (or real-time) been performed, normalizing for GAPDH loading control. Nonetheless, results by both cluster analysis (generated using microarray data) and PCR show down-regulation of TN RNA expression. TP1 and all genes selected for down-stream analysis were required to validate via IHC and PCR.

Genes are only accepted as reliable biomarkers if results of protein and RNA levels agree. With this in mind, protein expression was examined using clinical patient samples that were previously certified (by Pathologists) and analyzed for TN status. TMAs containing 98 different tissue cores were used for this analysis. Some 33% of TN samples on the TMA showed down-regulation when examined using TP1 antibody. An example of the protein staining pattern in non-TN compared to TN sample is given in Figure 3. All of the down-regulated TN samples displayed nearly negative TP1 protein levels. These are only the first set of experiments validating protein expression of TP1. Additional TMAs are being examined to improve the statistical power of the results.

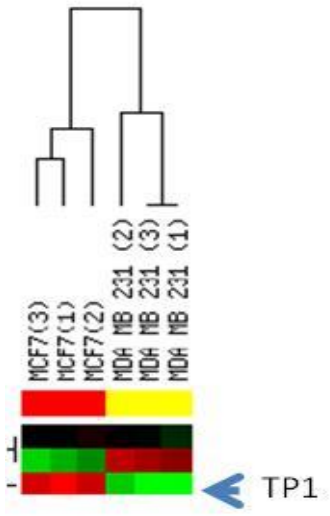

Figure 1. Hierarchical cluster analysis- TP1 is down-regulated in MDA MB231 (TN). Green decreased, red increased levels. Cluster must be performed with 3 or more genes. As a result irrelevant genes included in figure along with TP1.

Functionally, TP1 is a transcription factor. Transcription factors regulate transcription of other genes. Because there was an interest in identifying genes that might serve to drive the carcinogenic process, many of the genes identified as part of this study were processed to allow for identification of

transcription factors; TP1 was only one of those genes. Future studies will show if TP1 is regulated by, or regulates genes identified on the initial 49-list. As for the precise function of TP1, it is not known. It could be that 'loss of gene function' is key to the development of TN phenotype. Future studies here and by other investigators will have to be performed to demonstrate its possible role in TN cancers. Preliminary studies of TP1 are encouraging enough to expand the analysis of TN clinical patient samples and perform functionality studies.

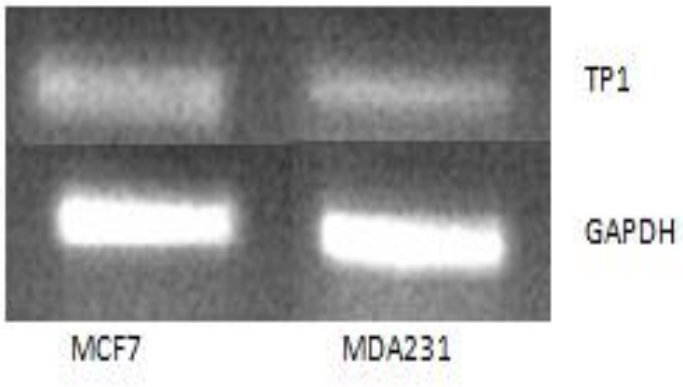

Figure 2. PCR- TP1 is downregulated in MDA MB231 (TN) compare to MCF7 (non-TN).

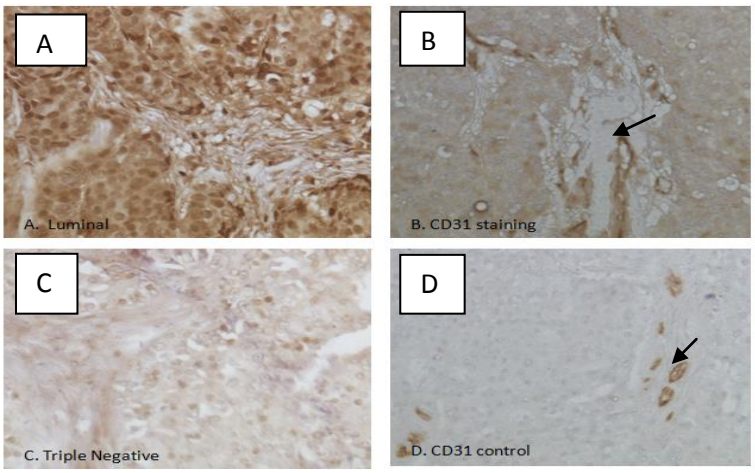

Figure 3. Immunohistochemistry- A: non-TN (positive TP1), B: non-TN (CD31, vessel control), C: TN (negative TP1), and D: TN-CD31 vessel control). Arrows point to CD31 positive blood vessels.

CONCLUSION

Preliminary data showed that Transcription factor 1 displayed promising results for further data analysis. We identified transcription factor 1as a gene that might be suitable as a signature associated with aggressive cancers (i.e., TN). In efforts to determine if the gene was differentially expressed in aggressive compared to less aggressive cancer, we examined the levels of transcription factor 1 in a luminal tumor (less aggressive) compared to a basal (aggressive) tumor. On a transcript level, RNA expression showed down-regulation/ loss of function. Similar to the transcript levels, protein analysis showed protein levels that were also down –regulated in some patient samples. It could be that the mechanism of down-regulation could affect aggressive behavior or metastatic potential.

ACKNOWLEDGEMENTS

This study was supported by Summer Undergraduate Research Program (SURP) of the College of Science and Technology at Texas Southern University. Extended thanks go to Carmen Gonzales, Delon Poole, and Richard North III.

REFERENCES

Sorlie T, Tibshirani R, Parker J, Hastie T, Marron JS. (2003) Repeated observation of breast tumor subtypes in independent gene expression data sets. *Proceedings of National Academy of Science* 100:8418–8423.

Minami CA, Chung DU, Chang HR. (2011) Management options in triple-negative breast cancer. *Breast Cancer* 5:175-199.

www.pantomics.com/TissueArrays/Human/Breast/BRC962.aspx

www.biology-online.org/dictionary/Transcription_factor

A STUDY ON THE COMBINED EFFECTS OF MICROGRAVITY AND SINGLE WALL CARBON NANOTUBES

Mohamed Coulibaly* and Dr. Jade Clement#

Department of Chemistry
College of Science and Technology, Texas Southern University
3100 Cleburne Street, Houston, TX 77004

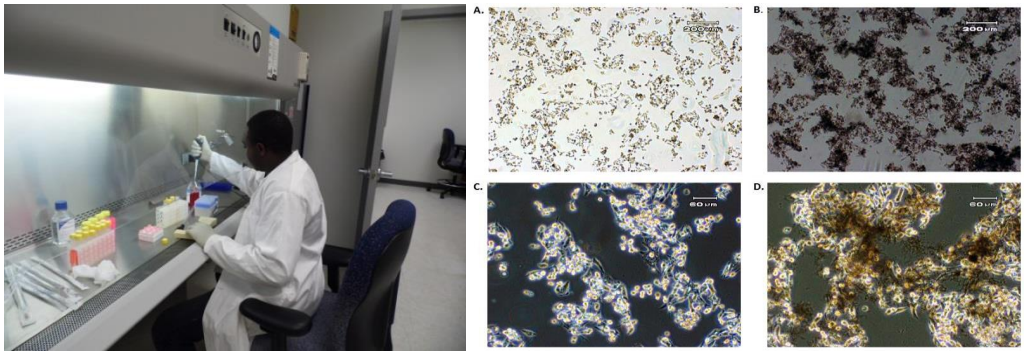

ABSTRACT

Microgravity is a major environmental factor that is hazardous to human health. Rotating Cell Culture Systems (RCCS) are a commonly used method to simulate the microgravity effect on cultured cells. We have compared the proliferation profiles of the HepG2 cells and its derivative cell line obtained by subjecting the cell to simulated microgravity (RCCS) culturing condition for 25 days followed by post microgravity recovery culture for 140 and 168 days, respectively. In a previous cell proliferation assay, we found that HepRC25D-a cell line (the cell line that undergone 140 day recovery post 25 day microgravity exposure) showed overall lower proliferation rates compared to its parental cell line, HepG2. In the current experiment using the XTT cytotoxicity assay, we found that the proliferation rates of the HepRC25D-b cell line (the cell line that had undergone 168 days of recovery culture) were nearly the same as that of its parental HepG2 cell line. In addition, we compared the survival rates of the HepRC25D-b and HepG2 cell lines treated with single wall carbon nanotubes. From our preliminary results on the combined effects of microgravity and carbon nanotubes, we could not definitely conclude if the simulated microgravity experience had rendered the HepRC25D-b cells a significant level of protection against the effects of the single wall carbon nanotubes.

Key words: *MicroRNAs, Cloning, PCR amplification, Double restriction enzyme digestion*

*SURP Fellowship Recipient
#Faculty Mentor

INTRODUCTION

Microgravity is a major hazardous environmental factor in space travel (Leach et al, 1990; Cogoli 1993; Aktov et al, 1992). Most cell types (from bacteria to mammalian cells) are sensitive to the effect of reduced gravity since most of the cells rely on the normal gravity on earth for them to grow and function properly. Microgravity effects on human health have much in common with earthbound health problems related to low physical activity or less mechanical loading associated with the aging population and people suffering from degenerative disorders. Continued research on microgravity effect on human cells will improve our understanding of space environmental response as well as many of our health-related problems (diabetes, osteoporosis, premature aging, etc.) on earth (reviewed by Clement JQ, 2012).

Because of the high cost of space flown experiments, ground-based methods for microgravity simulation have been developed and increasingly used in microgravity research. Ground-based simulated microgravity bioreactors such as the RCCS (rotating cell culture system) bioreactors are a commonly used method to simulate the microgravity effect on cultured cells (reviewed in Cogoli, 1993; Sonnenfeld & Shearer 2002; Sonnenfeld 2005). In a previous publication from our laboratory, we have documented that the microgravity effects on most genes of a human keratinocyte cell line can be recovered and the degree of recovery depends on the time duration of the microgravity exposures as well as the time periods of post exposure recovery (Clement et al, 2008).

Carbon nanotubes have significantly contributed to current nanotechnology development and application. Their small size, great strength, and their ability to conduct electricity and heat make them potentially useful in a wide variety of applications (Iijima 1991; Miller et al, 2005). These nanotubes pose a potential health risk that has yet to be clearly determined. Studies have found that carbon nanotubes may be harmful to living organisms which include pulmonary injury (Chou et al, 2008) and neurological damage (Belyanskaya et al 2010). Rodent studies have shown that inhaled nanotubes can cause fibrosis and inflammation in the lungs similar to asbestos exposure (Morimoto et al, 2011; Kobayashi et al, 2011). In addition, rodent studies have shown that SWCNT can induce reactive oxygen species causing liver damage (Patlolla et al 2011). Pristine nanotubes are perhaps the most hazardous to living organism due to their insolubility and relatively high metal content (such as Fe and Ni) which increase their toxicity (Schipper et al 2008). Some of the effects have partially been ameliorated by functionalizing carbon nanotubes with polyethelene glycol PEG (Heister et al, 2010). However, a recent study has shown that PEG functionalized nanotubes may cause some teratogenic effects in mice (Campagnolo et al 2013). Toward the realization of the full potential of nanotechnology and nanomedicine, it is important to further understand the biosafety nature of the nanomaterials. For safer space travel and further understanding of reduced gravity effects on human cells, it is important to study microgravity effects on human cell models. As a first step to observe the combined effects of microgravity and single wall carbon nanotubes, we performed *in vitro* cytotoxicity assays. The main objectives of current analysis were to test 1) if HepRC25D-b cells, derived from the human liver (HepG2) cells by culturing in simulated microgravity (RCCS) for 25 days would recover after 168 days of normal recovery culture to its pre-exposed parental cell line (HepG2) level in a cellular proliferation time course profile and 2) if the HepRC25D-b cell would response single wall carbon nanotubes in a similar or significantly differently survival proliferation profile compared to that of its parental cell line that has never been exposed microgravity.

METHODS

Cell Culture and Cell Exposure to Single Wall Carbon Nano-tubes (SWCNT)

The human hepatoblastoma cell line (HepG2) was purchased from the America Type Culture Collection. A derivative of the HepG2 cell line, HepRC25D-b, was derived previously by culturing HepG2 cells under simulated microgravity (RCCS, rotating cell culture system) for 25 days, and then cultured at normal gravity for 168 days. Both of the cell lines were cultured at 37^{o}C, 5%CO_2 in DMEM with 10% fetal calf serum. To compare the single wall carbon nanotube toxicity on these two cell lines, each of the two cell lines were grown on 96-well plates side by side together with their single wall carbon nanotube-treated counterparts. The cells were then assayed daily from day-1 to day-10, using the *in vitro* toxicology XTT assay.

in vitro Toxicology Assay

An *in vitro* toxicological study system using human cell lines is a relatively new trend of toxicological approach. We have applied an in vitro cytotoxicity assay as the main approach of this research is to investigate the proliferation rates an microgravity derived cell line in comparison with its parental cell line and to study the effects of the single wall carbon nanotubes on these human liver cell lines, using the *in vitro* cytotoxicity XTT assay system. The XTT *in vitro* toxicology assay system detecting the activities of mitochondrial dehydrogenase of living cells spectrophotometrically. The main

component of the XTT assay is the sodium salt of XTT (2,3-bis[2methoxy-4-nitro-5-sulfophenyl]2H-tetrosolium-5-carboxyanilide inner salt). In living cells, the mitochondrial dehydrogenase reduces the tetrazolium ring of XTT, giving an orange formazan derivative, which is soluble in water. The orange solution is spectrophotometrically measured in a microplate reader at a wavelength of 450 nm (Scudiero et al 1988; Roehm et al 1991). This assay has been shown to be reliable for measuring cell proliferation and viability in response to chemical exposures in transformed and tumor cell lines.

We performed a ten-day long time course XTT assay and followed the same procedure for all the time point processes except for day ten. We discarded the day-ten data due to technical variation. At each time point, the cells grown in a 96-well plate were removed from the incubator and placed into a laminar flow cell culture hood. A volume of 20 μL of the XTT solution (1 mg/mL) was added to each well of a multiwell plate. The cells were then returned to the incubator and incubated for 3 hours. At the end of the 3 hour incubation, the cells were removed and placed in the plate reader (Tecan Microplate Reader) for 1 minute agitation (mixing) and the absorbance at 450 nm and 690 nm (reference wavelength) were measured right after the agitation. The absorbance data were automatically recorded and then analyzed in Microsoft Excel to generate line graphs.

RESULTS AND DISCUSSION

In addition to studying the microgravity effects on cells and genes, we are also interested in if the affected genes and cells can eventually recover to their pre-exposure states. We applied a cell cytotoxicity approach to study the post microgravity recovery effect of a human liver cell line (HepG2). Recently, we used MTT cell proliferation assay in which the key reagent is the MTT, 3-(4,5-dimethylthiazol-2-yl)-2,5-diphenyl tetrazolium bromide, and found that the microgravity derived cell line (HepRC25D-a) displayed a lower overall rate of proliferation profile compared to the parental cell line. We hypothesized that a longer period of recovery culture allows the microgravity exposed cells eventually completely recover.

In the present study, we used a closely related cell line, HePRC25-b, which had undergone four additional weeks of post microgravity recovery period compared to HepRC25D-a. In addition to their proliferation rates, we also compared their survival rates when exposed to single wall carbon nanotubes (SWCNTs). We added the SWCNTs at the time of seeding the cells into the 96-well assay plates so that we could observe whether the SWCNTs exert any inhibitory effects on cell adhesion. Figure 1 shows some photographs of the HepG2 cells cultured in the presence and absence of the SWCNTs. It is noticeable that the SWCNTs formed black aggregates and deposited on the growing cells. The close association of these SWCNT particles may physically interrupt the cellular structures and functions. We

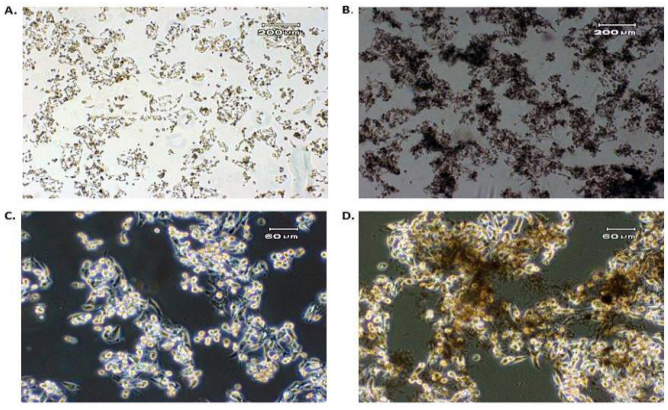

Figure 1. Human liver HepG2 cell line cultured in the presence and absence of the SWCNTs. A and C are lower and higher magnifications of the untreated HepG2 control. B and D are the lower and higher magnifications of the cells cultured in the presence of 50 μg/mL of the SWCNTs.

found that SWCNTs in our test concentrations did not noticeably interfere with cell adhesion whether in treated microgravity derived cell lines (data not shown) or their parental cell lines like HepG2 (Figure 1).

Figure 2 shows the time course experiment for the proliferation profile of the HepRC25D-b (microgravity derived cell line) compared to its parental cell line HepG2, and the survival trends of these cells in the presence of the SWCNTs. In a previous MTT based assay, we found that HepRC25D-a cell line (the cell line that had undergone 140 day recovery post 25 day microgravity exposure) showed a overall lower proliferation rates compared to its parental cell line. In the current experiment using the XTT cytotoxicity assay, we found that the cell proliferation rates of the HepRC25D-b cell line (the cell line that had undergone 168 days of recovery culture) were nearly the same as that of its parental cell line (Figure 2). This result indicated that the microgravity exposed HepRC25D-b cells had nearly completely recovered from the microgravity effect and returned to pre-exposure proliferation characteristics. We chose the XTT assay for the current experiment because it is much simpler in experimental procedure compared to the MTT assay we used in previous experiments.

In addition, survival rates of the HepRC25D-b and HepG2 cell lines treated with SWCNTs were compared. The results do not clearly indicate whether the simulated microgravity experience rendered the HepRC25D-b cells any level of protection against the toxic effects of the SWCNTs, since the proliferation of both cell lines were abrogated throughout the entire time course (Figures 2 and 3). The time course cell survival of the two cell lines was directly compare (Figure 3), even though the proliferation rates were very low for both of the cell lines. The microgravity-exposed cells seemed to have a slightly higher survival rate in days 3 through 5 of the time course, but no definite conclusions can be drawn from Figure 3 and further experiments at various relative dosage levels will be more informative.

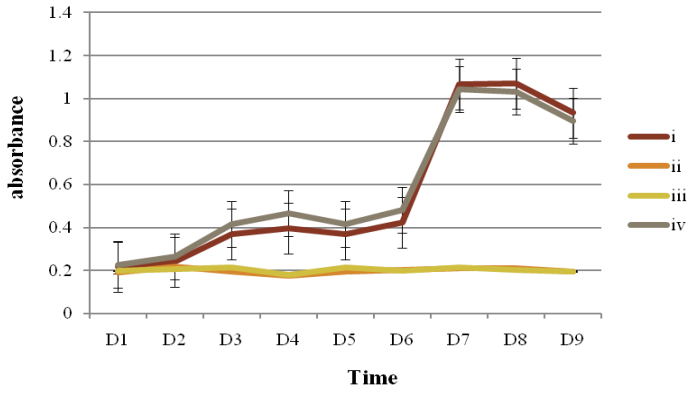

Figure 2. Time course proliferation of HepG2 and HepRC25D-b and their survival trends in the presence of the SWCNTs. i: proliferation curve for HepG2. ii: survival curve for single SWCNT exposed HepG2 cells. iii: survival curve of HepRC25D-b cells exposed to SWCNTs. iv: proliferation curve of the HepRC25D-b cells.

CONCLUSION

The microgravity derived cell line (HepRC25D-b) displayed a proliferation time course profile very similar to its parental cell line (HepG2), suggesting that the microgravity exposed cells had nearly completely recovered from the microgravity effect and returned to pre-exposure proliferation characteristics. Although the preliminary results of exposing these cells to SWCNTs from this experiment are inconclusive, it appeared that microgravity experience might render a slight protection against the toxic effects of the SWCNTs. Much more detailed further studies with various relative doses of the carbon nanotubes, especially at much lower doses of the tested material will provide more definitive information on future studies.

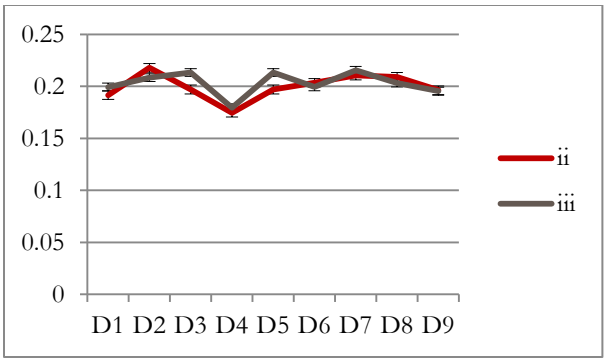

Figure 3. Comparison of cell survival profiles of HepG2 and HepRC25D-b in the presence of the SWCNT. ii: survival curve for SWCNT exposed HepG2 cells. iii: survival curve for cells exposed to SWCNT and HepRC25D-b cells.

ACKNOWLEDGEMENTS

This study was supported by Summer Undergraduate Research Program (SURP) of the College of Science and Technology at Texas Southern University.

REFERENCES

Atkov O. (1992). Some medical aspects of an 8 month's space flight. *Advances in Space Research* 12:343-345.

Belyanskaya L, Weigel S, Hirsch C, Tobler U, Krug HF, Wick P. (2009) Effects of carbon nanotubes on primary neurons and glial cells. *NeuroToxicology* 30:702-711.

Campagnolo L, Massimiani M, Palmieri G, Bernardini R, Sacchetti C, Bergamaschi A, Vecchione L, Magrini A, Bottini M, Pietroiusti A. (2013) Biodistribution and toxicity of pegylated single wall carbon nanotubes in pregnant mice. *Particle and Fibre Toxicology* 10:21-26.

Chou CC, Hsiao HY, Hong QS, Chen CH, Peng YW, Chen HW, Yang PC. (2008) Single-walled carbon nanotubes can induce pulmonary injury in mouse model. *Nano Letters* 8:437-445.

Clement JQ, Lacy SM, Wilson BM. (2008) Gene expression profiling of human epidermal keratinocytes in simulated microgravity and recovery cultures. *Genomics Proteomics and Bioinformatics* 6:8-28.

Clement JQ. (2012) Gene Expression Microarrays in Microgravity Research: Toward the Identification of Major Space Genes, Biotechnology/Book 2, E.C. Agbo, Ed., InTech

Cogoli A. (1993) Space flight and the immune system. *Vaccine* 11:496-503.

Heister E, Lamprecht C, Neves V, Tilmaciu C, Datas L, Flahaut E, Soula B, Hinterdorfer P, Coley HM, Ravi S, Silva P, McFadden J. (2010) Higher dispersion efficacy of functionalized carbon nanotubes in chemical and biological environments. *American Chemical Society Nano* 4:2615-2626.

Iijima S. (1991) Helitcal microtubules of graphitic carbon. *Nature* 354:56-58.

Iijima S. (2002) Carbon nanotubes: past, present, and future. *Physica B* 323:1-5.

Kobayashi N, Naya M, Mizuno K, Yamamoto K, Ema M, Nakanishi J. (2011) Pulmonary and systemic responses of highly pure and well-dispersed single-wall carbon nanotubes after intratracheal instillation in rat. *Inhalation Toxicology* 23:814-828

Leach CS. (1990) Medical considerations for extending human presence in space. *Acta Astronautica* 21: 659-666.

Miller J, Serrato R, Represas-Cardenas J, Kundahl G. (2005) The Handbook of Nanotechnology. John Wiley & Son.

Morimoto Y, Horie M, Kobayashi N, Shinohara N, Shimada M. (2011) Inhalation Toxicity Assessment of Carbon-Based Nanoparticles. *Accounts of Chemical Research* 46:770-781.

Niyogi S, Hamon MA, Hu H, Zhao B, Bhowmik P. (2002) Chemistry of single-walled carbon nanotubes *Accounts of Chemical Research* 35:1105-1113

Patlolla A, McGinnis B, Tchounwou P. (2011) Biochemical and histopathological evaluation of functionalized single-walled carbon nanotubes in Swiss-Webster mice. *Journal of Applied Toxicology* 31:75-83.

Roehm NW, Rodgers GH, Hatfield SM, Glasebrook AL. (1991) An improved colorimetric assay for proliferation and viability utilizing the tetrazolium salt XTT. *Journal of Immunological Methods* 142:257-265.

Schipper ML, Nakayama-Ratchford N, Davis CR, Kam NWS, Chu P, Liu Z, Sun X, Dai H, Gambhirm SS. (2008) A pilot toxicology study of single-walled carbon nanotubes in a small sample of mice. *Nature Nanotechnology* 3:216-221.

Scudiero DA, Shoemaker RH, Paull KD, Monks A, Tierney S, Nofziger TH, Currens MJ, Seniff D, Boyd MR. (1988) Evaluation of a soluble tetrazolium/formazan assay for cell growth and drug sensitivity in culture using human and other tumor cell lines. *Cancer Research* 48:4827-4833.

Sonnenfeld G, Shearer WT. (2002) Immune function during space flight. *Nutrition* 18: 899-903.

Sonnenfeld G. (2005) Use of animal models for space flight physiology studies, with special focus on the immune system. *Gravitational Space Biology Bulletin* 18:31-35.

CONTINUOUS CALCULUS VERSUS DISCRETE CALCULUS

FranChell Davidson* and Willie E. Taylor#

Department of Mathematics
College of Science and Technology, Texas Southern University
3100 Cleburne Street, Houston, TX 77004

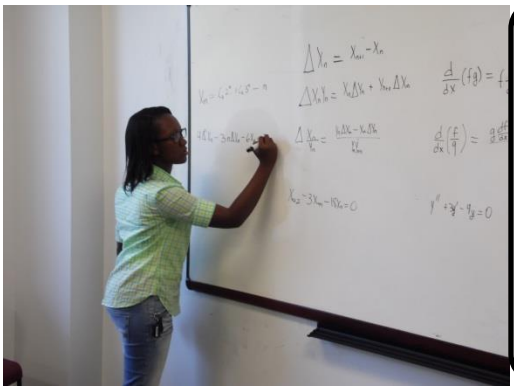

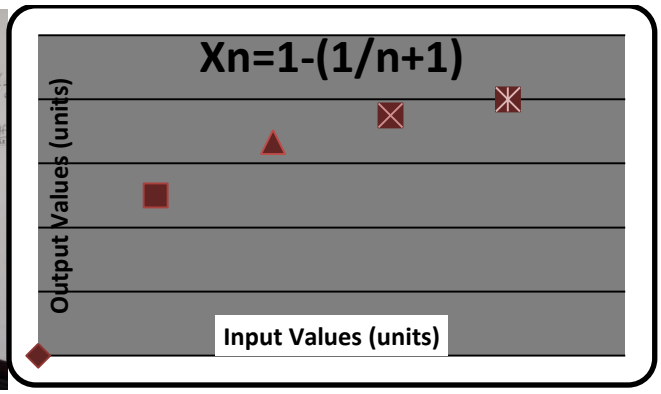

ABSTRACT

This project studied calculus from both the continuous and discrete points of view. While continuous functions are defined over intervals, discrete functions are sequences which are defined on inductive subsets of the integers. Various concepts from single variable calculus were studied together with their discrete analogues. Finally, methods for finding solutions of both linear differential equations and linear difference equations were investigated.

Key Words: *continuous calculus, discrete calculus, linear differential equation*

*SURP Fellowship Recipient
#Faculty Mentor

INTRODUCTION

This work investigates Calculus from the Continuous and Discrete points of view. Particularly, studying the solutions for the linear differential equations and linear difference equations are studied as well as discrete analogues of various formulas.

RESULTS

For a mathematics major it is important to understand the concept of a function. For centuries functions have been used to model natural phenomena and various processes, consequently, functions are extremely important. Continuous functions use intervals of numbers as their domains, while discrete functions use various subsets of the integers. Differential calculus studies limits, continuous functions, derivatives, and their properties. The difference calculus deals with discrete functions or sequences. The discrete analogue of a derivative is a difference. The modeling of various processes and natural phenomena use differential equations. The discrete analogue of a differential equation is a difference equation. Methods of solving these equations are similar.

Continuous Calculus vs. Discrete Calculus

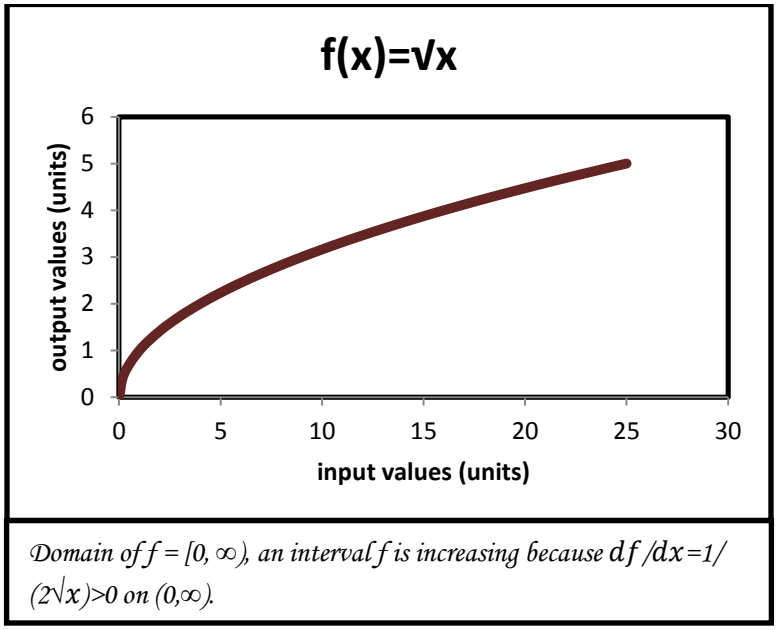

Figure 1. A graph showing continuous calculus.

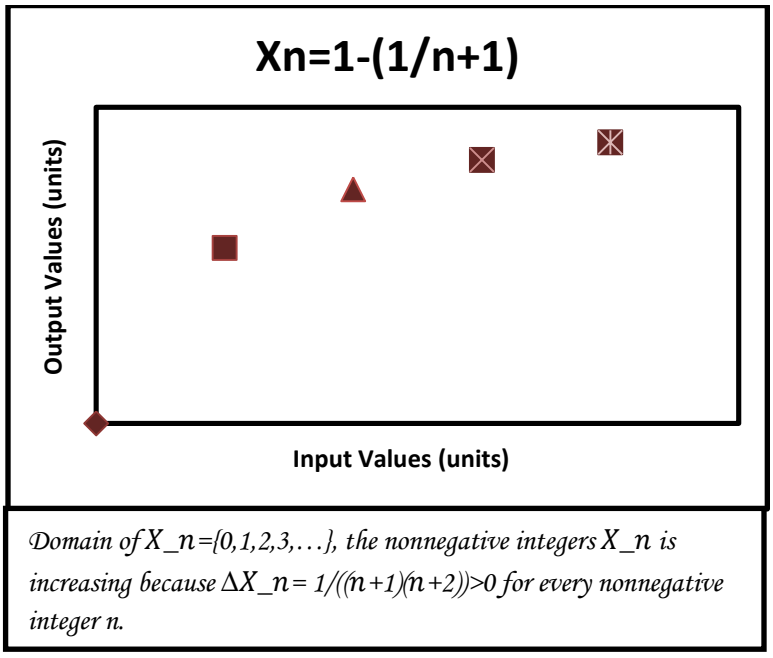

Figure 2. A graph showing discrete calculus.

Solving a second order differential equation

Given the second order differential equation y”− 3y’ + 2y = 0, the assumption is made that y = e^{mx}, Therefore, it is understood that y’ = me^{mx} and y’’ = m^2e^{mx}. These assumptions are substituted into the original differential equation. This gives the equation $m^2e^m - 3me^{mx} + 2e^{mx} = 0$. Since $e^{mx} \neq 0$, everything

is divided by e^{mx}, resulting in the characteristic equation $m^2 - 3m + 2 = 0$. This equation can now be factored and solved for the roots which are m = 2 and m = 1. The roots are used to write the basic solutions of $y_1 = e^{2x}$ and $y_2 = e^x$. The general solution is $y = C_1e^{2x} + C_2e^x$. This is a linear combination of y_1 and y_2.

Solving a second order difference equation

Given the second order difference equation $X_{n+2} - 6X_{n+1} + 9X_n = 0$, the assumption is made that $X_n = t^n$. Therefore, it is understood that $X_{n+1} = t^{n+1}$ and $X_{n+2} = t^{n+2}$. These assumptions are substituted into the original difference equation. This gives the equation $t^{n+2} - 6t^{n+1} + 9t^n = 0$. Since $t^n \neq 0$, everything is divided by t^n now resulting in the characteristic equation $t^2 - 6t + 9 = 0$. This equation can now be factored and solved for the roots. However, this equation has a repeated root of $t = 3$. Since, this is the case the basic solutions will be $U_n = 3^n$ and $V_n = n3^n$. The general solution is $X_n = C_13^n + C_2n3^n$, which is a linear combination of U_n and V_n.

Continuous Calculus vs. Discrete Calculus

Differential Equations	Difference Equations
E_1) $y'' - 3y' + 2y = 0$	e_1) $X_{n+2} - 3X_{n+1} - 10X_n = 0$
solution: $y = C_1e^{2x} + C_2e^x$	solution: $X_n = C_15^n + C_2(-2)^n$
E_2) $y'' - 6y' + 9y = 0$	e_2) $X_{n+2} - 6X_{n+1} + 9X_n = 0$
solution: $y = C_1e^{3x} + C_2xe^{3x}$	solution: $X_n = C_13^n + C_2n3^n$
E_3) $y'' + 4y = 0$	e_3) $X_{n+2} + X_n = 0$
solution: $y = C_1\sin 2x + C_2\cos 2x$	solution: $X_n = C_1\cos(n\pi/2) + C_2\sin(n\pi/2)$

CONCLUSION

Discrete Calculus and Continuous Calculus are very different. But finding solutions of differential equations and difference equations use similar techniques. An effort to unify the two kinds of calculus has started and is known as time-scale calculus. Dynamic equations play the role of differential and difference equations. Time-scale calculus is the integration of discrete and continuous calculus. Therefore, a complete understanding of discrete calculus and continuous calculus is useful in order to advance further in the field of mathematics.

ACKNOWLEDGEMENTS

This study was supported by Summer Undergraduate Research Program (SURP) of the College of Science and Technology at Texas Southern University.

USING PASSIVE RADIO-FREQUENCY IDENTIFICATION (RFID) AS A COMMUNICATION TOOL FOR DRIVERS' AWARENESS OF RISKS

Damon Hall* and Fengxiang Qiao#

Department of Transportation Studies
College of Science and Technology, Texas Southern University
3100 Cleburne Street, Houston, TX 77004

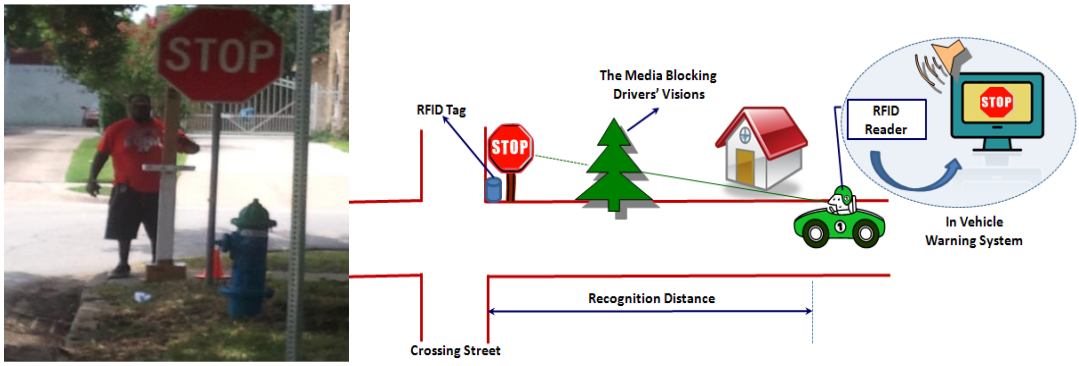

ABSTRACT

Stop signs at un-signalized intersections can easily be blocked by trees and other obstacles, which is a threat to safety. One of the practical solutions is to use the radio-frequency identification (RFID) device to automatically identify and track the presence of stop signs by attaching tags to or nearby those signs. The RFID readers receive signals from tags through electromagnetic fields to transfer information. A program to trigger the RFID can be compiled in the computer and the tags can be passive ones, which means they do not have their own power sources. The reader powers up the passive tags through emitted radio signals. The tags respond by sending back radio signals with the predefined ID information coded in the tags. As the receipt of signals from tags to readers really depend on the media in between the readers and the tags. In this research, the impacts of tag placement on signal transmission were tested. Working rages of 10 tags were tested, which is a good reference to the design of reliable RFID based smart guide singing system so as to reduce conflict events at un-signalized intersections.

Key Words: *Stop sign, RFID, Vehicle-to-infrastructure wireless communication, Intelligent transportation system*

*SURP Fellowship Recipient
#Faculty Mentor

INTRODUCTION

The RFID can be used to help drivers who face blockage on roadways and intersections (Gifford, 2006, Qiao and Yu, 2007). In the future it would be good to see RFID being used at block sites to ensure the safety of drivers and also to decline the number of car accidents that occur due to blockage of stop signs. Roadways account for a significant amount of crashes that occur in the U.S. In California on average 1.5 crashers per year occur at unsignalized intersections in rural areas, and 2.5 crashes per year occur at unsignalized intersections in urban areas (Bauer and Harwood, 1996). The RFID can be a feasible solution for drivers when it comes to roadways. It is counterintuitive that crashes are so concentrated at intersections since intersections take small portion of total trips within the entire transportation systems. One of the reasons is that at intersections, there are more traffic conflict points than on normal roadway segments, and sight distances at intersections are further constrained by obstacles such as trees, while drivers need to watch additional traffic from crossing streets (AASHTO, 2004). Many

crashes at unsignalized intersections are related to turning maneuvers. Left and right turn lanes remove vehicles waiting to turn from the through-traffic stream, thus reducing the potential for rear-end crashes

Qiao et al. (2012) and Qiao et al. (2013) proposed a RFID Based Smart Guide Signing System (Figure 1). The radio frequency (RF) receiver(s) are equipped inside the vehicles to transmit wireless signals to roadside tag(s) through wireless communication channels. This data will be further recognized by an in-vehicle signal processing, monitoring and display system, which will convey the represented message (e.g., STOP, YIELD, 30 MPH speed limit) to drivers through on-board display system or in-vehicle audio system. In the test by Qiao et al. in 2013, an active RFID system was used for the smart guidance system. Due to the too long working ranges (normally 700ft to 1.5 mile), this kind of smart guidance system may have some limitations. In this research, the research team is trying to seek for the possibility to use the passive RFID system for an even practical smart guidance system.

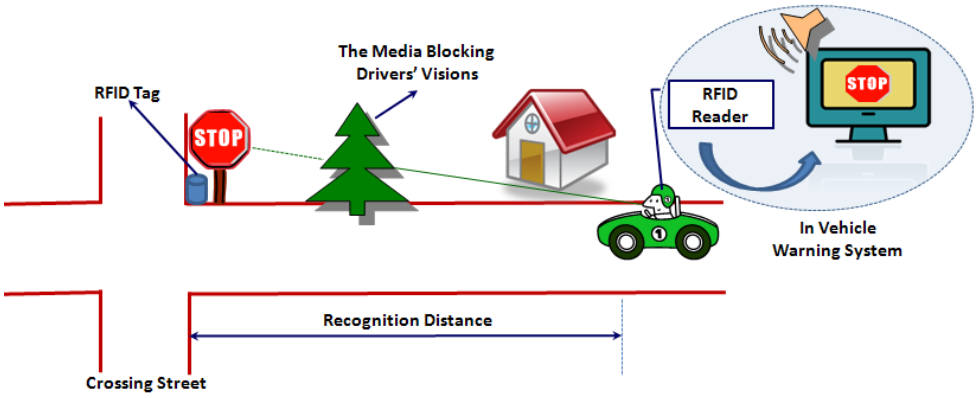

Figure 1. Illustration of a RFID based smart guide signing system (Adapted from Qiao et al, 2012 and Qiao et al, 2013).

Methods

The materials used in this research include: (1) a passive RFID system with one receiver and 10 tags (Figure 2); (2) one pair of "Talkabout" that helps the test assistants to communicate with each other; (3) a computer to read the information from RFID receivers through proper connections with RFID system and driven by a dedicated software by the manufacturer of the RFID system; and (4) an inverter that supplies power to the RFID system and associate computer when the tests are inside vehicles (Figure 3).

Figure 2. White rectangular receiver of the passive RFID system with connection cable to computer via USB port and a power adaptor for the operation of the receiver.

The method to construct a passive RFID based vehicle to infrastructure (V2I) system is similar to the one that Qiao et al. (2012) and Qiao et al. (2013) proposed in Figure 1. To eliminate the interferences among tags for different intersections and/or purposes within the detection range, our system uses a passive RFID system with a relative shorter range of detection. The detection range should cover the horizontal section of the roadway, plus a certain distance between the tags and the roadway edge. In this case, the tag in Figure 1 should be moved from under the STOP sign to where the "recognition distance" is warranted, which is about the location where the vehicle in Figure 1 is.

Figure 3. Inverter that helps to supply power from vehicles to the RFID system and associate computer when the tests are conducted inside vehicles.

The test was conducted in the trailer area in front of the Innovative Transportation Research Institute (ITRI) at TSU (Figures 6-7). One assistant holds a tag coming from far end towards the receiver, which is placed on a desk together with a connected computer. Once the tag signal is detected by the receiver and displayed on the computer, the assistant measures the distance between the tag and the receiver using a rolling ruler.

There are ten tests for each tag so as to eliminate the measurement errors. The same procedure repeats for ten times as there are a total of ten tags tested. The tested distance are logged into an excel spreadsheet for further data process.

RESULTS AND DISCUSSION

The test results are listed in Table 1. For the ten tested tags with ten tests each, the average working range of RFID tag is 154.4 ft with a standard deviation of 21.8. The average detection range for each tag various from 109.7ft to 184.7ft. For a single test, the minimum detection range is 71.5ft, and the maximum detection range is 206.4ft.

The detected working range is sufficient enough for the detection of a roadside traffic sign or other information from a coming vehicle driving along a roadway as in most cases, the road width is normally less than the minimum range from the test (71.5ft). To further analyze the coverage of the detection range over roadway lanes, it is necessary to check the standardized lane width in the national design manual.

The American Association of State Highway and Transportation Officials (AASHTO, 2004) provides guidance for widening lanes through horizontal curves to provide for the off-tracking requirements of large trucks. Lane width does not include shoulders, curbs, and on-street parking areas. Table 2 lists the ranges of lane widths for various types of roadways by AASHTO (2004). Due to the special needs on merging and safety, the width for one lane on ramps ranges from 12ft to 30ft. Since there is normally only

one to two lanes on each ramp, the total lane width should be 24ft to 60ft. Considering about the additional width on shoulder lanes, the shortest RFID detection range (71.5ft) is already sufficient.

For other roadway types including freeway, arterial road, collectors and local streets, the maximum lane width is 12ft for both rural and urban roadways (see Table 2). The minimum working range (71.5ft) can cover about 6 lanes. In the case of the need to extend the working range of the RFID system, two tags can be placed one each end of the roadway. This will double the working range for receivers inside the vehicles to detect necessary information from tags.

Each tag has its unique code that can be detected by the receivers inside vehicles, it would be very easy to figure out which tag is for which bound in the case that the roadway has two directions and there is a need to place tags for each direction. Besides, the detection system (on the receiver side) can combine the use of Global Positioning System (GPS). In this case, the identification and nature of tags can be further figured out by the system.

Table 1. Test results of the working ranges of 10 tags related to the RFID receiver.

			Test										Total	Average (ft)
			1	2	3	4	5	6	7	8	9	10		
Tag	1	ft	110	115	193	167	94	153	150	146	164	166	1458	146.3
		in	8	9	6	11	8	1	0	2	7	4	56	
	2	ft	164	193	158	137	141	153	166	157	144	160	1573	157.8
		in	4	9	10	4	6	1	8	2	0	11	55	
	3	ft	159	179	180	161	179	205	145	162	171	176	1717	172.1
		in	3	0	11	8	1	3	4	8	7	8	53	
	4	ft	170	159	171	163	171	160	206	187	186	167	1740	174.5
		in	11	5	7	8	6	0	5	6	0	10	58	
	5	ft	145	152	105	91	97	94	101	112	92	104	1093	109.7
		in	8	3	9	1	6	3	4	8	0	8	50	
	6	ft	119	121	135	157	164	186	144	114	157	201	1498	150.1
		in	3	1	3	1	7	4	8	7	0	0	34	
	7	ft	192	168	205	181	176	193	180	185	187	175	1842	184.7
		in	7	11	10	4	2	9	8	1	3	6	61	
	8	ft	182	165	188	178	202	198	155	121	115	115	1619	162.3
		in	6	10	0	1	6	7	1	9	7	3	50	
	9	ft	123	135	151	152	153	168	130	134	106	71	1323	132.8
		in	4	10	11	0	10	11	0	3	6	6	61	
	10	ft	156	194	143	157	169	144	145	124	157	141	1530	153.5
		in	9	8	8	5	0	7	10	2	6	0	55	

The above discussion proves that the tags (which should be placed on the roadside) can be properly detected or read by the RFID receiver (which should be placed inside a vehicle) accurately. This passive RFID based smart guidance system can be used and put in affect. The earlier and correct detection of a traffic sign that is blocked by obstacles would definitely increase the safety of all involved vehicles in the surrounding area. This will also reduce the chance of traffic violations such as running STOP/YIELD sign. The on time warning of a traffic sign will enable drivers to reduce the vehicle speed at a comfortable deceleration rate, which is associated with less vehicle emissions and thus improves air quality. The RFID

system properly guides vehicles to smoothly pass intersections. This will also help reduce travel time and congestion, and contribute to the efficiencies of transportation system.

Table 2. Range for Lane Width.

Type of Roadway	Rural		Urban	
	US (feet)	Metric (meters)	US (feet)	Metric (meters)
Freeway	12	3.6	12	3.6
Ramps (1-lane)	12-30	3.6-9.2	12-30	3.6-9.2
Arterial	11-12	3.3-3.6	10-12	3.0-3.6
Collector	10-12	3.0-3.6	10-12	3.0-3.6
Local	9-12	2.7-3.6	9-12	2.7-3.6

(Source: AASHTO, 2004)

CONCLUSION

In this paper the concept of the passive RFID is presented as a tool that can read long distance and help drivers that face roadways blockage. There were important factors that affected the quality performance of the passive tags that were analyzed and tested. The results show that the RFID is sufficient for long range reading. The test results showed high dependency on the nature of the employed RFID systems.

ACKNOWLEDGEMENTS

This study was supported by Summer Undergraduate Research Program (SURP) of the College of Science and Technology at Texas Southern University. This study was also supported by the Tier 1 University Transportation Center TranLIVE, the National Science Foundation (NSF) under grants #1137732, and the Innovative Transportation Research Institute at TSU. The assistants from TSU undergraduate students Kevin Rodriguez and Deyanira Rangel during field tests, and the helps from undergraduate students Mark Etim and Emmanuel Ogbeh, and graduate students Xiaobing Wang are also appreciated.

REFERENCES

American Association of State Highway and Transportation Officials (2004). A Policy on Geometric Design of Highway and Street, 5th Edition.

Bauer KM, Harwood DW. (1996) Statistical models of at-grade intersection accidents. Report No. FHWA-RD-96-125, Federal Highway Administration.

Gifford J. (2006). RFID Applications in Transportation Operations. Presented at Research Opportunities in Radio Frequency Identification (RFID) Transportation Applications Conference, October 17-18.

Qiao F, Yu L. (2007) Potential Applications of Radio Frequency Identification (RFID) in Transportation Operation and Intelligent Transportation System (ITS), Proceedings of The 4th International Conference on Cybernetics and Information Technologies, Systems and Applications: CITSA 2007, jointly with The 5th International Conference on Computing, Communications and Control Technologies: CCCT 2007, Orlando, Florida, USA, July 12-15.

Qiao F, Yu L, Fatholahzadeh R, Yuan X. (2012) Smart Guide Signing System Using RFID as an Intelligent Sensor. Proceedings of the ASCE Earth Space Conference, Hawaii, April.

Qiao F, Wang X, Yu L, Jia J. (2013) Using RFID to Improve Drivers Awareness of STOP Sign at Unsignalized Intersections. Proceedings of the 92nd Transportation Research Board Annual Meeting, Paper number 13-1585, Washington DC, January .

BIO ELECTROMAGNETISM: EFFECTS OF ELECTROMAGNETIC ON LIVING TISSUES, CELLS, AND ORGANISMS

Kanees Khan* and Graham Thomas#

Department of Electronics Engineering Technology
College of Science and Technology, Texas Southern University
3100 Cleburne Street, Houston, TX 77004

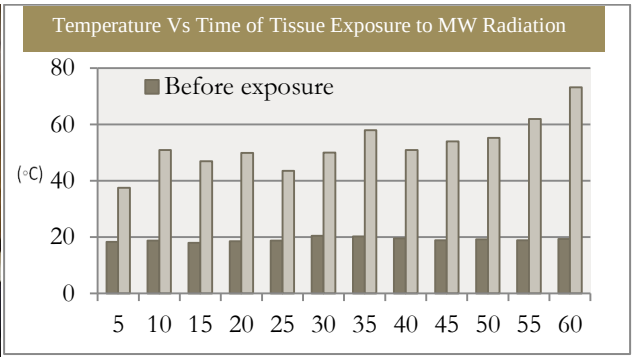

ABSTRACT

There are possible hazardous health effects of exposure to electromagnetic radiation emitted from mobile phones on the human body. The effect is more pronounced if phone is kept in pocket or near testicular organs. Present review examines concerns of radiation interaction on biological tissue. Such radiation could be harmful and cause mutagenic changes in reproduction pattern and leads to infertility, decreased sperm count, enzymatic and hormonal changes, DNA damage, and apoptosis formation. Exposure to high power microwave radiation could also damage biological tissues such as skin. A one dimensional multi-layer model is presented to characterize skin temperature rises and burn processes resulting from skin exposure to microwaves radiation. The skin tissue exposure to microwave radiation was predicted depending on blood perfusion rate, thermal conductivity, power density, and exposure time. The research will utilize Penne's equation and Fourier Law to calculate the amount of heat transferred to the tissue sample. In our research we are going to look at the effects of microwave radiation on skin tissue by looking at the rising temperature based on time exposure to microwave radiation. In order to measure the temperature due to radiation we will use microwave so it will give strong blast of microwave energy to flesh (pork). The reasons for pork flesh because it has the same consistency as human flesh. We are using the tissue for investigating our hypothesis. Data collected suggest the radiation caused the temperature of tissue to increase from an average room temperature of 19.1 °C to 73.2 °C. The range of temperature was 37.5 °C to 73.2 °C. The first sample was heated for 5 seconds and time exposure of sample to microwave radiation increase by intervals of 5 seconds up to 60 seconds for final sample.

Key Words: *electromagnetic radiation, microwave radiation, skin damage*

*SURP Fellowship Recipient
#Faculty Mentor

INTRODUCTION

Bio-Electromagnetism is the study of the interaction between electromagnetic fields and biological creatures. The study of Bio electromagnetics include electrical or electromagnetic field produced by living cells, tissue or organisms. Michael Faraday was the scientist who contributed to the fields of electromagnetism. Michael Faraday discovered the electromagnetic induction on the magnetic field around a conductor carrying a direct current, which established the basis for the concept of the electromagnetic fields. Bio Electromagnetism is a discipline that examines the electric or electromagnetic effects that arise in biological tissues such as the behavior of excitable tissue, the magnetic field at and

beyond the body, the response of excitable cells to electric and magnetic field stimulation, and the essential electric and magnetic properties of the tissue.

Research currently taking place investigates the hazards of electromagnetic field on living tissue or cells. The rapid development of wireless communication technology and the widespread use of mobile phone has become common device in society. These devices emit some form of electromagnetic radiation. Several studies have recommended that men should not carry mobile phones in their front trouser pocket. Exposure to mobile phone signals or storage of mobile phone close to the testes affects sperm counts, mortality, viability, and structure." (Kesari, Kumar, Nirala, Siddiqui, &Behari, 2012). In the study of males attending an infertility clinic in Poland, Wdowiak found an increased percentage of sperm cells of abnormal structure and a decrease in sperm mobility associated with the duration of exposure to mobile radiations. Research also suggests that microwaves radiation from mobile phone may include chromosomal instability and lead to increased cancer risk. Such radiation could be harmful and cause mutagenic changes in reproduction pattern and leads to infertility, decreased sperm count, enzymatic and hormonal changes, DNA damage, and apoptosis formation. Research also suggests that microwaves radiation from mobile phone may include chromosomal instability and lead to increased cancer risk as shown in Figure 1.

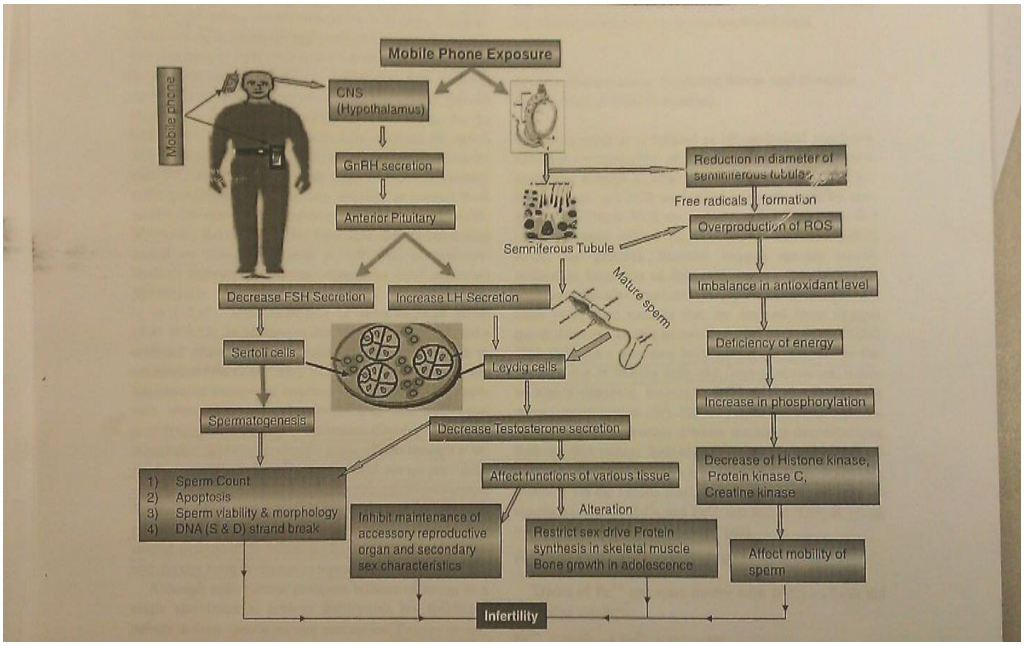

Figure 1. Mobile phone Exposure (Adapted from Kesari et al. 2012).

Health concerns regarding potential hazards due to human exposure of microwaves radiation have been growing. It is therefore necessary to develop proper standards, which could definitely determine acceptable as well as dangerous doses of exposure for humans or other biological tissues. Radar and radar communication devices, navigation equipment, medical devices, weapon detection devices, industrial heating devices, smart weapons, laser surgery equipment, and microwaves ovens are increasingly using high power microwave sources. This forces scientists to focus on possible related health risk for those working with these devices. Exposure to microwaves at sufficiently high intensities produces a perceptible increase in tissue temperature, and the energy absorbed by an organism depends on frequency, power, and exposure time. In this research we are going to look at nature of electromagnetic radiation, propagation of electromagnetic radiation, and source of electromagnetic radiation, such as microwaves. Microwaves with a wavelengths ranging from as long as one meter to as short as one millimeter with

frequencies between 300 MHz (0.3 GHz) and 300 GHz "The penetration depth of microwaves is small and the heating takes place near the body surface at the skin"(Ozen, 2003).

At high-power levels it becomes even more important to quantify the safety limits related to a specific absorption and thermal hazards. Thermal wave is a sound wave in a solid which has a short wavelength. A thermal wave model of bio-heat transfer was used to analyze heat and burn injury of tissues exposed to microwave radiation. One dimensional multi-layer model is presented to characterize skin temperature rises and burn processes resulting from skin exposure to microwaves. The researcher will utilize Penne's equation and Fourier Law to calculate the amount of heat transferred to the tissue sample. In this research we are going to look at the effects of microwave radiation on skin tissue by measuring and recording the rising temperature based on time exposure to microwave radiation. In order to measure the temperature due to radiation we will use microwave (Owen, 700Watts) so it will give strong blast of microwave energy to flesh (pork). The reasons for pork flesh because it has the same consistency as human flesh. We used dead tissues for investigating our hypothesis.

METHODS

First the researcher collected twelve organic tissues and measures the room temperature of the pork flesh. After recording the room temperature of pork flesh the researcher use microwave (Ovwn 700Watts) to expose the each individual organic tissue to microwave radiation. The first sample was heated for 5 seconds and time exposure of sample to microwave radiation increase by intervals of 5 seconds up to 60 seconds for final sample. Data collected suggest the radiation caused the temperature of tissue to increase from an average room temperature of 19.1 °C to 73.2 °C (Shown below Table 1). The researchers observed each tissue sample in microscope device and draw the resulted cell structure (shown in figure 1-1). As been notice that the cell structure gradually changed from being a regular cell in to the burn and breakage of tissue as exposure to microwave radiation increased from 5 to 60 sec. The reason for usage of short time period exposure to microwave radiation is to represent the low dose radiation exposure and the long time period to represent the long term exposure to microwave radiation on biological tissues.

In order to calculate the heat observe by the tissue sample Fourier Law was used. Fourier Law equation is shown below.

$$\rho C\tau \frac{\partial^2 T}{\partial t^2}[\tau W_b C_b+\rho C]\frac{\partial T}{\partial t} - W_b C_b (T_b-T) - k\nabla^2 T = Q_r$$

ρ = Density [kg/m^3]
C = Specific heat [J/kg °C]
k = Thermal condition [W/m °C] of tissue
T= Tissue temperature [°C]
t = Time (sec)
C_b = Heat of blood
W_b = Blood perfusion rate [kg/m^{3}s]
T_b = Artery temperature [°C]
τ = Thermal relaxation time

RESULTS AND DISCUSSION

The data (Table 1) indicate that the radiation increased the temperature of the pork tissues from the average room temperature (19.1 °C) to 73.2 °C after 60 seconds of exposure. The range of temperature after the exposure to microwave radiation for 5 to 60 seconds was between 37.5 °C and 73.2 °C.

The graph below shows the observation and examination of difference between before and after exposure of microwave radiation (Figure 2). Before exposure of microwave radiation the sample (pork flesh) temperature is constant in a range of 18.4 to 19.4 ºC and after exposure to microwave radiation temperature began from 37.5 °C at 5sec and rises up to 73.2 °C at 60 sec. The huge changes in the increase of temperature lead heat transfer to increase from 18.68 °C to 126 °C (Figure 3) cause a major burn and brake down to the sample tissue. These results conclude that high amount of microwave radiation in short period of time are similar to exposing living tissue to a low dose of microwave radiation for long period time could damage the sample tissue will be similar to human tissue.

The sample was examined under a microscope before exposure to the microwave radiation. As shown

Table 1. Measurement of heat effect due to microwave (MW) radiation.

	Measurement of heat effect due to microwave (MW) radiation											
time (sec)	5	10	15	20	25	30	35	40	45	50	55	60
before exposure (°C)	18.4	18.8	18.8	18.6	18.8	20.5	20.3	19.6	18.9	19.2	18.9	19.4
after exposure (°C)	37.5	51	47	49.9	43.6	50.1	58	51	54	55.3	62	73.2
Heat Observe (kJ)	18.7	59.2	50.9	56.8	35.8	47.1	73.2	54.8	68.1	70.5	93.4	126

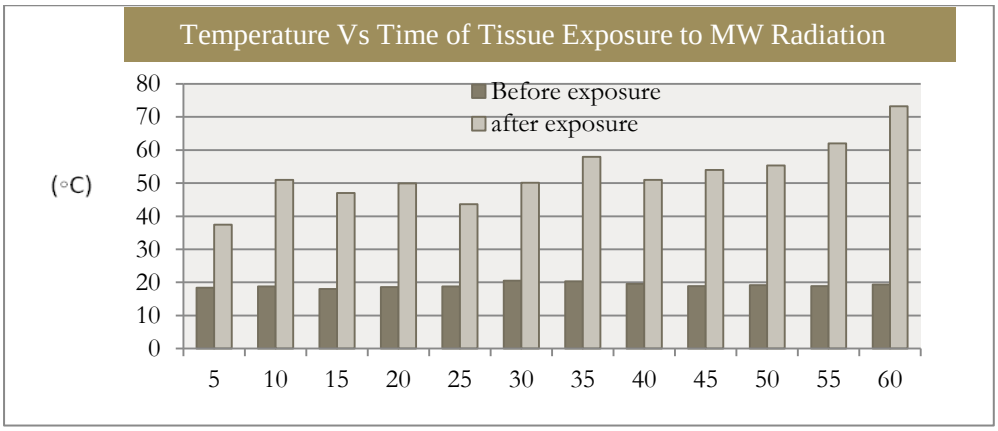

Figure 2. Temperature vs. Time of Tissue Exposure to Microwave (MW) Radiation.

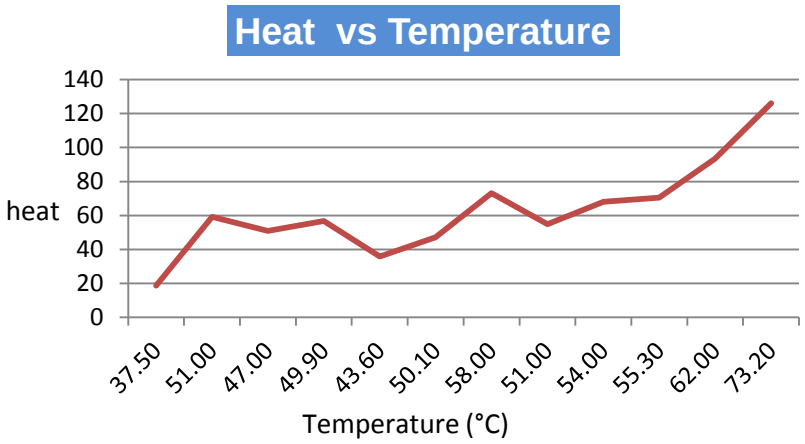

Figure 3. Heat vs. Temperature

in Figure 4, the unexposed cells are very compacted and regularly shaped but the exposed cells seem to be dispersed and irregularly shaped. This observation is even more pronounced as each successive sample is exposed to the radiation for longer time periods. See below for diagram of cell structure before and after exposure. As shown in Figure 4, the cell gradually change from a normal structure of regular cell into the burn an breakage to the cell structure as the microwave radiation increased from 5 sec to 60 sec.

CONCLUSION

Health concerns regarding potential hazards of human exposure to microwaves radiation have been growing. It is therefore necessary to develop proper standards, which can definitely determine acceptable

exposure to humans. A thermal wave model of bio-heat transfer was used to analyze heat and burn injury of tissues exposed to microwave radiation. Every successive increase in time caused a corresponding increase in temperature was observed which indicated that heat was transferred to the samples from the microwave radiation. The heat absorbed by the tissue samples caused severe degradation of the cell structure of the samples. These results can possibly be an indication that long term exposure of the human tissue to electromagnetic radiation can cause irreversible damage to sensitive cell and tissue structure. On the other hand the rapid development of wireless communication technology and the widespread use of mobile phone has become common device in society. These devices emit electromagnetic radiation.

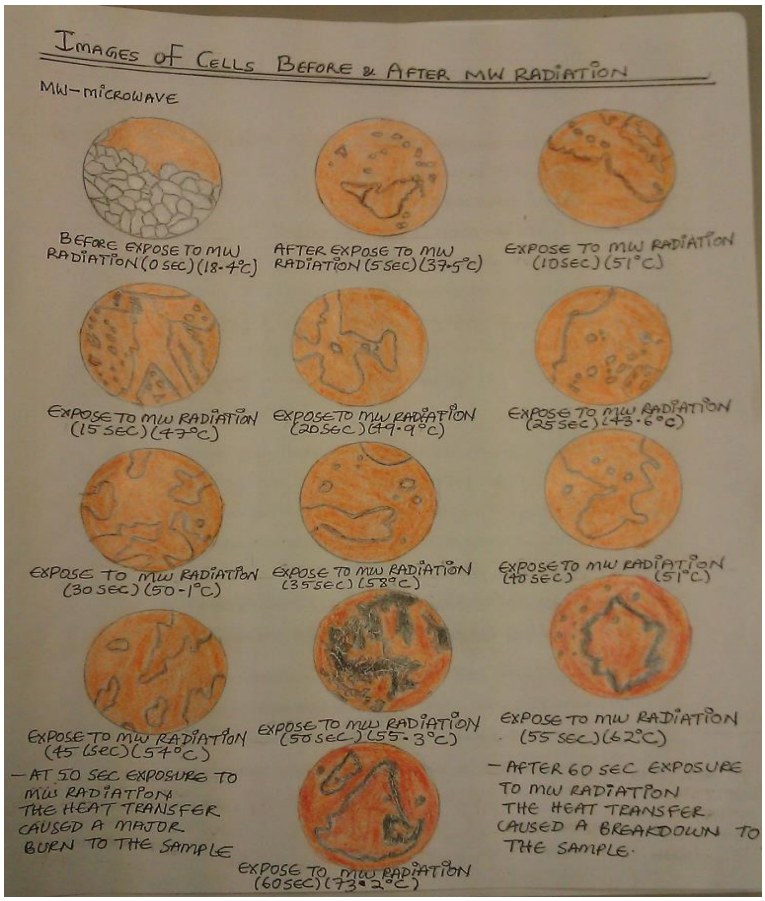

Figure 4. Results of cell structure changes after the exposure to microwave radiation.

ACKNOWLEDGEMENTS

This study was supported by Summer Undergraduate Research Program (SURP) of the College of Science and Technology at Texas Southern University.

REFERENCES

Kesari, Kavindra Kumar, et al. (2013) Biophysical Evaluation of Radiofrequency Electromagnetic Field Effects on Male Reproductive Pattern. *Cell biochemistry and biophysics* 65:85-96.

Ozen, Sukru, Selcuk Helhel, and Suleyman Bilgin. (2011) Temperature and Burn Injury Prediction of Human Skin Exposed to Microwaves: A Model Analysis. *Radiation and environmental biophysics* 50:483-439.

Liu Y, Liang Z, Yang Z. (2008) Computation of electromagnetic dosimetry for human body using parallel FDTD algorithm combined with interpolation technique. *Progress In Electromagnetic Research* 82:95-107.

A STUDY ON THE COMBINED EFFECTS OF MICROGRAVITY AND BISPHENOL A ON HUMAN LIVER CELLS

Ray Mbonu* and Jade Clement#

Department of Chemistry
College of Science and Technology, Texas Southern University
3100 Cleburne Street, Houston, TX 77004

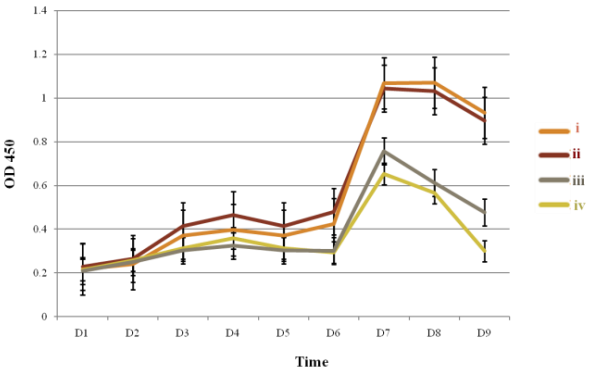

ABSTRACT

The existence of Bisphenol A (2,2-bis[4-hydroxyphenyl]propane, BPA) in the environment is a major public health concern. BPA can be absorbed when ingested, inhaled, or through the skin and is detectable in 90% of the U.S. population. BPA effects on cells and organism vary in severity and modes of action, especially when different doses are applied. Microgravity is a major space environmental factor that is hazardous to human health. In this research report, we summarize our experimental observations on the toxicity of bisphenol A on human liver cells that had recovered from an experience of simulated-microgravity for 25 days (HepRC25D-b) versus the parental cell line (HepG2) that has never been exposed to simulated microgravity. We performed time-course XTT cytotoxicity assay for cell viability analysis using various doses of BPA. Our results of BPA toxicity experiment with the two closely related cell lines (differing only in their experience with microgravity) has allowed us to tentatively conclude that 1) At lower doses (25 μM and 50 μM), BPA showed significant toxicity to log phase HepG2 and HepRC25D-b cells. 2) At higher doses (100 μM and 200 μM), BPA virtually completely abrogated the proliferation of cells and no log phase growth was detected for both of the two cell lines. 3) Within the lower doses of BPA exposures, it was discernable that microgravity experience slightly reduced the survival rates at log phase and post log phase of HepRC25D-b.

***Key Words**: Microgravity, Bisphenol A, XTT cytotoxicity assay, Cell proliferation, Log phase*

*SURP Fellowship Recipient
#Faculty Mentor

INTRODUCTION

Bisphenol A (2,2-bis[4-hydroxyphenyl]propane, BPA) is a plasticizer used in the manufacturing of polycarbonate plastics and epoxy resins. BPA is found everywhere in the environment. Every year, 6 billion pounds is produced and 100 tons is released in to the environment (Vandenberg et al, 2009). BPA is commonly used in everyday products such as beverage containers, food cans, baby bottles, dental sealants, etc. (Olea et al, 1996; Brotons et al, 1994; Biles et al, 1997). It can be absorbed when ingested, inhaled, or through the skin. As a result, around 90% of all Americans have detectable levels of BPA (Vandenberg, et al., 2007). Laboratory studies have also linked BPA to a number of these diseases. BPA

has been shown to cause increased incidence of breast cancer in mice (Jenkins et al, 2012) and increase susceptibility to precancerous lesions in rats (Ho et al, 2006) as well as having links to obesity, diabetes, and other metabolic disorders (DeCoster & Larebeke, 2012). At doses as low as 10μM, BPA has been shown to alter gene expression in some cell lines (Tilghman et al, 2012). BPA effects challenge the traditional toxicological assumption that dose makes the poison. BPA has been shown to have a non-monotonic dose response (Jenkins et al, 2012).

Crewmembers of space flights are exposed to microgravity. Microgravity is known to be a major hazardous factor in space travel. It has been shown to cause immune system dysfunction, muscle atrophy and neurological alterations to name a few (Leach et al, 1990; Cogoli 1993; Aktov et al, 1992). Because of the high cost of space flown experiments, ground-based methods for microgravity simulation have been created to simulate the effect of microgravity similar to those seen in the space environment. Rotating Cell Culture Systems (RCCS) are a commonly used method to simulate the microgravity effect on cultured cells. Such ground-based microgravity simulation experiments at the cellular and molecular levels have expanded our understanding of the underlying molecular and cellular alterations induced by microgravity.

In the present study, we performed a time-course XTT cytotoxicity assay on human liver cells that had been exposed to a simulated microgravity and post microgravity recovery culture conditions. XTT cytotoxicity assay is an effective method in determining changes in cell proliferation as well as toxicity. We compared the two cell lines HepRC25D-b (recovered from a 25 day microgravity experience) and HepG2 (the parental cell line that have never experienced any microgravity condition) regarding their survival viability profiles in various doses of BPA.

METHODS

Cell Culture and Treatments with Bisphenol A

An *in vitro* toxicological study system using human cell lines is a relatively new trend of toxicological approach, giving specific time- and dose-dependent toxicological response curves at relatively lower cost. The main approach of this research is to study the effect of BPA's impact on human liver cell lines, using the *in vitro* cytotoxicity XTT assay system. The human hepatoblastoma cell line (HepG2) was purchased from the America Type Culture Collection. A derivative of the HepG2 cell line, HepRC25D-b, was derived previously by culturing HepG2 cells under simulated microgravity (RCCS, rotating cell culture system) for 25 days, and then cultured at normal gravity for 168 days. Both of the cell lines were cultured at 37^{o}C, 5% CO_2 in DMEM with 10% fetal calf serum. To compare bisphenol A toxicity on these cell lines, each of the two cell lines were grown on 96-well plates and treated with bisphenol A at 0 μM, 25 μM, 50 μM, 100 μM, and 200 μM, respectively. The cells were assayed daily from day-1 to day-10, using the *in vitro* toxicology assay (described below).

In vitro Toxicology Assay

To evaluate the effect of bisphenol A toxicity, we applied the XTT *in vitro* toxicology assay that assesses the activity of mitochondrial dehydrogenase activities of viable cells. The XTT assay is a spectrophotometric toxicological method and its main component is the sodium salt of XTT (2,3-bis[2methoxy-4-nitro-5-sulfophenyl]2H-tetrosolium-5-carboxyanilide inner salt). In living cells, the mitochondrial dehydrogenase reduces the tetrazolium ring of XTT, giving an orange formazan derivative, which is soluble in water. The orange solution is spectrophotometrically measured in a microplate reader at a wavelength of 450 nm (Scudiero et al 1988; Roehm et al 1991). XTT detrazolium salts has been shown to be reliable reagents used in colorimetric assays for measuring cell proliferation and viability in response to chemical exposures in transformed and tumor cell lines.

The procedure is as follows. At each time point, the cells grown in a 96-well plate were removed from the incubator and placed into a laminar flow hood for cell and tissue culture. 20 μL of the XTT solution (1 mg/mL) was added to each well in a multiwell plate. The cells were then returned to the incubator and incubated for 3 hours. After the 3 hour incubation, the cells were removed and placed in the plate reader (TeCan Microplate Reader) for 1 minute agitation (mixing) and the absorbance at 450nm

and 690 nm (reference wavelength) were measured right after the agitation. The absorption data were automatically recorded and then analyzed in Microsoft Excel.

RESULTS AND DISCUSSION

To examine whether the HepRC25D-b cells would display a similar or significantly different survival curve in response to bisphenol A when compared to that of its parental cell line HepG2 which had never experienced the microgravity, we performed a time course XTT assay. The results of this time course experiment with bisphenol A are shown in Figures 1, 2, 3, and 4.

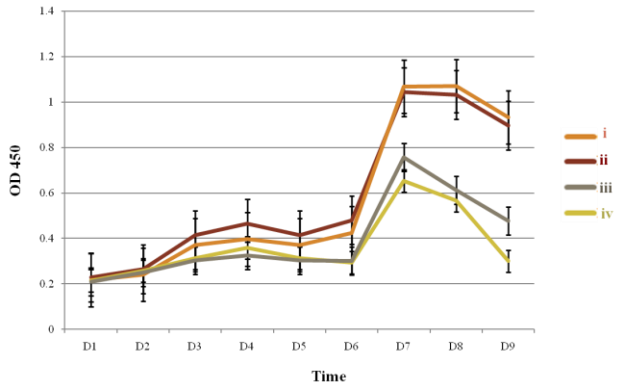

Figure 1. Cell Survival and Proliferation Rates in the Presence of 25 µM bisphenol A (BPA). i: proliferation curve of HepG2 cells in the absence of BPA. ii: proliferation curve of HepRC25D-b cells cultured in the absence of BPA. iii: survival curve of HepG2 cells at 25 µM BPA. iv: survival curve of the HepRC25D-b cells in response to BPA at a dose level of 25 µM.

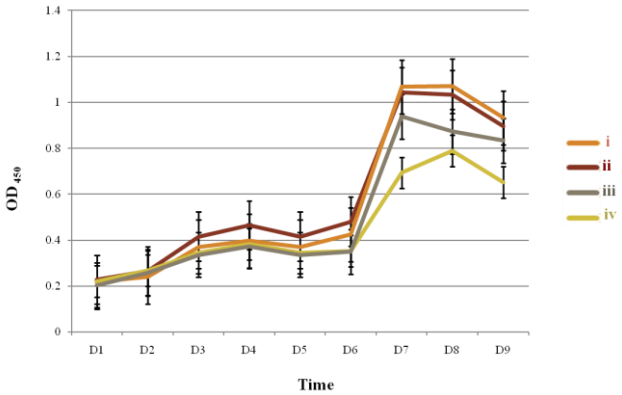

Figure 2. Cell Survival and Proliferation Rates in the Presence of 50 µM bisphenol A (BPA). i: HepG2 cell proliferation rates for the nine days cultured in the absence of the tested toxicant BPA, ii: nine-day time course of the RCCS derivative cell line, HepRC25D-b cells ,cultured in the absence of tested toxicant, iii: line graph shows the time course response of HepG2 cells to the toxicant BPA at a dose level of 50 µM, iv: line graph shows the time course response of the HepRC25D-b cells to the toxicant BPA at a dose level of 50 µM.

The data in Figure 1 shows the time course cellular proliferation rates and BPA toxicity profiles of the two cell lines (HepG2 and HepRC25D-b) cultured in the presence and absence of 25 µM bisphenol A. The two cell lines showed very similar proliferation curves in the absence of bisphenol A. Both of the cell lines also displayed a similar survival curves when treated with 25 µM BPA. However, minor differences are perceivable. It seemed that the survival curve of the microgravity exposed cells fell behind the non-microgravity exposed cells between day 6 and day 9, at log phase and onward. It is clear from Figure 1

that BPA at a concentration as low as 25 μM has significantly inhibited the proliferation of both of the two cell lines. Figure 2 shows the time course growth and toxicity trends for microgravity-exposed human liver cell line and its parental cell line cultured in the presence and absence of 50μM BPA.

After rechecking the original data and the steps of the analysis, the existing data of this experiment showed that at the dose level of 50 μM BPA, the proliferation rates of the HepG2 and HepRC25D-b cell lines were higher than that at 25 μM BPA level (compare Figure 1 and Figure 2). The reason for this is not certain. It could be a manifestation of the non-monotonic dose response nature of BPA (Jenkins et al., 2012). It could also be caused by the particular positions of the tested cells in the 96-well plates. We will perform further experiments to clarify the issue. The XTT assay was also performed with much higher doses of BPA, 100 μM (Figure 3) and 200 μM (Figure 4).

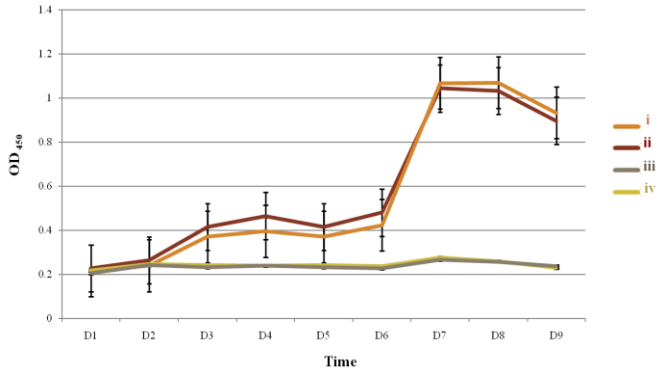

Figure 3. Cell Survival and Proliferation Rates in the Presence of 100 μM bisphenol A (BPA). i: HepG2 cell proliferation curve in the absence of BPA. ii: proliferation curve of HepRC25D-b cells cultured in the absence of BPA. iii: survival curve of HepG2 cells in the presence of 100 μM BPA. iv: survival curve of the HepRC25D-b cells in response to BPA at a dose level of 100 μM.

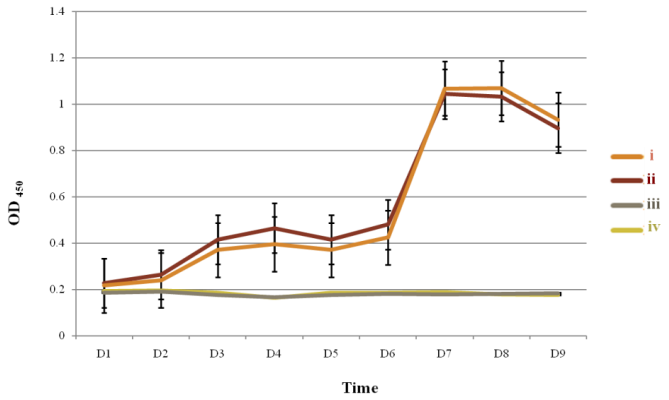

Figure 4. Cell Survival and Proliferation Rates in the Presence of 200 μM bisphenol A (BPA). i: proliferation curve of HepG2 cells in the absence of BPA. ii: proliferation curve of HepRC25D-b cells cultured in the absence of BPA. iii: survival curve of HepG2 cells at 200 μM BPA. iv: survival curve of the HepRC25D-b cells in response to BPA at a dose level of 200 μM.

Figure 3 shows these two cell lines cultured in the presence or absence of 100 μM BPA. Both of the two cell lines were essentially completely overcomed by the toxicity of BPA at 100 μM, they did not survive at such a high dose (Figure 3). We have also tested the cells at an even higher dose of 200 μM BPA and the cells did not survive at all at this highest dose tested (Figure 4). Both of the higher dosages show a high level of toxicity from the first time point onward. The results showed a large difference in

cellular response to BPA between the concentrations of 50 μM and 100 μM (compare Figure 2 and Figure 3). Further experiments will be performed to include BPA concentrations between 50 μM and 100 μM.

CONCLUSION

Our preliminary results of BPA toxicity experiment with two closely related cell lines differing only in their experience with microgravity has allowed us to tentatively draw the following main conclusions: 1) At lower doses (25 μM and 50 μM), BPA showed significant toxicity to log phase HepG2 and HepRC25D-b cells, 2) At higher doses (100 μM and 200 μM), BPA essentially completely abrogated the proliferation of cells and no log phase growth was detected at these high levels of BPA for any of the two cell lines and 3) with the lower doses of BPA, it was discernable that microgravity experience slightly reduced the cell survival at log phase and post log phase of cell growth.

ACKNOWLEDGEMENTS

This study was supported by Summer Undergraduate Research Program (SURP) of the College of Science and Technology at Texas Southern University.

REFERENCES

Atkov O. (1992) Some medical aspects of an 8 month's space flight. *Advances in Space Research* 12:343-345.

Biles J, McNeal T, Begley T, Hollifield H. (1997) Determination of bisphenol-A in reusable polycarbonate food-contact plastics and migration to food simulating liquids. *Journal of Agricultural and Food Chemistry* 45:3541-3544.

Brotons J, Olea-Serrano M, Villalobos M, Olea N. (1994) Xenoestrogens released from lacquer coating in food cans. *Environmental Health Perspectives* 103:608-612.

Cogoli A. (1993) Space flight and the immune system. *Vaccine* 11:496-503.

De Coster S, von Larebeke N. (2012) Endocrine-disrupting chemicals: associated disorders and mechanisms of action. *Journal of Environmental and Public Health,* 52 pages

Ho SM, Tang WY, Belmonte de Frausto J, Prins GS. (2006) Developmental exposure to estradiol and bisphenol A increases susceptibility to prostate carcinogenesis and epidenetically regulates phosphodiesterase type 4 variant 4. *Cancer Research* 66:5624-5632.

Jenkins S, Bentancourt AM, Wang J, Lamartiniere CA. (2012) Endocrine-active chemicals in mammary cancer causation and prevention. *Journal Steroid Biochemistry Molecular Biology* 129:191-200.

Leach CS. (1990) Medical considerations for extending human presence in space. *Acta Astronautica* 21:659-666.

Olea N, Pulgar R, Perez P, Olea-Serrano F, Rivas A, Novillo-Fertrell A. (1996) Estrogenicity of resin-based composites and sealants used in dentistry. *Environmental Health Perspectives* 104:298-305.

Roehm W, Rodgers GH, Hatfield SM, Glasebrook AL. (1991) An improved colorimetric assay for proliferation and viability utilizing the tetrazolium salt XTT. *Journal of Immunological Methods* 142:257-265.

Scudiero DA, Shoemaker RH, Paull KD, Monks A, Tierney S, Nofziger TH, Currens MJ, Seniff D, Boyd MR. (1988) Evaluation of a soluble tetrazolium/formazan assay for cell growth and drug sensitivity in culture using human and other tumor cell lines. *Cancer Research* 48:4827-4833.

Tilghman SL, Bratton MR, Segar CH, Martin EC, Rhodes LV, McLachlan JA, Wiese TE, Nephew KP, Burow ME. (2012) Endocrine disruption regulation of microRNA expression in breast carcinoma cells. *PLoS ONE* 7: e32754.

Vandenberg L, Hauser R, Marcus M, Olea N, Welshons W. (2007) Human exposure to bisphenol A (BPA). *Reproductive Toxicology* 24:139-177.

Vandenberg L, Maffini M, Sonnenschein C, Rubin B, Soto A. (2009) Bisphenol-A and teh great divide: a review of controversies in the field of endocinre disruption. *Endocrine Reviews* 30:75-95.

SUSTAINABLE PRODUCTION OF VEGETABLES USING HYDROPONIC SYSTEM AND ALGAL BIOFUELS

[1]Kelly Newton* and [2]Hyun-Min Hwang#

[1]Department of Biology, [2]Department of Environmental and Interdisciplinary Sciences
College of Science and Technology, Texas Southern University
3100 Cleburne Street, Houston, TX 77004


ABSTRACT

There are growing interests in constructing sustainable and environment friendly buildings that require less energy consumption for cooling and heating and utilization of renewable solar and wind driven energy. One of the solutions is constructing green roof to improve insulation. However, many existing buildings were not designed to support conventional soil-based green roof. This study investigated effectiveness of soil-free hydroponic system as an alternative green roof. Three climber plants (*Epipremnus aureum, Hedera algeriensis, Hedera nepalensis*) were placed in a pilot scale flow-through hydroponic system to test whether hydroponic system is feasible for growing climber plants. *H.algeriensis* and *H.nepalensis* grew at a steady rate of about 1 cm/week but growth rate of *E.aureum* was less than 0.2 cm/week. Three vegetables (cucumber, squash, tomato) were also tested whether hydroponic system is feasible for roof gardening. Tomato didn't grow well with the system tested in this study but cucumber and squash grew successfully with growth rates of 5 and 8 cm/week, respectively. Phytoplankton has gained more attention due to their capacity in removal of carbon dioxide and toxic volatile organic carbon in the air and generation lipids that can be converted to biofuel. Freshwater phytoplankton (*Botryococcus braunii)* was incubated for two weeks in a solution containing mineral nutrients and vitamins (F2 solution). Lipids were collected from dried phytoplankton cells using hexane. The collected lipids can be thermally fractionated to produce readily usable biofuel. The present study showed both hydroponic system and phytoplankton incubation can significantly contribute to the sustainability of modern society with less ecological footprint.

Key Words: *Sustainability, Hydroponic system, Green roof, Algal biofuel*

*SURP Fellowship Recipient
#Faculty Mentor

INTRODUCTION

Conventional agricultural practices to grow crops and vegetables require large amount of water for irrigation and agricultural chemicals such as fertilizers, herbicides, and insecticides. Degraded water quality is a ubiquitous issue around farming areas. The obvious benefit of a hydroponic system is much less water quality degradation. Hydroponic systems can produce vegetables with only a fraction of water and fertilizers compared to that required for conventional agricultural practices because hydroponic

system recirculates nutrient amended water continuously. No excess fertilizers will be released into nearby watershed and almost no herbicides are required at all for the hydroponic system that is a great alternative in producing vegetables with minimum water quality degradation. Hydroponic system can be also applied to build green roof that is a sustainable cooling system that leads to less energy consumption especially during summer in sun belt states like Arizona, California, Louisiana, and Texas.

Modern world is highly dependent on fossil fuels such as gasoline and diesels for transportation that creates various unwanted issues related to environmental pollution and global climate change. Since the fossil fuel consumption rates are extremely higher than their production rates, the supply of fossil fuels will be limited in the near future. Fossil fuel consumption is responsible for large scale environmental pollution such as oil spill as well as tremendous amount of emission of global warming gases like carbon dioxide that are big concerns for humans and wildlife. Therefore, there is a growing interest regarding development of sustainable energy such as biofuels (Beal et al., 2012; Ghasemi et al, 2012).

This study was conducted to develop an effective way to grow, harvest, and convert algae into a biofuel as well as to create a sustainable hydroponic system design that will be able to support vegetation that has various demands. Both of these studies have public and environmental benefits, and have been the focus of urban sustainability and environmental pollution mitigation.

METHODS

A hydroponic system was constructed using PVC pipes, water circulation pumps, and water tanks (Figure 1). Commercially available nutrient stock solution (Solutions A) for hydroponic growth was amended into distilled water to make 248 ppm of salt solution. The solution A contained 7% nitrogen, 7% potassium, 5% calcium, 1% phosphate, and 0.5% magnesium. Three types of ivy plants (*H. algeriensis, H. nepalensis,* and *E.aureum*) were inserted into the system after removing soil from the roots. The ivy plants were exposed to artificial light for 12 hours and followed by no light for 12 hours for three weeks. The plants were measured by four sets of criteria: plant length, leaf number, color, and new growth (e.g., budding). Two controls were included to validate the efficiency of the hydroponic system. One set of plants was kept in pots with soil and another set of plants were kept in jars containing nutrient free water. Another hydroponic system was constructed to test the growth of vegetables with a slightly different nutrient stock solution (Solution B), containing 5% nitrogen, 5% potassium, 5% calcium, 5% phosphate, 1.5% magnesium, and 1% sulfur.

Figure 1. Hydroponic system having no soil in PVC pipes.

A photobioreactor was developed for the biofuel production. A small fraction of *Botryococcus braunii* was incubated using F2 solution for 10 days and added to a clear Plexiglas tube containing 2 L of F2 solution amended water. The tube was exposed to an artificial light continuously to allow the

phytoplankton to grow faster (Figure 2). After two weeks, phytoplankton cells were filtered and dried in an oven for 24 hours. Dried algae cells were extracted with hexane to collect lipid (Wuertz et al., 2009) that can be converted into biofuel for combustion engines.

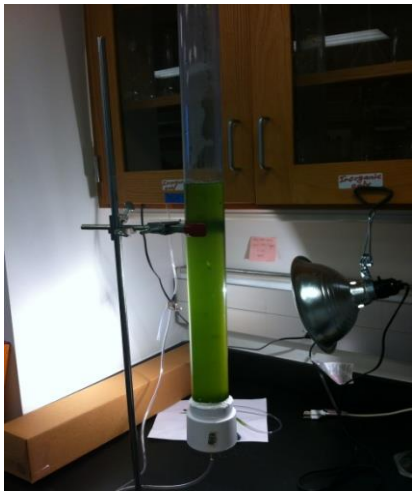

Figure 2. Algae growing in a plexiglass tube exposed to artificial light.

RESULTS AND DISCUSSION

H. algeriensis and *H. nepalensis* in the hydroponic system grew at a steady rate of about 1 cm per week (Figure 3) but *E. aureum* grew at much slower rate (2.9 mm/week). The coloring of the plants remained consistent. When these plants remained in pots with soil, their growth rates were relatively similar. This study demonstrates these plants can grow consistently in the hydroponic system, having no soil. This hydroponic system can be used to build green roof without applying soil on the roof that is a great advantage for building not designed to support excessive weight of soil.

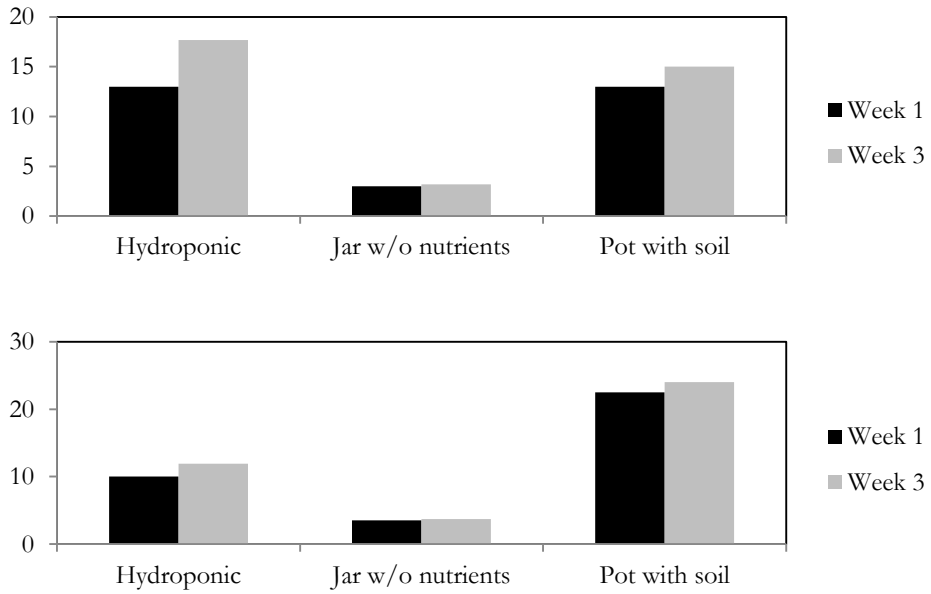

Figure 3. Height (mm) of *H. nepalensis* (top) and *H. algeriensis* (bottom) in a hydroponic system for three weeks.

A preliminary test conducted to identify optimum nutrient concentration ranges to feed the hydroponic systems indicated that between 372 and 496 ppm and 248 and 496 ppm solutions were most suitable ranges for cucumber and squash, respectively. So all vegetables were grown with 372 ppm of solution in the hydroponic growth tests. From week one to week three the tomato plant only grew 3.64 cm and lost 19 leaves, indicating that the hydroponic system used in the present study was not suitable for tomato. Remarkable growth was observed in both cucumber and squash plants contained in the hydroponic system over the three weeks. The cucumber plant grew from 11.5 cm to 27.9 cm and 19 new buds appeared. Squash had a 25.06 cm of growth, 6 new leaves, and 10 new buds over the three weeks (Figure 4). Leaf colors of cucumber and squash remained consistent throughout the entire experiment that is another indication of the successfulness of this practice (Figure 5). On average, the vegetative plants showed a growth rate of about 5 to 8 cm per week in the hydroponic systems.

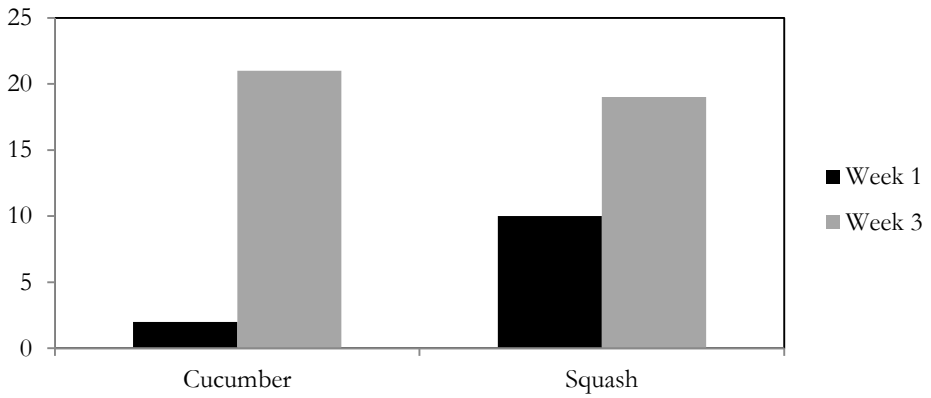

Figure 4. Growth (by number of buds) of cucumber and squash in a hydroponic system.

Week 1 Week 3

Figure 5. Growth of squash in a hydroponic system.

CONCLUSION

The present study provides evidence that the hydroponic system eliminates the need for soil and associated limitations such as climate changes, while still reaping the benefits of agriculture. In addition, the processes employed in the present study can also help in areas where there is little to no fertile soil to cultivate. Because hydroponic system recirculates nutrient amended water within a closed system, no excess nutrients will be released into nearby watersheds. It is another benefit of hydroponic system minimizing water quality degradation. The hydroponic system tested in the present study can be also used

to build green roof without applying soil on the roof that is a great advantage for building not designed to support excessive weight of soil.

Acknowledgements

This study was supported by Summer Undergraduate Research Program (SURP) of the College of Science and Technology at Texas Southern University.

References

Beal CM, Hebner RE, Webber ME, Ruoff RS, Seibert AF, King CW. (2012) Comprehensive Evaluation of Algal Biofuel Production: Experimental and Target Results. *Energies* 5:1943-1981.

Ghasemi Y, Rasoul-Amini S, Naseri AT, Montazeri-Najafabady N, Mobasher MA, Dabbagh F. (2012) Microalgae Biofuel Potentials: Review. *Applied Biochemistry and Microbiology* 48:126-144.

Woertz I, Feffer A, Lundquist T, Nelson Y. (2009) Algae Grown on Dairy and Municipal Wastewater for Simultaneous Nutrient Removal and Lipid Production for Biofuel Feedstock. *Journal of Environmental Engineering* 135:1115-1122.

EXPLICATION OF BRANCHED CHAIN AMINO-ACID TRANSAMINASE 1 IN TRIPLE NEGATIVE BREAST CANCER THAT COULD SERVE AS A RELEVANT BIOMARKER

Richard North, III* and Audrey Player#

Department of Biology
College of Science and Technology, Texas Southern University
3100 Cleburne Street, Houston, TX 77004

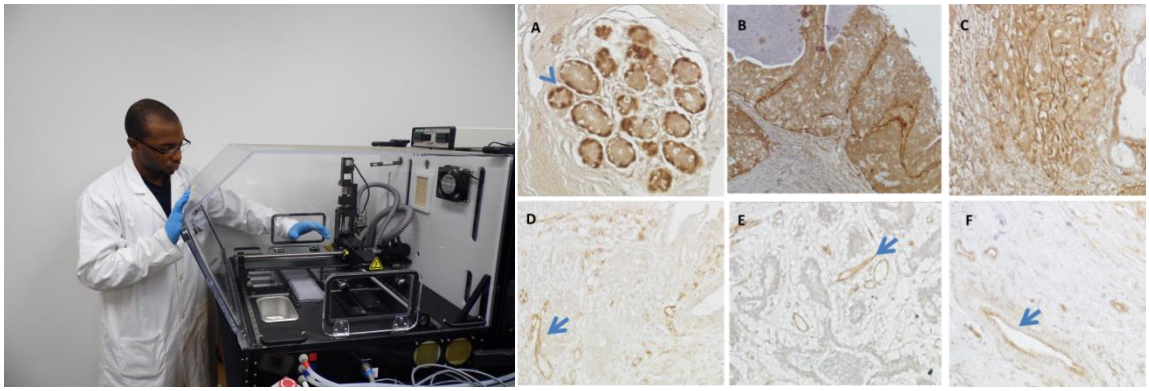

ABSTRACT

Triple negative (TN) breast cancer is defined in part by being an aggressive type of cancer that results in low patient survival rates. Little is known about the genetics of the cancers, so charactering its genome is the first step towards defining genes that might affect survival. Purpose of this study was to identify genes differentially expressed in TN cancers and validate their reliability as biomarkers. Branched chain amino-acid transaminase 1 (BCAT1) was one of several genes identified. Focus of this study was to perform initial studies to determine possible utility of the gene. BCAT1 expression levels were examined to determine if the gene would be a potential biomarker for TN cancers. BCAT1 levels were examined in MDA 231 (representing TN) and MCF7 (non-TN breast cancer) cell lines. RNA levels were analyzed using Polymerase Chain Reaction (PCR). Examination of protein levels was done using Immunohistochemistry (IHC) using tissue microarray (TMA) complied from clinical patient samples. BCAT1 RNA levels were higher in TN compared to non-TN breast cancer cell lines. However, on the protein level, there was no difference in BCAT1 in TN compared to non-TN sample. At the protein level, BCAT1 expression could not distinguish TN and non-TN clinical samples. In conclusion, BCAT1 would not be a useful gene to study for its utility as a biomarker in TN tumors

***Key Words**: Breast cancer, Genes, Branched chain amino-acid transaminase 1, PCR*

*SURP Fellowship Recipient
#Faculty Mentor

INTRODUCTION

Breast cancer is one of the most common malignancies in women of the United States. Although it is often spoken in terms of one disease, there are many different types of breast cancers, likely based on their original progenitor cell types. The cancers begin with anomalies associated with cells found in the ducts of the breast. Early data classify these cells as basal or luminal and/or stem-related cell types. Specific mutagenesis and differences in the genetics of these cell types are thought to lead to the different breast cancers. A number of studies have been performed in efforts to characterize breast tumors and

better understand their differences. Early data by Perou et al (ref) show that based on their genetics, breast cancers respond differently to therapies, has different pathological appearances, and although many follow a similar pattern of development, some are clearly more aggressive than others. It is the more aggressive cancers that display higher metastatic potential. These observations are informative, but investigators are a long way from fully understanding breast cancers.

It is important to understand breast cancers in general, but it is particularly important to understand the genetics of the aggressive / metastatic type cancers, because these are the ones that shorten patient survival and kill the patient. Aim of more recent studies is to characterize the metastatic / aggressive cancers, and identify particular genes that are useful for diagnoses or as possible therapeutic targets. As therapeutics, if the newly identified genes are key to the carcinogenic process, they might be effective at moderating the disease and prolonging patient survival. Major focus of the current study is to characterize gene expression in tumors previously defined as either aggressive or less-aggressive breast cancers with the goal of identifying genes that might serve to distinguish the two basic types. Once specific genes are identified, they would be examined for reliability and utility as biomarkers and ultimately therapeutic targets. Previous data show that TN tumors display highly aggressive behavior compared to non-TN tumors. As a result, TN tumors are used as model system in this study in efforts to identify genes related to aggressive/metastatic potential. TN tumors are defined as negative for 3 different genes; estrogen receptor, progesterone receptor, and ERRB2. Of all the breast cancers, TN represents 10-20% of the cancers. Non-TN breast represent a variety of different cancer types, obviously positive for these three receptors. Other investigators have successfully used transcriptome analysis to characterize breast cancers. Data presented here utilized Affymetrix microarray to compare TN to non-TN breast cancers samples and identify genes differentially expressed between the groups. Following transcriptome analysis, the BCAT1 gene was found up-regulated in TN compared to non-TN and considered a candidate for study. BCAT1 gene is a c-myc target that catalyzes the first reaction in the catabolism of essential branched chain amino acids leucine, isoleucine and valine. BCAT1 overexpression has been used as a diagnostic marker in nasopharyngeal and glioblastoma tumors. For this study, BCAT1 RNA and protein levels were examined to determine the gene's possible reliability as a marker for breast cancers.

METHODS

Affymetrix U133 plus 2 gene expression hybridizations were performed previously following suggestions of the manufacturer (Affymetrix.com) using MDA MB231 (TN) cell line and MCF7 (non-TN) cell line, each in triplicate. Affymetrix microarray contained 54, 675 genes and Expressed Sequence Tags (EST) corresponding to all known and purported genes. Datasets generated from hybridizations were deposited on National Cancer Institute's mAdb website (madb.nci.nih.gov). For data analysis, MDA MB231 (TN; group 1) was compared to MCF7 (non-TN; group 2). Grouped samples were normalized using Robust Multiarray analysis (RMA), and group comparisons performed using T-test. Gene expression differences between the 2 groups were identified using the T-test, and filtered based on genes showing at least 2-fold difference, with statistical p-values <0.01. A list of 49 (of 54,675) genes were identified as different between the 2 groups. The 49-gene-list was then compared to publically available patient datasets deposited on Gene Expression Omnibus (GEO); this allowed for comparisons between cell line and patient datasets and to some degree comparison to datasets generated by other investigators. Data associated with clinical samples was retrieved from Gene Expression Omnibus (GEO; www.ncbi.nlm.nih.gov/geoprofiles) using search-terms "Affymetrix and triple negative breast cancer". The GEO-GDS4069 dataset was one of the GEO datasets used for comparison to cell line datasets. GDS4069 included normal, non-basal/luminal, and basal breast cancer samples. Basal-breast cancer samples were all TN aggressive type samples. Hierarchical clustering (HC) analysis was performed using programs available on mAdb.

RNA gene expression levels were examined by converting mRNA to cDNA and analysis of the relative quantities between the different cell lines. To generate cDNA, 1 μg of total RNA (from cell lines) was mixed with iScript Reverse Transcriptase (RT) and master mix (BioRad.com), containing dNTPs, RT buffer and oligo dT primer, and processed as suggested by the manufacturer.

BCAT1 (and GAPDH as the control) primers were generated using Primer 3 program (biotools.umassmed.edu/bioapps/primer3_www.cgi). Primers were synthesized by IDTDNA. PCR was performed using melting temperature of 56deg for 29cycles. PCR products (for analysis of gene expression levels) were analyzed using 1% agarose gel electrophoresis.

TMA were used to examine the protein levels in tissues previously diagnosed as TN or other stages/types of breast cancer. Immunohistochemistry (IHC), which is an analysis of protein levels, was performed according to recommendation by manufacturer, including the antigen retrieval of TMA tissues. As a control for tissue quality, TMAs were examined for CD31 staining (demonstrating localization of blood vessels). Only 'core samples' showing positive CD31 staining were used for interpretation of BCAT1 results. Protein levels (i.e., staining intensities) were scored from 0-5 (with 5 representing most intense staining or protein levels).

RESULTS AND DISCUSSION

Principle objective of this study was to identify genes that were reliably differentially expressed in TN cancers. Genes would then be studied to determine their clinical utility. Because a host of studies showed that transcriptome analysis was a suitable method for identifying markers, microarray analysis of the transcriptome was used for this study. BCAT1 was one of several genes shown to be differentially expressed between TN and non-TN cell lines. Microarray data showed that BCAT1 transcript levels were higher in the TN cell line (Figure 1). Comparison analysis showed gene expression in TN samples was 7X higher with a p-value <0.00000005 (data not shown). The same samples were analyzed using the qualitative PCR method. Similar to results using microarray, the MDA MB231/TN samples showed higher levels of BCAT1 (Figure 2). This was the first time the gene was identified as differentially expressed in TN samples. BCAT1 expression in breast cancers was validated by data-mining publically available microarray datasets deposited at GEO. Even though BCAT1 was over-expressed, investigators involved in the GEO studies did not document or observe BCAT1 as a gene-of-interest. Tens of thousands of genes are interrogated on the microarray platforms, making it easy for investigators to overlook particular genes. Which genes are uncovered can be based on how the analyses are performed. Analysis of the same high-throughput datasets by different investigators can lead to somewhat different sets of 'genes-of-interest', explaining how BCAT1 might have been over-looked in the GEO studies.

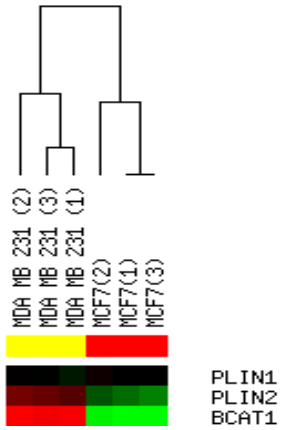

Figure 1. HC of BCAT1 using data values generated on Affymetrix microarray. BCAT1 transcript levels were higher (red) in MDA MB231/TN cell lines compared to MCF7 non-TN (green). Clustering can only be performed using 3 or more genes, so PLIN1 and 2 were added for clustering purposes.

Previous investigators have shown high levels of BCAT1 in other types of cancers, most notably, nasopharyngeal. Zhou et al (Molecular Cancer 2013) used knock-down studies to examine the possible role of BCAT1 in nasopharyngeal cancer cells. Their results showed that BCAT1 affected cell proliferation, migration and invasion in the carcinomas. The authors suggested that BCAT1 contributed to mechanisms related to fueling cancers and spurring their growth. Following microsatellite analyses, they suggest over-expression might be due to genomic amplification; some 45% of the samples demonstrating

over-expression of the RNA transcript also displayed genomic amplification of the BCAT1 gene. Data in this current study has only gone so far as to observe over-expression of transcript levels in TN cell lines. It is too early to speculate as to the contribution of BCAT1 transcript on the aggressive, migratory behavior of TN cancers.

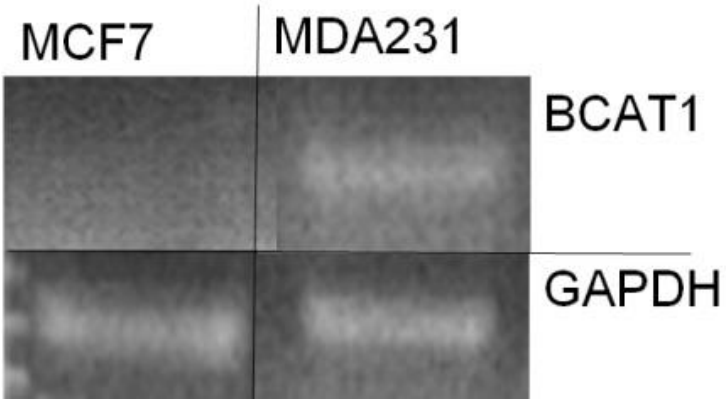

Figure 2. PCR analysis of BCAT1 cDNA generated using MDA MB231 and MCF7 cell line material. GAPDH gene levels were used as control. Consistent with results initially observed in microarray, higher levels of BCAT1 were observed in cell cultured cell lines.

A gene can only be seriously considered as a marker, if it demonstrates differential expression in clinical patient samples. Performance in clinical samples is critically important because they represent tissues (and genotypes) as will be observed in real patients. For validation of any marker, retrospective studies must be performed using archival tissue samples collected from patients. These types of analyses are most easily performed on the more stable protein product using immunohistochemistry. This in mind, current study focused on identifying genes that were first found to be differentially expressed on the transcript level, and validated as differentially expressed on the protein level in clinical samples.

Similar to results observed for transcript levels, Zhou et al found over-expression of BCAT1 protein in nasopharyngeal tissue samples. That was not the case when clinical samples from TN breast cancers were examined. BCAT1 levels were indiscriminately high in normal, non-TN and TN breast cancers, not showing differential expression on the protein level. In breast clinical samples, BCAT1 showed distinct and very intense cytoplasmic staining in all samples analyzed (Figure 3). BCAT1 appeared to be located in regions common to basal cells of the normal tissues (3A; arrow head). This is consistent with genes related to TN genotype, as TN tumors are thought to originate from basal cells lining the lumen of the ducts. BCAT1 might be considered for study as a potential basal cell related marker/gene. Staining was not related to high antibody concentrations, because when lower levels were administered, a similar pattern and distribution of staining was observed (data not shown). Remarkably, the staining pattern in breast tissue was similar to that observed in nasopharyngeal tissues. Current study shows differential BCAT1 on the transcript level, not at the protein level. de Bont *et al*. (2007) observed similar results.

CONCLUSION

The primary goal was to identify a biomarker that distinguishes TN breast cancer from all other types of less aggressive breast cancer; if found, the TN-specific gene could be studied for its clinical utility. BCAT1 was identified and transcript levels found to be differentially expressed in TN cell lines. However, at the protein level, BCAT1 expression could not distinguish TN and non-TN clinical samples. In conclusion, BCAT1 would not be a useful biomarker to characterize in TN tumors.

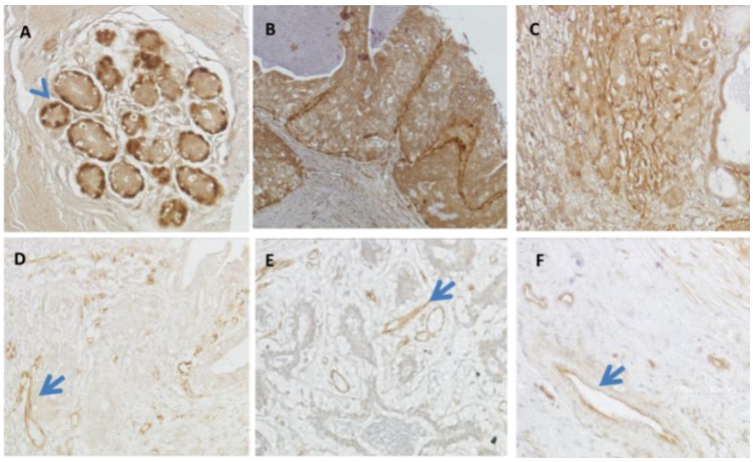

Figure 3. Immunohistochemistry analysis of BCAT1 protein levels in clinical patient samples. A= normal breast tissue BCAT1, B=non-TN breast tissue BCAT1, C= TN breast tissue BCAT1. C= normal breast tissue CD31 control, E=non-TN breast tissue CD31 control, F=TN breast tissue CD31 control. Arrow (no head; A) designates localization of BCAT1 in basal regions of lumen. Arrows (with head) show localization of CD31 in blood vessels / vascularity in medulloblastoma. de Bont et initially thought that BCAT1 might be a marker to distinguish metastatic medulloblastomas. That was not the case. RNA transcripts showed differential expression in medulloblastomas, but protein levels (as demonstrated by IHC) were the same in non-metastatic and metastatic medulloblastoma tissues. Differential regulation (in both their and this study) is clearly on the level of the transcript. How this might affect migration (if it does at all) is not known. Regulation of the transcript could be the focus of other studies most likely related to long antisense and/or micro-RNAs (miRNA). Interestingly enough, expression analysis of miRNA showed a potential candidate which was differentially expressed in TN compared to non-TN (data not shown; experiments performed by AP).

Acknowledgements

This study was supported by Summer Undergraduate Research Program (SURP) of the College of Science and Technology at Texas Southern University. Extended thanks go to Kayla Burrell, Carmen Gonzalez and Delon Poole.

References

Sorlie T, Tibshirani R, Parker J, Hastie T, Marron JS. (2003) Repeated observation of breast tumor subtypes in independent gene expression data sets. *Proc Natl Acad Sci* 100:8418–8423.

Minami CA, Chung DU, Chang HR. (2011) Management options in triple-negative breast cancer. *Breast Cancer* 5:175-99.

madb.nci.nih.gov/ (madb website)

www.ncbi.nlm.nih.gov/geoprofiles/ (GEO link)

frodo.wi.mit.edu/ (primer sequence)

www.pantomics.com/TissueArrays/Human/Breast/BRC962.aspx (immunohistochemistry)

www.biology-online.org/dictionary/Transcription_factor

GENOTOXIC EFFECTS OF GRAPHENE OXIDE ON SACCHAROMYCES CEREVISIAE

Nafisat Omotayo* and Ayodotun Sodipe#

Department of Biology
College of Science and Technology, Texas Southern University
3100 Cleburne Street, Houston, TX 77004

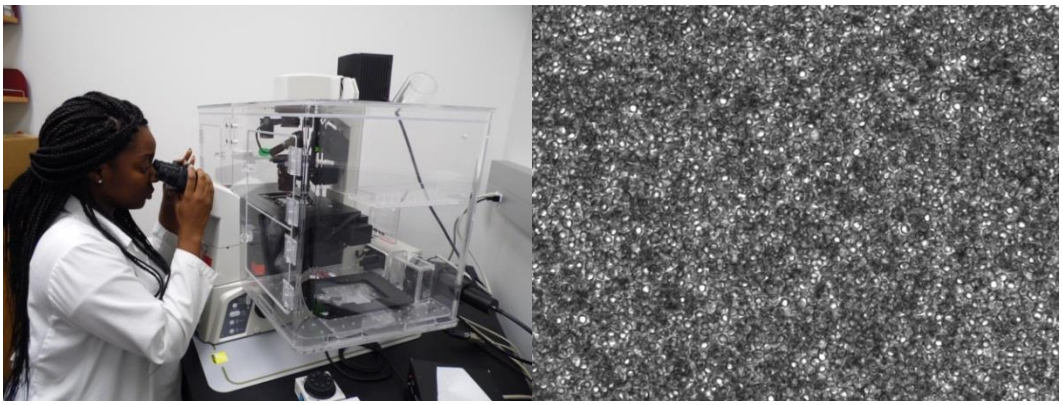

ABSTRACT

Graphene oxide, a compound of carbon, has seized the scientific community by storm. It is a single or multi-atomic-layered material made by the oxidation of graphite crystals, that is both flexible and a great conductor of electricity and heat. It has exclusive mechanical, electronic, and optical properties, which have shifted researchers focus towards biomedical areas such as precise DNA bio sensing and drug delivery. The focus of this study was to visualize any DNA damage that may occur to the yeast saccharomyces after exposure to graphene oxide. In our study, we labeled the antibody RAD17 with the fluorescent dye fluorescein isothiocynate (FITC) to visually compute any DNA damage that may occur. Our experimental design was organized into twenty conditions which included five controls, and two replicas. The graphene oxide was prepared from a stock solution with a concentration of 0.005g/ml or a 0.5% concentration. It was then optimized and prepared to varying concentrations of 500µg/ml, 750µg/ml, and 1000µg/ml. The results presented knowledge regarding the cell line saccharomyces. The cell structure of saccharomyces cerevisiae includes a cell wall of chitin, mannoproteins, and β – glucans. The extracellular cell wall of saccharomyces may have played a role in preventing graphene oxide from entering the cell, thus obstructing the graphene from affecting the yeast. The lack of graphene entering saccharomyces could have averted any potential effects that graphene may have had on the cells.

Key Words: *Genotoxicity, Graphene oxide, Saccharomyces cerevisiae, Antibody RAD17*

*SURP Fellowship Recipient
#Faculty Mentor

INTRODUCTION

Graphene plays a major role in advanced, cost-effective carbon-based flexible and transparent electronics. It has significantly high-strength, high-transparency, is flexible and is a superior thermal and electric conductor. Industrialists are endeavoring to discover cost-effective methods to manufacture bulk quantities of graphene for commercial applications ("Graphene Oxide – Properties and Practical Applications"). There are many ways in which graphene oxide can be functionalized, depending on the desired application. For optoelectronics, biodevices or as a drug-delivery material, for example, it is possible to substitute amines for the organic covalent functionalization of graphene to increase the

dispersability of chemically modified graphene in organic solvents. It has also been proved that porphyrin-functionalized primary amines and fullerene-functionalized secondary amines could be attached to graphene oxide platelets, ultimately increasing nonlinear optical performance.

In order for graphene oxide to be usable as an intermediary in the creation of monolayer or few-layer graphene sheets, it is important to develop an oxidization and reduction process that is able to separate individual carbon layers and then isolate them without modifying their structure. While the chemical reduction of graphene oxide is currently seen as the most suitable method of mass production of graphene, it has been difficult for scientists to complete the task of producing graphene sheets of the same quality as mechanical exfoliation, for example, but on a much larger scale. Once this issue is overcome, we can expect to see graphene become much more widely used in commercial and industrial applications (De La Fuentes, 2013).

There are former studies regarding the genotoxicity of graphene nanoplatelets in hMSC's (human mesenchymal stem cells). Human mesenchymal stem cells are a fundamental factor in tissue engineering and were isolated from umbilical blood in this study (Akhavan et al, 2012). The experiment tested the genotoxicity of reduced graphene oxide nanoplatelets, which were synthesized by sonication of PEGylated graphene oxide sheets and followed by a chemical reduction using hydrazine and bovine serum albumin. It examined the influences of reduced graphene oxide nanoplatelets on hMSC's through DNA fragmentations and chromosomal aberrations. The rGONPs showed genotoxic effects on the stem cells through DNA fragmentations and chromosomal aberrations, even at low concentration of 0.1 mg/mL. The results presented essential knowledge for more efficient and innocuous applications of graphene sheets and particularly nanoplatelets in upcoming nanotechnology-based tissue engineering as, e.g., drug transporter and scaffolds (Akhavan et al, 2012). Wang et al. (2013) investigated the genotoxicity of graphene oxide to human lung fibroblasts (HLF) cells. The results indicated that the genotoxicity of graphene oxide was concentration dependent and was more severe than the cytotoxicity to human fibroblast cells. This study found that the electronic charge on the surface of graphene oxide played a vital role in the toxicity of graphene oxide to human fibroblast cells.

The significance of this study lies within the results. If the graphene oxide does not damage the DNA in saccharomyces and is proven nontoxic, graphene oxide can be used in biomedical applications, drug delivery, and biosensors. In contrast, if the graphene is proven to be toxic within the saccharomyces cerevisiae, it can still be used as an application screening test.

METHODS

Cell Culture

The cell line saccharomyces cerevisiae was cultured in a liquid media composed of YPD (Yeast Peptone Dextrose) broth and DI water. The media was then autoclaved for an hour to sterilize any microorganisms within the liquid. A colony of saccharomyces was transferred from an agar petri dish into the media and left to grow at room temperature (25°C) in an incubator for a period of three days. The samples were then removed and placed into well plates with their respective concentration of graphene oxide for their allotted time.

Graphene Oxide Preparation

The graphene oxide was purchased from Angstron Materials and prepared from a stock solution dispersed in DI water at a 0.5% concentration. The graphene oxide was then diluted to 500µg/ml, 750µg/ml, and 1000µg/ml concentrations into deionized water and stored in the dark at 4°C.

Labeling Antibodies

The Pierce® FITC Antibody Labeling Kit and anti-RAD17 from Thermo Scientific aided in labeling the antibody RAD17. The labeling buffer contained a dilution of Borate Buffer (0.67M) and DEPC treated water with 1mg of RAD17. It was then incubated, purified in purification resin, and stored in a refrigerator (4°C). Before the labeled antibody was purified in spin columns, the columns were filtered

with PBS for 10 minutes and centrifuged at 1000 rpm for one minute to pre vet the spin columns. This helped to prevent the actual antibody from remaining in the filter after being centrifuged.

Graphene Oxide Exposure

The samples were incubated in 96 well plates for 0, 16, 24, 48, and 72 hours respectively. The samples were labeled S1 – S20 to differentiate between trials, times, and concentrations. Samples 1, 2, 3, 4, and 5 (the controls after 0 hours) were kept in a well plate and viewed. Samples 6, 7, 8, 9 and 10 were exposed and incubated with concentrations of graphene oxide: 0µg/ml, 500µg/ml, 750µg/ml, and 1000µg/ml for 16 hours. Samples 11, 12, 13, 14 and 15 were exposed and incubated with concentrations of graphene oxide: 0µg/ml, 500µg/ml, 750µg/ml, and 1000µg/ml for 48 hours. Samples 16, 17, 18, 19 and 20 were exposed and incubated with concentrations of graphene oxide: 0µg/ml, 500µg/ml, 750µg/ml, and 1000µg/ml for 72 hours. After the allotted time, the samples were placed on microscopic slides, fixed on the slide by flame and washed in a 10% Triton X for 10 minutes. They were then washed in phosphate buffer solution (PBS) three times and viewed under a microscope.

Sample Analysis

This experiment was replicated twice independently and viewed using a Nikon Eclipse Ti inverted microscope with and without the FITC filter. This filter made it possible to visualize any DNA damage that occurred, in the form of fluorescent foci, to saccharomyces from the exposure to graphene oxide.

RESULTS AND DISCUSSION

Graphene oxide has promising applications in bioimaging, diagnostics and therapeutics (Liu et al, 2012). It has the ability to play a novel role in biomedical applications and aid the scientific arena in making many innovative discoveries for the betterment of mankind. Because of the numerous advantages that graphene oxide provides, it is imperative to test graphene for any potential toxicity. In former studies performed, graphene oxide had a concentration and dose dependent toxicity on the particular cells that were exposed to it. These findings gave us an inkling of what to expect in the results of our particular experiment.

In this study we wanted to test the possible genotoxic effects of the carbon based chemical graphene oxide on the yeast, saccharomyces cerevisiae. To investigate this idea, we cultured our cell line saccharomyces in a liquid media and exposed and incubated our samples over a period of 0 hours, 16 hours, 24 hours, 48 hours, and 72 hours with varying concentrations of graphene oxide (500µg/ml, 750µg/ml, 1000µg/ml). Before exposing the saccharomyces to the graphene oxide, the antibody RAD17 was labeled with the fluorescent dye FITC to aid in visualizing any form of DNA damage that may occur through the production of foci. RAD17 is one of the proteins expressed in the yeast saccharomyces cerevisiae after any form of DNA damage is induced within the cell. If any DNA damage had occurred, the FITC labeled antibody RAD17 would fluoresce under the FITC filter in the form of foci (a way to determine if the cell has been damaged).

After exposure of the cell line to graphene oxide and sample analysis with the *Nikon Eclipse Ti*, there was a reoccurring theme. The yeast cells within samples 1 – 5, our controls, were alike in many avenues. The cells were oval in shape with a clear outer cell wall and intact nucleus. The experimental samples that had been incubated with graphene oxide were highly similar to the controls. The cells maintained their cell wall and there seemed to be no effect on the actual cell under all magnifications regardless of the time exposure or the graphene oxide concentration. The samples were first viewed under a monochrome image and then viewed with a FITC filter to check for any appearance of foci in the sample. Under the FITC filter, no foci were seen. The yeast had slight auto fluorescence but maintained its shape and cell wall despite the time and dosage of graphene oxide.

Despite the increased dosage of graphene oxide alongside the time exposed, there were no imminently visible effects of the chemical graphene oxide on the yeast cell saccharomyces cerevisiae. The lack of penetration of graphene oxide into the cell wall of saccharomyces may have played a role in the absence of any DNA damage. The nucleus and vacuoles within the cell were not affected by the

graphene oxide, therefore forgoing any chance of toxic effects. Although RAD17 is a protein that is expressed in response to DNA damage in saccharomyces, it may not be expressed as well as its other counterparts. As we only labeled the antibody RAD17, it could have made it difficult to see any form of foci or reactive oxygen species that may have been induced in reaction to the graphene oxide.

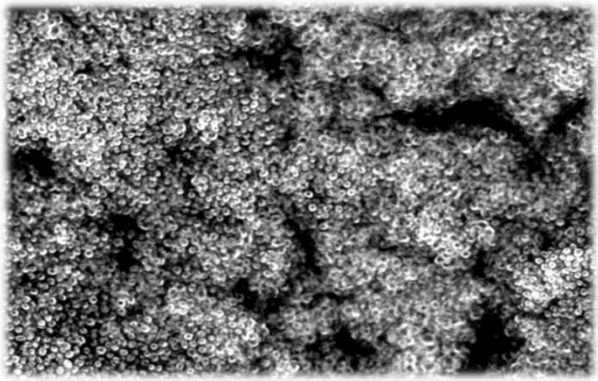

Figure 1. S5 yeast control after 72 hours (40x magnification).

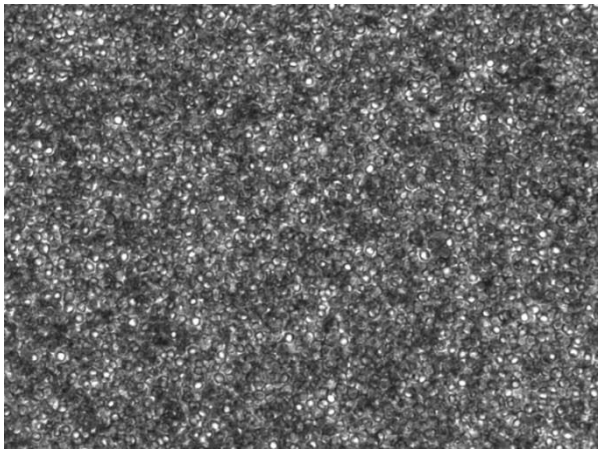

Figure 2. S20 yeast after 72 hour exposure to graphene oxide (40x magnification).

CONCLUSION

This study demonstrated that after the exposure of saccharomyces cerevisiae to various concentrations of the chemical graphene oxide, there was no interaction between the graphene oxide and the accharomyces. This could be due to the thick cell wall of the yeast preventing the dye from entering the cell and affecting the yeast. An additional explanation may lie within the protein RAD17. RAD17 is one of the proteins expressed in response to DNA damage in the yeast saccharomyces cerevisiae (Paulovich et al, 1998). The antibody RAD17 was specifically labeled with FITC so any DNA damage would be visible under a FITC filter. Since there were no detectable foci seen with FITC, it can be concluded that the protein RAD17 may not express well in response to reactive oxygen species. Therefore, more sensitive assays need to be applied to see the multi-generation genotoxic effect in saccharomyces.

Table 1. Physical changes of yeast cells after exposure to graphene oxide**.**

	Time (hours)				
Dosage	0	16	24	48	72
0µg/ml	Cells cylindrical in shape. Cell wall intact. **S1**	Maintains shape and size. No visible change. **S2**	Yeast cell maintained shape and size. **S3**	Same shape. Cell wall remains. **S4**	Cells still maintain shape and size compared to 0 hours. **S5**
500µg/ml	Cells cylindrical in shape. Cell wall intact. **S6**	Remains size, shape. No foci seen under FITC filter. **S7**	Maintains shape and size. **S8**	No apparent physical change. **S9**	Sample looks similar to control. No physical change or foci. **S10**
750µg/ml	Cells cylindrical in shape. Cell wall intact. **S11**	No obvious change to cell. **S12**	No apparent physical change. **S13**	Maintains shape and size. **S14**	No obvious change seen within cell. No foci seen. **S15**
1000µg/ml	Cells cylindrical in shape. Cell wall intact. **S16**	Maintains shape and size. **S17**	No change evident in sample. **S18**	Cell wall intact. No visible damage viewed under microscope. **S9**	Cell wall remains upheld with no apparent damage or foci under fluorescent filter. **S20**

S1: 0 hours, 0µg/ml. **S2:** 16 hours 0µg/ml. **S3:** 24 hours, 0µg/ml. **S4:** 48 hours. 0µg/ml.
S5: 72 hours. 0µg/ml. **S6:** 0 hours. 500µg/ml. **S7:** 16 hours. 500µg/ml. **S8:** 24 hours. 500µg/ml.
S9: 48 hours. 500µg/ml. **S10:** 72 hours. 500µg/ml. **S11:** 0 hours. 750µg/ml. **S12:** 16 hours.750µg/ml.
S13: 24 hours. 750µg/ml. **S14:** 48 hours. 750µg/ml. **S15:** 72 hours. 750µg/ml. **S16:** 0 hours. 1000µg/ml.
S17: 16 hours. 1000µg/ml. **S18:** 24 hours. 1000µg/ml. **S19:** 48 hours. 1000µg/ml. **S20:** 72 hours. 1000µg/ml.

ACKNOWLEDGEMENTS

This study was supported by Summer Undergraduate Research Program (SURP) of the College of Science and Technology at Texas Southern University. We would like to express appreciation for Francis Ogbonnia, Shari Galvin, Shantel Nwanguma, and Sarah Glenn for their help. Special thanks go to *Obaid Ullah* for her help.

REFERENCES

Akhavan O, Ghaderi E, Akhavan A. (2012) Size-dependent genotoxicity of graphene nanoplatelets in human stem cells. *Biomaterials* 33:8017-8025.

De La Fuentes J. Graphene Oxide - What Is It? (www.graphenea.com).

Liu JH, Yang ST, Wang H, Chang Y, Cao A, Liu Y. (2012) Effect of size and dose on the biodistribution of graphene oxide in mice. *Nanomedicine* 7:1801-1812.

Paulovich AG, Armour CD, Hartwell LH. (1998) The Saccharomyces cerevisiae RAD9, RAD17, RAD24 and MEC3 genes are required for tolerating irreparable, ultraviolet-induced DNA damage. *Genetics* 150:75-93.

Wang A, Pu K, Dong B, Liu Y, Zhang L, Zhang Z, Duan W, Zhu Y. (2013) Role of surface charge and oxidative stress in cytotoxicity and genotoxicity of graphene oxide towards human lung fibroblast cells. *Journal of Applied Toxicology* 33:1156-1164.

BIOINFORMATICS APPROACHES TO DECODING THE MITOCHONDRIAL GENOME OF PALAWAN PEACOCK-PHEASANT *POLYPLECTION NAPOLEONIS*

Tommy Quach*and Hector Miranda#

Department of Biology
College of Science and Technology, Texas Southern University
3100 Cleburne Street, Houston, TX 77004

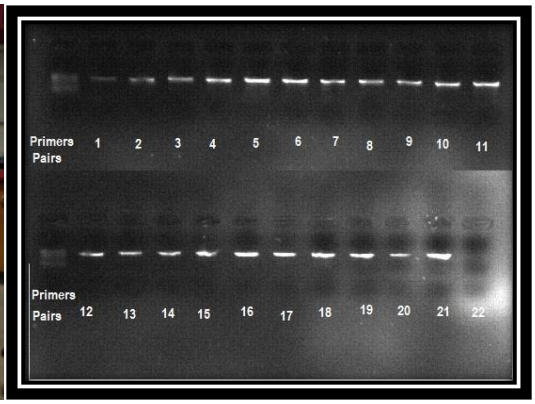

ABSTRACT

Throughout many decades, many researchers and scientist have debated over the controversial issue of the traces of origin and trend of popular divergences from the Southeastern flock of the Palawan Peacock Pheasants. To be more specific, the genus *Polyplectron* are separated into seven different species whereas the experiment for this summer will focus specifically on the *Polyplectron napoleonis.* With the significant amount of information from two articles that argues about the trend of these Southeastern birds from two different perspectives proven with different studies, it has empowered the strike of interest of declaring which paper is correct based upon the data obtained. The first hypothesis demonstrated that species of the Southeastern flock of Peacock Pheasants migrated from the mainland to the islands of Taiwan, while the second hypothesis disputed with a contradictory idea that the flock of Peacock Pheasants actually migrated from islands of Taiwan to the mainland. Researchers have defined the traces of migration upon these Peacock Pheasants as "island hopping" leading to popular divergences and growth in population of these species. As we sequence the entire mitochondrial genome of *Polyplectron napoleonis*, we plan to observe the phylogenic relations with other species under the same genus. Considering that the entire closed circular molecule consist of 16,000 base pairs, 13 protein-coding genes, 2 rRna genes, and 22 tRNA genes, the gene order and gene coding strands illustrates similar characteristics with other birds.

Key words: *Palawan Peacock Pheasants, migration, mitochondrial genome sequencing*

*SURP Fellowship Recipient
#Faculty Mentor

INTRODUCTION

Complete mitochondrial genome (mtgenome) sequences are increasingly being used in addressing questions on the basal evolution of birds. Recently, the mitochondrial genomes have been used to investigate the basal origin and diversification of birds prior to the K/T boundary (Paton *et al*., 2002; Harrison *et al*., 2004; Pacheco *et al*., 2011). The number of complete bird mitochondrial genomes have been constantly increasing in GenBank, Although single genes such as cytochrome oxidase 1 (cox1) are considered standard for species-level phylogenies or identification (DNA barcoding), the mitogenome provides a larger dataset to address more complex issues that can be addressed by a single or a few genes.

The phylogeography of *Polyplectron* is somewhat enigmatic. Studies based on *cytb* and *D-Loop* (control region) and nuclear ovomucoid intron G suggest *P. napoleonis* as basal to the *Polyplectron* clade (Kimball *et al*., 2001; Kimball and Braun, 2008). However, this phylogeny is not congruent with the most recent phylogenetic report for the clade (Eo *et al*., 2009). In contribution to better understand the evolution of *Polyplectron*, we characterize the complete mitochondrial genome of the Palawan Peacock-pheasant *Polyplectron napoleonis.*

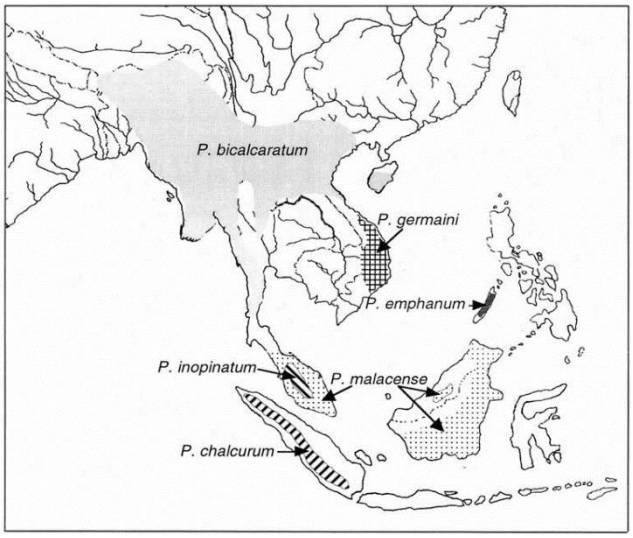

Figure 1. A map illustrating distribution of Polyplectron napoleonis relative to five other species.

The Palawan Peacock-pheasant *Polyplectron napoleonis*, is regarded as the most spectacular of the genus *Polyplectron*. It is endemic to the island of Palawan and currently categorized by the by the International Union for the Conservation of Nature (IUCN) as Vulnerable (Birdlife International, 2005). The population estimates for this *P. napoleonis* ranges from 10,000 (McGowan and Garson, 1995) to 50,000 individuals (Mallari *et al*., 2011). It mainly inhabits primary and secondary forest up to 800 m in elevation. Although there is strong pressure from deforestation and hunting, *P. napoleonis* is currently not considered as vulnerable but not endangered. However, this conservation status may change as environmental exploitation continues in a small tropical island such as Palawan.

METHODS

Specimen source and DNA extraction:

DNA extraction was performed using DNAeasy Tissue kit (Qiagen) following manufacturer instruction to obtain DNA from fresh tissue sample. Primers were designed using Primer3Plus.

Primer design and PCR amplification:

Primers were designed using Primer3Plus and Geneious Pro 5.5 (Biomatters, New Zealand). However, we did not use degenerate primers to avoid amplification of non-target loci. The Polymerase Chain Reaction (PCR) is a technology that allows DNA to be amplified through numerous cycles(35 cycles) just from a couple or single strands of DNA. Within the process of PCR, it consist of 3 main stages: Denaturing, Annealing, and Extension/Elongation. Primary PCR was conducted using TAKARA LA (Roche) and amplification of smaller (usually 800 bp) secondary PCR was made using the primary PCR product as template. PCR was carried out in a total volume of 25 uL containing 10-50 ng of template DNA, 4 µL of deionized water, 4 µL 10 mM of each dNTP, and 8 µL of AmpliTaq 360 Gold Polymerase Master Mix (Life Technologies). A total of 27 primer pairs were used. In cases where internal primer pairs failed, two strategies were adopted: 1.PCR using the forward primer and the reverse primer of the

adjacent 3'-end fragment, or the reverse primer of the target fragment and the forward primer of the 5' adjacent fragment, and 2. designing new species-specific primers using the known flanking sequences for 'two-way primer walk'. The PCR cycles were as follows: one cycle of 10 min at 95°C, 35 cycles of 20 s at 95°C, 20 s at 60°C, and 50 s at 72°C. The process was completed with a final elongation at 72°C for 10 min. These parameters were adjusted to optimize PCR product quality. All amplifications were performed on Veriti Thermal Cycler (Life Technologies). The approximate waiting time for the process of polymerase chain reaction to complete was approximately 1.5-2 hours for each trial run. By the time PCR is finished, the products should be thousands-million copies of base pair just from a single stranded DNA. Errors in between preparing and processing these primers are a major area where caution needs to take place in order to prevent a human error or contamination in the products.

DNA sequencing and contig assembly

The PCR products were detected by applying through the process of gel electrophoresis in 1.0% agarose gel and purified using Exo-Sap-IT (Affymetrix, CA). Amplified products were sequenced bidirectionally on an ABI-PRISM 3730 sequencer using BigDye Terminator, version 3.1, Cycle Sequencing Kit (Applied Biosystems) by Eurofins mwg/Operon (Alabama USA). Raw chromatograph sequences were manually checked using FinchTV (http://www.geospiza.com/Products/finchtv.shtml). Both forward and reverse sequences were aligned and consensus assembled using ClustalW (Larkin *et al*., 2007). Contig assembly was accomplished in Geneious Pro 5.5 (Biomatters, New Zealand).

Gene annotation and analysis

Transfer RNA genes analysis and secondary structure inference were done using tRNAscan-SE (Lowe and Eddy, 1997) and verified by sequence alignment with other published pheasant sequence Genebank annotations. Protein-coding genes (PCG) and ribosomal RNA genes (rRNAs) were identified and open reading frames were translated after homology establishment of inferred open reading frames from alignment with published *P. bicalcaratum* (NC012900) and *P. germaini* (KF422893, *in press*). Translation of PCG open reading frames was made in ExPASy (Artimo *et al*., 2012)

RESULTS AND DISCUSSION

Genome organization

Based upon our results obtained from data interpreting and data analysis, the mitogenome of *N. napoleonis* is a closed-circular molecule of 16,700 bp (GenBank accession number XXXXXX). Not only does the the genome contains 13 protein-coding genes, 2 rRNA genes and 22 tRNA genes, but the Gene order and gene coding strand is consistent with those observed in galliformes and other birds. Furthermore, data illustrate that there are similarities with $tRNA^{Glu}$ and *nd6* where they are found immediately adjacent to the control region instead of being located between the *nd5* and *cytb* genes as in other vertebrates (Desjardins and Morais, 1990). Except for *nd6*, all protein-coding genes are transcribed at the complementary Heavy (H) strand. The overall base composition is 23.9 % T; 29.5 A, 32.3 % C, and 14.3 % G with a total A + T content of 53.4%. Two reading frames overlaps occur on the same strand: *atp8* and *atp6* overlap by 8 nt, *nd4L* and *nd4* by 5 nt. All of the protein-coding genes begin with the ATG start codon, except for *cox1* which has a GTG start codon.

Protein-coding genes and codon usage

The mitogenome of *P. napoleonis* contains 13 protein-coding genes typical of metazoans. In addition, there were no unexpected stop codons observed within PCGs. The initiation and stop codons are shown in the table were the codons are assembled in Table 1. All protein-coding genes use the standard ATG start codon, except for *cox1*which has GTG start codon. This differs from *P. germaini* which has the typical ATG start codon (Omeire *in press*). This non-standard putative codon for *cox1* have also been observed in metazoans (Okimoto and Wolstenholme 1990, Caterino and Sperling 1999). Seven out of 13 PCGs have TAA stop codons, two have AGG (cox1 and nd6), and three PCGs (*nd2*, *cox2* and *nd4*) have incomplete stop codon of just T- nucleotide. The AGG stop codon in vertebrates has been noted as rare stop codon

Table 1. Characteristics of the species' sequence.

	Position			Codon				
Gene	From	To	Size (bp) Nucleotide	Amino Acid	Initiation	Stop	Intergenic nucleotides	Strand
Control region	1	1169	1169				0	N/A
$tRNA^{Phe}$	1170	1236	67				0	H
12S rRNA	1237	2215	979				0	H
$tRNA^{Val}$	2216	2289	74				0	H
16S rRNA	2290	3887	1598				-1	H
$tRNA^{Leu}$(UUR)	3887	3960	74				+9	H
nd1	3970	4944	975	325	ATG	TAA	0	H
$tRNA^{Ile}$	4945	5018	74				+6	H
$tRNA^{Gln}$	5025	5095	71				-1	L
$tRNA^{Met}$	5095	5163	69				0	H
nd2	5164	6202	1039	346	ATG	T-	0	H
$tRNA^{Trp}$	6203	6281	79				+6	H
$tRNA^{Ala}$	6288	6359	72				-2	L
$tRNA^{Asn}$	6358	6420	63				+12	L
$tRNA^{Cys}$	6433	6498	66				-1	L
$tRNA^{Tyr}$	6498	6568	71				+1	L
cox1	6570	8120	1551	517	GTG	AGG	-7	H
$tRNA^{Ser}$(UCN)	8112	8186	75				+2	L
$tRNA^{Asp}$	8189	8257	69				+1	H
cox2	8259	8942	684	228	ATG	TAG	+1	H
$tRNA^{Lys}$	8944	9010	67				0	H
atp8	9011	9176	165	55	ATG	TAA	-8	H
atp6	9167	9850	684	228	ATG	TAA	-1	H
cox3	9850	10633	784	261	ATG	T-	+1	H
$tRNA^{Gly}$	10635	10702	68				0	H
nd3	10703	11054	352	117	ATG	TAA	+1	H
$tRNA^{Arg}$	11056	11124	69				0	H
nd4l	11125	11421	297	99	ATG	TAA	-5	H
nd4	11415	12792	1377	459	ATG	T-	0	H
$tRNA^{His}$	12792	12860	69				+1	H
$tRNA^{Ser}$(AGY)	12862	12926	65				+2	H
$tRNA^{Leu}$(CUN)	12929	12999	71				0	H
nd5	13000	14817	1818	606	ATG	TAA	+4	H
cytb	14822	15964	1143	381	ATG	TAA	+3	H
$tRNA^{Thr}$	15968	16036	69				0	H
$tRNA^{Pro}$	16037	16112	76				+5	L
nd6	16118	16639	522	174	ATG	AGG	+1	L
$tRNA^{Glu}$	16641	16709	69				0	L

(Wolstenstein and Fauron 1995). TAA termination of the incomplete T- by post-transcriptional polyadenylation is assumed to be operational (Ojala et al. 1981).

Transfer RNA and ribosomal RNA genes

The *P. napoleonis* contains the typical set of 22tRNA genes, which are interspersed between rRNAs and protein-coding genes. All 22 tRNA genes can fold into a typical cloverleaf structure, except for tRNA-Ser (AGN) which may be lacking the DHU arm (Figure 2). Eight tRNAs are coded on the complementary L strand, while the remaining 14 tRNAs are transcribed at the Heavy (H) strand. The three tRNA clusters (IQM, WANCY, and HSL) are well conserved in *P. germaini*, typical of vertebrate mitochondrial genomes. The two ribosomal RNA genes (12S and 16S) are located between $tRNA^{Phe}$ and $tRNA^{Val}$ (981 bp), and between $tRNA^{Val}$ and $tRNA^{Leu}$ (UUR) (1598 bp), respectively. These mismatches are possibly corrected by RNA-editing mechanisms (Lavrov et al. 2000). As in all metazoans, there are two rRNA genes in *P. napoleonis*, the small and large ribosomal genes (12S rRNA and 16S rRNA). The 12S rRNA is located in between tRNA-Phe and tRNA-Val, and the 16S rRNA is located between tRNA-Val and tRNA-Leu (UUR). The length of 12S rRNA is 979 nt long with 49.2% AT content, while the 16S rRNA 1598 nt long with 54.3% AT content.

The Control-region

The control region was determined to be 1169 bp, well within the observed range among Galliformes, but one bp shorter than that reported for *P. bicalcaratum* (Shen et al. 2009). Overall, the mitogenome sequence pairwise sequence similarity between P. napoleonis and P. bicalcaratum was 93.3 %. With these information provide, it is safe to say that a conclusion can be made once all species are processed and analyzed.

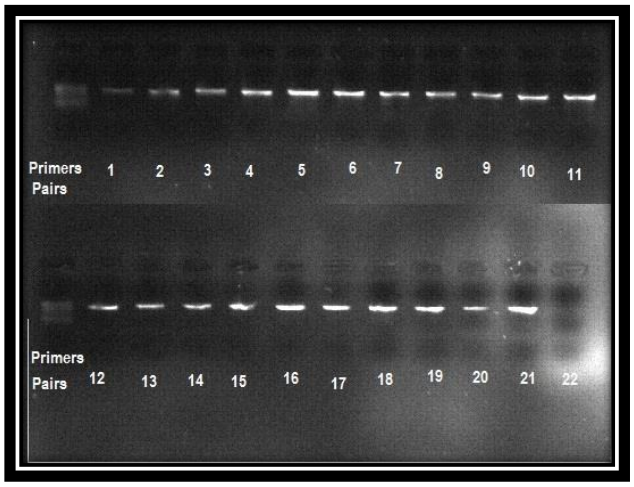

Figure 2. Amplified PCR result of the first 22 primer pairs in 1% agarose gel.

CONCLUSION

Generally speaking, this experiment has had a positive outcome for this particular research project. Based on the data presented, it is safe to state that there are enough information to have a distinct conclusion on the origin of migration of the Palawan Peacock-Pheasant once the rest of the species have been gathered, processed, and analyze with the template. In addition, our results does show that are numerous types of similarities between the Palawan Peacock-Pheasant *Polyplectron Napoleonis*. To be more specific, there is a high percentage (93%) similarity of the mitogenome sequence between the *Polyplectron napoleonis* and *Polyplectron bicalcaratum*. This result can create a scientific and ideal conclusion that there are some type resemblance and similarities between the origins of migration

between these two species. Overall, I have learned and consumed numerous of scientific information and lessons within the fields of genetics and evolution from this project. Not only has it enhanced my knowledge about the genetic/evolution field of science, it also has opened my perspective on how many scientists and research apply these processes in our daily lives

Figure 3. Sequence alignment, assembly and annotations of the complete mitochondrial genome of P. napoleonis with Genious Pro 5.5.

ACKNOWLEDGEMENTS

This study was supported by Summer Undergraduate Research Program (SURP) of the College of Science and Technology at Texas Southern University. We appreciate the assistance from Ms. Shaunte Abdin for helping, explaining, and illustrating how to proceed with polymerase chain reaction procedure, gel electrophoresis, and using the genious program to analyze our results.

REFERENCES

BirdLife International 2005. Polyplectron germaini. 2006. IUCN Red List of Threatened Species. IUCN 2006.

Desjardins P, Morais R. (1991) Nucleotide sequence and evolution of coding and noncoding regions of a quail mitochondrial genome. *Journal of Molecular Evolution* 32:153-161.

Desjardins P, Morais R. (1990). Sequence and gene organization of the chicken mitochondrial genome. A novel gene order in higher vertebrates. *Journal of Molecular Biology* 12:599-634.

Eo SH, Bininda-Emonds ORP, Carroll JP. (2009) A phylogenetic supertree of the fowls (Galloanserae, Aves). *Zoologica Scripta* 38:465-481.

Harrison GL, McLenachan PA, Phillips MJ, Slack KE, Cooper A, Penny D. (2004) Four new avian mitochondrial genomes help get to basic evolutionary questions in the late Cretaceous. *Molecular Biology and Evolution* 21:974-983.

Kimball RT, Braun EL. (2008) A multigene phylogeny of Galliforms supports a single origin of erectile ability in non-feathered facial traits. *Journal of Avian Biology* 39:438-445.

Kimball RT, Braun EL, Ligon JD, Lucchini V, Randi E. (2001) A molecular phylogeny of the peacock-pheasants (Galliformes: Polyplectron spp.) indicates loss and reduction of ornamental traits and display behaviours. *Biological Journal of Linnean Society* 73:187–198.

Lowe TM, Eddy SR. (1997) tRNAscan-SE: a program for improved detection of transfer RNA genes in genomic sequence. *Nucleic Acids Research* 25:955-964.

Pacheco M A, Battistuzzi FU, Lentino M, Aguilar RF, Kumar S, Escalante AA. (2011) Evolution of modern birds revealed by mitogenomics:timing the radiation and origin of major orders. *Molecular Biology and Evolution* 28:1927-1942.

Paton T, Haddrath O, Baker AJ. (2002) Complete mitochondrial DNA genome sequences show that modern birds are not descended from transitional shorebirds. *Proceedings of the Royal Society of London, Biological Sciences* 269:839-846.

Shen YY, Shi P, Sun YB, Zhang YP. (2009) Relaxation of selective constraints on avian mitochondrial DNA following the degeneration of flight ability. *Genome Research* 19:1760-1765.

PRELIMANARY ASSESMENT OF VOLATILE ORGANIC COMPUNDS (VOCS) IN INDOOR PARKING FACILITIES IN THE GREATER HOUSTON AREA

Raven B. Reed* and Bobby L. Wilson#

Department of Chemistry
College of Science and Technology, Texas Southern University
3100 Cleburne Street, Houston, TX 77004

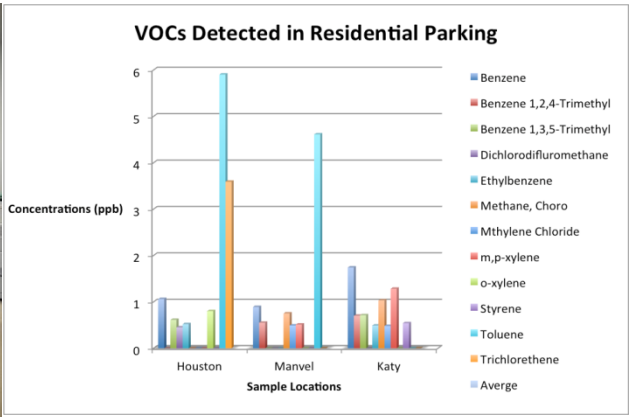

ABSTRACT

Automobiles have been widely known as sources of (Volatile Organic Compounds) VOC emissions in outdoor environments; however, the impact of these emissions indoor has not yet been studied in detail and needs to be developed. Two different types of indoor parking facilities have been assessed for the VOC concentrations, which include residential attached parking garages, and commercial ground parking garages. For this assessment, Houston, Texas, a representative big city, was chosen because of its high dependency on private transportation via cars by its citizens, the numerous petrochemicals industries emitting VOCs, and the several days each year that it experiences a high ozone level. These factors significantly increase Houstonians' exposure to VOCs. Indoor air samples were collected using 6-L stainless steel canisters for 24-h period and analyzed using a modified version of EPA Method TO-15, which is TSU-TO15 with GCMS coupled to cryogenic pre-concentrator. The eight most abundant VOCs were identified in each sample. Six out of the eight VOCs identified are classified as hazardous air pollutant based on EPA regulations. This research found that the concentrations of VOCs are higher in attached residential parking garages following, ground commercial parking garages. It can be assumed that the VOCs are greater where there is little to no ventilation.

Key Words: *residential attached parking garages, commercial ground parking garages, volatile organic compounds (VOCs), indoor air*

*SURP Fellowship Recipient
#Faculty Mentor

INTRODUCTION

Worldwide air quality has been an issue for the atmosphere and living species such as (plants, animals, fungi etc.) This study focuses on humans, which fall under the living species Kingdom Animalia. In the United States, large industrialized cites are exposed to higher concentrations of VOCs due to emissions. Mass transit systems have been implemented to ease traffic and VOCs. The most common transportation mode is the automobile. Humans are exposed to VOCs by three main activities involving its use: in- vehicle exposure during commuting, refueling, and in transit (within parking garages). Research studies have indicated that between home, school, and work 92% of a person's life is spent

indoors (Klepeis, 2003). The quality of indoor air can have a significant impact on human health and the well being of an individual. A wide variety of health effects are caused by exposure to indoor air pollutants.

VOCs are major air pollutants in the environment that are easily released into air. These compounds vaporize at various temperatures and rates depending on their volatility. Air pollution can be classified as either indoor or outdoor. VOC emission sources may be found in any indoor environment, including particulate matter, gases, vapors, biological materials, and fibers. A previous study by the U.S. Environmental Protection Agency (EPA) in 1999 found that 29% of total volatile organic compounds (TVOC), 34% of total oxides of nitrogen, and 51% of all carbon monoxide emissions were attributable to automobile emissions (McGaughey, 2004). The Environmental Protection Agency (EPA) lists some symptoms of VOC exposure. The ability of organic chemicals to cause adverse health effects varies greatly from those that are highly toxic, to those with no known effect. As with other pollutants, the extent and nature of the health effect will depend on many factors including level of exposure and length of time exposed. Adverse health effects include; eye and respiratory tract irritation, headaches, dizziness, visual disorders, and memory impairment are among the immediate symptoms that some people have experienced soon after exposure to some organics. Many organics are known to cause cancer in animals; some are known to cause cancer in humans. EPA's Office of Research and Development's "Total Exposure Assessment Methodology (TEAM) Study" (Volumes I thorough IV, completed in 1985) found levels of about a dozen common organic pollutants to be 2 to 5 times higher indoors than outside (U.S. EPA, 2012). EPA Team studies indicated that concentrations could persist in the air long after the activity is completed.

In the presence of nitrogen oxides and sunlight, many of these compounds contribute to ozone formation. The emission of VOCs into the atmosphere comes from both biogenic and anthropogenic sources. Biogenic being produced by living organisms or of biological process and anthropogenic being produced by human activity. However, the emissions from anthropogenic sources are the ones of the most concern, particularly in industrialized areas. In an industrialized area such as Houston, Texas, the sources of VOC emissions come not only from automobiles but also from other human activities such as refineries and petrochemical facilities. Despite the widely known fact that Houston has several days throughout the year with high ozone levels and VOC concentrations, there are limited numbers of studies on VOCs in outdoor and indoor air quality in Houston, Texas. Houston will start the research on indoor air quality for many cities to follow. Samples will be obtained and analyzed.

METHODS

Summa stainless steel canisters were used to collect indoor air samples with 6 liters volume made by Entech Instruments, Inc. (Simi Valley, California). These canisters were coated by silonite™ with a maximum pressure allowed in the canister of 40 psig. During sample collections, indoor air was drawn through canister with a rate of 3.4 ccm. The airflow was managed by CS1200 instruments using restrictors from Entech Instruments, Inc. (Simi Valley, California). This restrictor was calibrated by a flowmeter made by Alicat Scientific flow calibrator model 01-39-20035 (Alicat Scientific, Tucson, Arizona) before and after each sample collection.

Sample Collection

Two different types of indoor parking facilities in Houston, Texas, were selected to represent air quality in indoor parking facilities in urban areas. These parking facilities include residential attached garages, and ground parking garages. Some restrictions were applied for particular types of sampling locations. The attached garages are located within residential area while the ground parking facilities are located in commercial areas. It is expected that the indoor air at sampling locations are not influenced directly by particular local emission sources; therefore, it is adequate for representing the mixture of VOCs in indoor air environments. Detailed locations of the sampling sites are summarized as follow:

Table 1. Sampling Site Description.

Parking Type	Location	Description
Residential Attached Garage	Houston, TX	House
	Manvel, TX	House
	Katy, TX	House
Commercial Parking Garage	East Garage at TSU	University
	West Garage at TSU	University

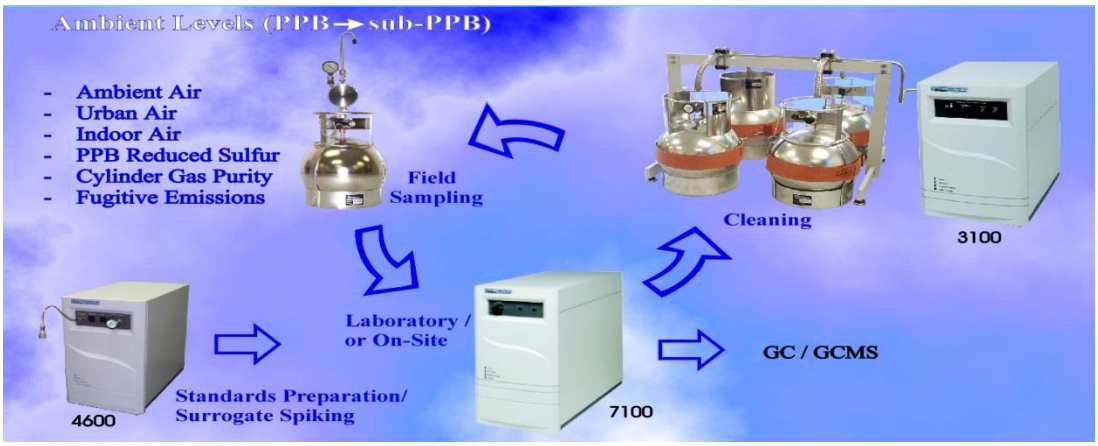

Figure 1. Diagram showing the sample collection procedure.

Sample Analysis

Samples were taken over 4 day periods for 24hrs per day. At the end of each sampling period, each canister was tightly closed with its cap and stored at room temperature until the analysis. All analysis was taken with in 7days. After the completion of the samplings, the canisters were transported to the laboratory and analyzed. Samples were analyzed by gas chromatography (GC) coupled with the mass spectrometer (MS) with the selected ion monitoring (SIM) mode. Prior to gas chromatography and mass spectrometer, samples are concentrated by the preconcentrator model 7100A (Entech Instruments, Inc., California). The preconcentrator freezes all organic compounds found in the ambient air. Helium was used as a carrier gas because nitrogen is found in ambient air.

Quality Assurance and Quality Control (QA/QC)

The regularly applied quality assurance and quality control experiments included regular multi-point calibration, blank check for canisters, continuing calibration verification (CCV), canister cleaning, and canister tracking sheet. One internal standard was used to maintain performance, stability of the MS, and also to quantify the compound detected. Some of these gases have been identified as markers for automobile emissions such as benzene, toluene, ethylbenzene, and m,p-xylene. All samples were analyzed less than 7days after they arrived in the laboratory, which is within the 30day time frame to acquire accurate data.

RESULTS AND DISCUSSION

Volatile organic compounds identified

Twenty air samples from five locations were collected and analyzed by GCMS. The eight most abundant target compound VOCs have been identified in every single attached garage, parking facility. EPA classifies most of the VOCs found in this study as hazardous air pollutants. The results are presented in the following table:

Table 2. Volatile organic compounds identified in attached residential and ground parking garages.

Benzene	Methane, Chloro
Benzene 1,2,4-Trimethyl	Methylene Choride
Benzene 1,3,5-Trimethyl	m,p-xylene
Chloroform	Carbon Tetrachloride
Dichlorodifluromethane	Trichloromonfluoromethane
Ethylbenzene	Styrene

Dichlorofluoromethane (known as Freon 21), chloromethane, and trichloromonofluoromethane have been categorized as airborne halocarbons, and they are mainly used as refrigerants. There are not many studies associated with these three compounds especially in indoor environments; however, it has been reported that in the ambient air their site. In addition, a study in Mumbai, India, by Srivastava (2004) found that there is also possibility that the presence of chlorinated compounds may be attributable to the sea emission. The city of Houston is located about 70 miles from the Gulf of Mexico, and the observed concentrations of chlorinated compounds may be also attributed to marine sources.

Among the twelve VOCs found, toluene was the most abundant compound in every type of indoor parking facility. The concentrations are measured by volume is parts per billion (ppb). For toluene, the mean exposure level in attached garages (5.785 ppb) is the highest followed by ground parking (3.8475 ppb). Other VOCs such as ethylbenzene, m,p-xylene, and benzene were also higher in attached residential garages compared to the same types of VOCs in ground parking garages. Previous studies mentioned several factors that contributed to the high benzene, toluene, ethylbenzene, and xylene concentration in indoor attached garage such as material stored inside and human activities (Wallace, 1993, Guo, 2003). Guo *et al*. (2003) mentioned significant differences on indoor toluene concentrations due to differences in fuel types used for cooking (liquefied petroleum gas or natural gas), while frequency of house cleaning has been identified as a source of higher benzene, toluene, ethylbenzene concentrations in homes.

It was suspected that the concentration of TVOCs would be higher in residential parking garages than in ground parking garages because of the more compounds being stored in a residential parking garage with little to no ventilation. As shown in Figures 2 and 3 the TVOCs are 4.678ppb and 2.536ppb commercial parking garages. As a consequence, TVOCs in residential attached garages is the highest followed by commercial parking garages. Observation during the sampling period revealed that attached garages are extensively used to store several types of chemicals and household machinery; therefore, it is possible that the indoor air quality in attached garages was greatly influenced by emissions from these materials. These chemicals include paints, household cleaners, motor oil, and small machine such as lawn mowers, and blowers.

In terms of ventilation design, the situation in commercial parking facilities is different from that in attached garages. It is assumed that storage functions in underground and ground parking facilities are the same; therefore, the difference is only in the availability of ventilation. In both commercial ground and underground indoor parking facilities, ventilation design is important for maintaining a good air quality. During the experiment most of the ground parking facilities chosen as sampling locations were located in the same multi-story commercial parking facilities with no mechanical ventilation. Despite not having mechanical ventilation, they primarily rely on the natural opening in the car entrance/exit system to maintain good air quality inside. Consequently, VOCs emitted inside will be expected to stay even longer due to the short circulation of the ventilation airflow. On the other hand, the ground parking has the more natural ventilation, which can prevent air pollutants from being trapped inside the facilities. This result is supported by Chan and Chow (2004) who studied performance of car park ventilation system in Hong Kong and mentioned several factors that contributed to the magnitude of VOCs indoor such as ventilation, random engine operating time, number of cars entering/leaving car park, degree of congestion, and level of occupancy of the parking lot.

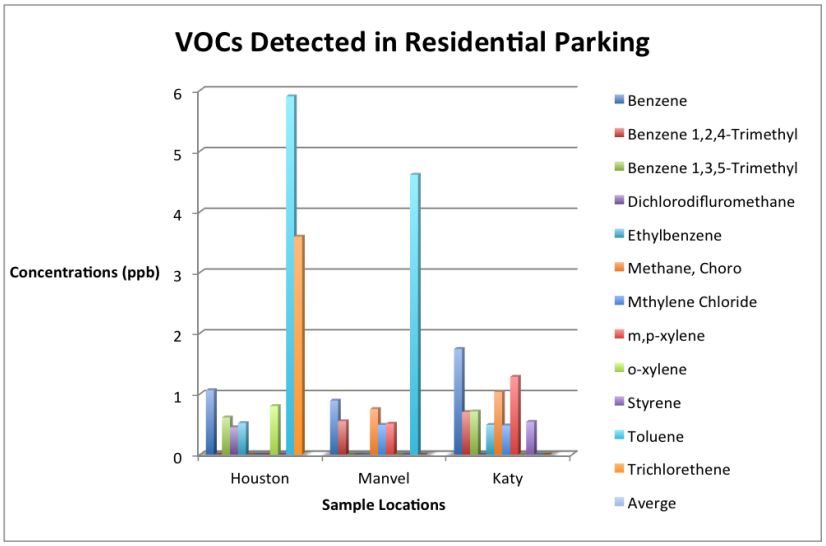

Figure 2. Compounds Identified in Attached Residential Parking Garages

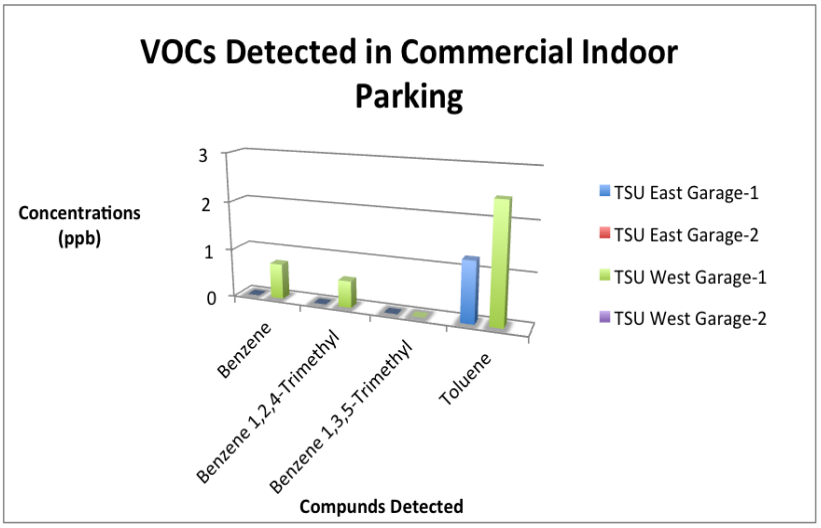

Figure 3. Compounds Identified in Commercial Ground Parking Garages.

Result of this study also revealed that the average percentage of VOCs profiles of ground parking facilities are found to be similar when compared with attached garages. The average samples from ground parking facilities had toluene as the highest portion (40%), followed by m,p-xylene (20-22%), benzene (16-17%), and ethylbenzene (8-9%). It is believed that their air quality was closely associated with the traffic pattern such as the low-driving speed, frequent acceleration/deceleration, and idling.

CONCLUSION

Different types, magnitudes, and sources of VOCs were identified from in indoor parking facilities in Houston. It was also found that attached residential garages have the highest TVOC concentrations followed by ground commercial parking facilities. Toluene to benzene, and m,p-xylene to benzene ratios confirmed that several factors affected these conditions such as the material stored, ventilation, and automobile emissions. In attached garages, the impact of material stored in them has a more significant

effect than automobile emissions and the availability of ventilation. While in ground parking facilities, the automobile emissions and ventilation availabilities are more significant determinants of air quality than the material stored in them.

This study leads to the question of whether indoor parking facilities can increase the risk of human exposure to VOCs. Since many of the VOCs are hazardous to human health; this risk should be considered as a part of total risk of human exposures to VOCs during their daily activities. While Houstonians have already been exposed to high VOC concentrations from outdoor environment activities (e.g. traffic, refineries, and petrochemical facilities), additional activities causing VOC exposures will add to the total risk significantly. These results will not only be a beneficial reference to assess the risk of exposure when combined with human activity patterns and concentration of pollutants in microenvironments, but also to establish strategies for reducing human exposure to VOCs. Future study recommended is to sample and analyze VOCs in underground parking garages.

ACKNOWLEDGEMENTS

This study was supported by Summer Undergraduate Research Program (SURP) of the College of Science and Technology at Texas Southern University. We also express our gratitude to Siobhan Tarver for her support in sample collection and laboratory analysis.

REFERENCES

Chan MY, Chow WK. (2004) Car park ventilation system: performance evaluation. *Building and Environment* 39:635-643.

Duffy BL, Nelson PF. (1997) Exposure emission of 1,3-Butadiene and benzene in the cabins of moving motor vehicles and buses in Sydney, Australia. *Atmospheric Environment* 31:3877-3885.

Edgerton (1990). Ambient volatile organic compounds at selected sites in Bankok city, Thailand. *Chemosphere* 6:673-679.

Kristanto GA, Conley FL, Thomas RL, Wilson BL. (2004) Assessment of Volatile Organic Compounds (VOCs) in Indoor Parking Facilities in Houston, Texas" *Environmental Toxicology Program, Department of Chemistry, Texas Southern University, Houston, TX.*

Hoglund PG. (2004) Parking, energy consumption and air pollution. *Science of the Total Environment* 334-335:39-45.

McGaughey GR, Desai NR, Allen DT, Seila RL, Lonneman WA, Fraser MP, Harley RA, Pollack AK, Ivy JM, Price JH. (2004) Analysis of motor vehicle emissions in a Houston tunnel during Texas Air Quality Study 2000. *Journal of Atmospheric Environment* 38:3363-3372.

Na K, Kim YP, Moon KC. (2003) Diurnal characteristics of volatile organic compounds in the Seoul atmosphere. *Atmospheric Environment* 37:733-742.

U.S. Environmental Protection Agency. (2012) An Introduction to Indoor Air Quality (IAQ) Volatile Organic Compounds (VOVs). U.S. EPA/Office of Radiation and Indoor Air, Indoor Environments Division, Washington, DC.

U.S. Environmental Protection Agency (1997) Compendium Method TO1: Determination of volatile organic compounds (VOCs) in air collected in specially-prepared canisters and analyzed by gas chromatography/mass spectrometry (GC/MS). Compendium of methods for the determination of toxic organic compounds in ambient air. Second Ed. U.S. Environmental Protection Agency, Cincinnati, OH.

Wallace LA. (2001) Human exposure to volatile organic pollutants: Implications for indoor air studies. *Annual Review of Energy and the Environment* 26:269-301

National Institute of Standards and Technology. Chemistry Web Book (webbook.nist.gov/chemistry)

U.S. Environmental Protection Agency. Indoor Air Quality (www.epa.gov/iaq)

HOW MUCH ENERGY CAN TSU STUDENTS SAVE? – WATER PURIFICATION SYSTEMS VERSUS BOTTLED WATER AND BIKES VERSUS CARS

[1]Tyneshia Thomas* and [2]Hyun-Min Hwang#

[1]Department of Biology, [2]Department of Environmental and Interdisciplinary Sciences
College of Science and Technology, Texas Southern University
3100 Cleburne Street, Houston, TX 77004

ABSTRACT

The purpose of this research is to see how much energy is consumed by TSU students through the use of bottled water versus water purification systems on campus and through riding buses and bikes appose to driving cars for commute. During the first part of this study, the amount of energy consumed throughout the life cycle (cradle to grave) of bottled water was calculated. Consumption of bottled water has been steadily increasing since the late 1990s in the United States. Approximately 32 to 54 million barrels of oil were used to make 33 billion liters of bottled water in the U. S. in 2007. The estimated total amount of energy consumed from plastic bottle production to landfill is 25.3 mL of diesel per water bottle, indicating that about 267,000 L of diesel is consumed by TSU students through drinking bottled water for 5 years on campus. The second half of this research focused on the amount of gasoline that can be saved through riding buses and bikes appose to driving a car. A survey with 100 TSU students revealed that each student drives approximately 80 km on average to commute between homes and TSU campus. Coupled with 8.78 km/L of fuel economy (weighted average for students' vehicles) indicates that TSU students consume 55.4 million L of gasoline for 5 years for commuting, which is equivalent to 61,000 tons of CO_2 emission. This study demonstrates that changes of our life styles and personal behavior and support from institutes and city administration and public policies can save energy as well as reduce the carbon footprint that will significantly contribute to the mitigation of unwanted impacts of climate change.

Key words: *Life cycle assessment, Bottled water, Water purification system, Energy consumption, Environment friendly commuting*

*SURP Fellowship Recipient
#Faculty Mentor

INTRODUCTION

We use fossil fuel energy directly and indirectly for almost all parts of our life. No matter the time of the day energy is exerting itself in one manner or the other. But what if the energy was compared to other forms of energy in order to conserve it and save money and resources. Will utilizing less energy potentially preserve the environment? That's the purpose of this experiment. To compare the energy consumption of the same task being done in different ways, the amount of energy required for the different approach need to be investigated.

Many people feel that the tap water in the greater Houston area is not favorable for drinking and consume bottled water instead of tap water. Each year, billions of portable and disposable plastic bottles are produced for drinking water. About 43 million barrels of oil was used to produce 33 billion liters of bottled water in the U.S. in 2007 (IBWA, 2013) and the amount of bottled water we consume has been steadily increasing. In order to produce portable plastic bottles, we need to make polyethylene terephthalate (PET), which generated from petroleum (IBWA, 2013). So we consume energy during the entire life cycle of the PET bottles, including petroleum extraction, refining, PET bottle manufacturing, water filling, and transportations to local retail stores and eventually to recycling facilities or landfill sites (Figure 1). One option to avoid energy consumption for PET bottles is using on-site water purification systems that can be connected to municipal tap water faucets.

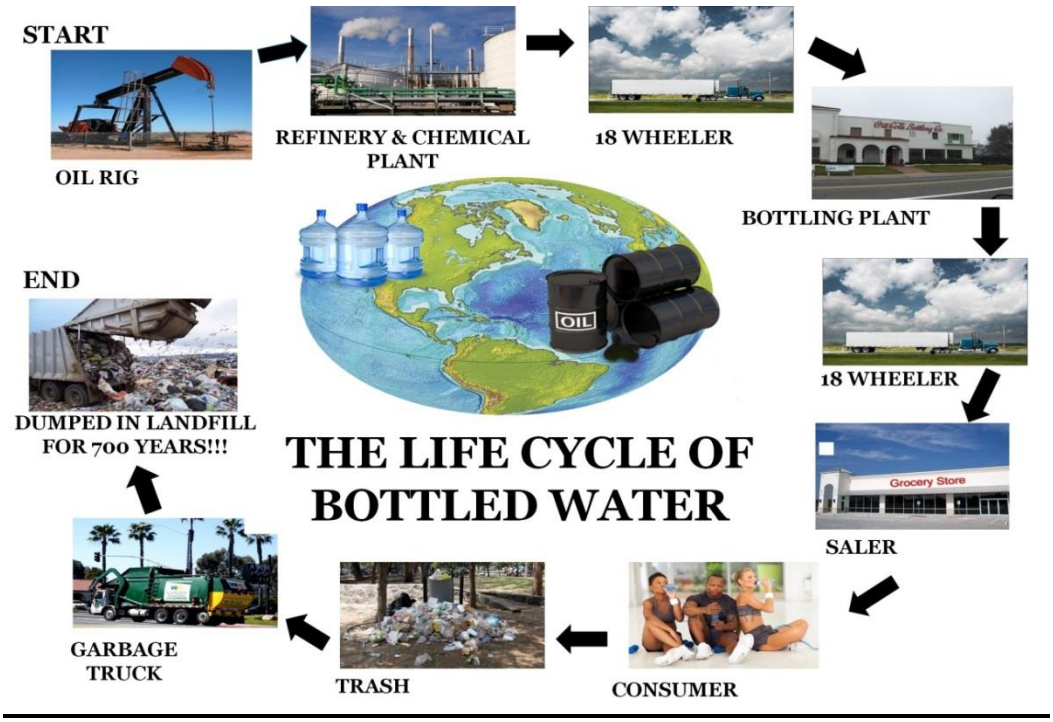

Figure 1. Life cycle of disposable plastic bottles for drinking water.

One of the major aspects of modern life of people in the U.S. is driving personal vehicles to commute between homes and work places. Students also drive tens of kilometers daily for commuting. Fuel consumption by driving personal vehicles accounts for 30% of the total energy consumption of typical Americans.

This research will take a closer look at how much energy can be saved by Texas Southern University (TSU) students through using water purification system on TSU campus instead of drinking bottled water and by using public transportation and bicycles instead of driving personal vehicles.

METHODS

Bottled water vs. Water purification system

The first part of this project was to acquire how much energy is used during a life cycle (from production to landfill) of disposable PET bottles that have been used for drinking water. The life cycle of disposable PET bottles is conceptualized in Figure 1. The material (polyethylene terephthalate) used to make plastic bottles is a thermoplastic polymer resin produced from ethylene glycol and dimethyl terephthalate that are generated from petroleum. Once PET bottles are produced, they are transported to

water bottling factories that are typically located near big cities. Water filled PET bottles are transported to local retail stores to sell to consumers. After the consumption, PET bottles are collected for recycle or disposal in landfill. So the total amount of energy consumed for PET bottles include all energy used during the life cycle of the disposable PET bottles.

Required information for this life cycle assessment was obtained from a student survey, a short interview with staff of water bottling companies, literatures, and the internet. A survey performed with 100 TSU students revealed that each TSU student drinks 1.74 bottles of water each day on campus. In order to calculate amount of fuels used to transport water filled PET bottles from bottling facilities to local retail stores, a short interview was taken by speaking with a representative of Coca-Cola. Fuel efficiency of a loaded 18 wheeler truck is about 4 miles per gallon, which is equivalent to 1.69 km/L (www.whitehouse.gov). Average distances from water bottling factories to TSU campus and to landfill sites are 40 km and 32 km, respectively (Thomas Net, 2013). We assumed that all consumed PET bottles are collected on the campus and disposed at landfill sites.

We assumed that one reverse osmosis water purification system will be installed for each floor in each building on TSU campus. There are 40 buildings and each building has 3 floors on average. Because no information regarding the amount of energy used to make a water purification unit, retail price is converted to the amount of diesel using a conversion factor of $2.5/gallon (= $0.66/L). After an initial installation of the water purification system, additional operation cost is for filter replacement for 5 years of estimated life.

Bikes vs. Automobiles

The second part of this project was to calculate the amount of energy TSU students use to drive automobiles vs. to use public transportation and bicycles. A survey of 100 students was taken to get the average distance a student drives to and from TSU. Then a study of the student parking lot was taken to see the type of automobile students drive on campus. Once that information was acquired, a weighted average of each type of vehicle (car, truck or suv) was used to calculate fuel efficiency (miles per gallon = km per liter) for students to commute each day. Fuel economy rate was obtained from the Department of Energy fuel economy site (www.fueleconomy.gov). The total amount of fuels consumed by students for commuting was calculated by dividing the distance between home and TSU campus by the weighted average fuel efficiency of vehicles on campus and compared to the amount of fuel used to ride bused and bikes for commuting.

RESULTS AND DISCUSION

Water purification system vs. Bottled Water

Forty three million barrels of crude oil was used to produce 33 billion liters of bottled water in 2007. Assuming average size of a PET bottle is 0.5 L, 33 billion liters is converted to 66 billion plastic bottles. U.S. refineries produce an average of about 10 gallons of diesel fuel from one barrel (42 gallons) of crude oil. So 43 million barrels of crude oil can be converted to 1.62 billion liters of diesel that is equivalent to 24.5 mL of diesel per 1 PET bottle.

According to that representative each 18 wheeler truck typically holds 25 large pallets. Each pallet holds 48 cases and each case holds 24 water bottles so each fully loaded 18 wheeler truck can hold 28,800 PET bottles. So the amount of diesel to be used to transport water bottles from factories to campus and empty bottles to landfill sites is 0.79 mL per bottle. Therefore, total energy consumed during the life cycle of a PET bottle is equivalent to 25.3 mL of diesel. Because each TSU student drinks 1.74 bottles of water each day, total amount of diesel consumed by all TSU students through drinking bottled water is 418 L

per day. Students come to the campus 4 days a week for 16 weeks for each semester, so they consume total 53,500 L per year. For comparison with the energy consumption by water purification system that will be operated for 5 years, yearly energy consumption through drinking bottled water is multiplied by 5, resulting in 267,000 L during 5 year.

In order to install one water purification system for each floor for all building on TSU campus, total 120 purification systems need to be installed initially. Retail price of a water purification system is appropriate is about $200. One hundred twenty of this purification system can support 1.74 bottles of water for each TSU student every day. The total cost for initial installation of 120 purification systems is $24,000. Because the majority of the retail price of these products is derived from non-energy related activities such as labor of employees in manufacturing companies, marketing, and margins for manufacturer and retailers, only 10% of this price is considered energy related cost, which is $2,400. Then, it can be converted to 3,640 L of diesel ($2,400 × L/$0.66). Assuming that the filters are replaced once for each semester, total cost for filters for the remaining 9 semesters is $76,800. Again only 10% of this is considered energy related cost, which is $7,680. Then it can be converted to 11,600 L of diesel. Combining initial installation and filter replacement during 5 years of life time of the water purification systems, total 15,240 L of diesel is consumed to support drinking water for all TSU students.

Comparison of these two cases shows that about 250,000 L of diesel can be saved when we use water filtration system instead of consuming bottled water. The total amount of energy required for water purification system is only about 6% of the energy used during the life cycle of bottled water. Although it is not included in this study, disposal of 10 million PET bottles require much greater space in landfill sites compared to that for 120 water purification systems and about 1,000 sets of filters. This study clearly shows that we can reduce significant amount of energy consumption and consequently reduce significant amount of greenhouse gas emission by changing from bottled water to water purification system.

Table 1. Amount of diesel consumed from the production of bottled water to disposal in landfill.

Energy used to produce bottled water	24.5 mL/bottle
Energy used to transport from manufacturing factories to TSU campus and to landfill sites	0.79 mL/bottle
Total energy consumed during life cycle of PET bottles used by TSU students	25.3 mL/bottle
Total energy consumed during life cycle of PET bottles used by TSU students for 5 years	267,000 L
Total energy required to operate water purification systems at TSU buildings for 5 yeas	15,250 L
Total energy savings by changing from bottled water to water purification system	251,750 L

Bikes vs. Automobiles

The survey showed that the average student drives approximately 50 miles (= 80 km) round trip each day to commute between homes and TSU campus. These miles coupled with 20.75 miles per gallon (weighted average of automobiles on campus), 8.78 km/L, resulting in that each student uses 9.11 L of gasoline each day (Table 2). It is not expected for students to ride a bike for commuting this long distance, but if students use public transportation (e.g., buses) and bikes together, significant amount of fossil fuels can be saved, and consequently reducing the carbon footprint of each student on campus**.** We assumed that students come to the campus 4 days a week, 16 weeks per semester and they attend TSU 5

years before they graduate. Although, a small increase of fuel consumption for bused to carry TSU students needs to be considered for more accurate assessment, we assumed that no additional fuel is required for buses because they are already in operation throughout the Houston area. Total gasoline that can be saved by all TSU students for 5 years by using buses and bicycles is 55.4 million L. Assuming all gasoline is converted to CO_2 and H_2O during combustion, approximately 61,000 tons of CO_2 emission can be reduced.

Table 2. Amount of gasoline used to drive personal vehicles for TSU students for commuting .

Amount of gasoline utilized to drive a car to and from school	9.11 L/day
Total gasoline savings by a TSU students for 5 years	5,830 L
Total gasoline savings by all TSU students for 5 years	55.4 million L

CONCLUSION

In conclusion, a large amount of energy can be saved by changing from the consumption of bottled water to the utilization of on-site water purification systems. These purification systems will not only save energy in the form of crude oil, but it will also save money for students not buying bottled water. The students at Texas Southern can also save energy by not driving personal vehicles to commute between homes and campus. Changes of our life styles and personal behavior and support from institutes and city administration and public policies, we can save energy as well as reduce the carbon footprint that will significantly contribute to the mitigation of unwanted impacts of climate change.

ACKNOWLEDGEMENTS

This study was supported by Summer Undergraduate Research Program (SURP) of the College of Science and Technology at Texas Southern University. Thanks to everyone who took time to assist my research by answering survey questions, sending me articles, and educating me on the purification process of water. Jerry Geisler, Susan Smyer, Brenda Templeton and Eric Garza Jr. from Water Works Education Center NE Houston, Claire Scoggin from the Museum of Natural Science and Daniel Wuan from Public Works Drinking Water.

REFERENCES

FACT SHEET: Opportunity For All: Improving the Fuel Efficiency of American Trucks – Bolstering Energy Security, Cutting Carbon Pollution, Saving Money and Supporting Manufacturing Innovation (www.whitehouse.org)

Fuel economy. (2013) U.S. Department of Energy (www.fueleconomy.gov)

IBWA. (2013) Bottled Water Production. (www.bottledwater.org/education/bottled-water-production).

Thomas Net (2013) Plastic Bottle Manufacturing - Product Sourcing and Supplier Discovery Platform. (www.thomasnet.com/articles/materials-handling/plastic-bottle-manufacturing).

A Renaissance of EXCELLENCE

TSU Texas Southern University
College of Science and Technology